Report: Bauxite-related resources in the ESEE region and REE – focus on Croatia, Hungary, Montenegro and Slovenia

24 February, 2020

17089 REEBAUX: Prospects of REE recovery from bauxite and bauxite residue in the ESEE region
University of Zagreb Faculty of Science (UNIZG-PMF)
Version: 2

This activity has received funding from the European Institute of Innovation and Technology (EIT), a body of the European Union, under the Horizon 2020, the EU Framework Programme for Research and Innovation

Contributed by (in alphabetical order)

Matija Bedeković
Lóránt Biró
L. Bódi
Andrea Čobić
Goran Durn
Hana Fajković
Hans-Jurgen Gawlick
Hartwig Gielisch
Nikola Gizdavec
Anamarija Grbeš
Nikolina Ilijanić
Erli Kovačević Galović
Ivona Ivkić
Mate Lesko
Florian Lowicki
Ferenc Madai
Slobodan Miko
Andrea Mindszenty
Ana Mladenović
V.Z. Nagy
Slobodan Radusinović
Csaba Szabó
Dominik Teskera
Nenad Tomašić
Janez Turk
Igor Vlahović
Gyula Záray

Partner institutions: Croatian Geological Survey, DMT, Eötvös Loránd University, Geological Survey of Montenegro, Montanuniversität Leoben, Slovenian national building and civil engineering institute, University of Miskolc, University of Zagreb – Faculty of Mining, Geology and Petroleum Engineering, University of Zagreb – Faculty of Science

This activity has received funding from the European Institute of Innovation and Technology (EIT), a body of the European Union, under the Horizon 2020, the EU Framework Programme for Research and Innovation

CONTENT

This activity has received funding from the European Institute of Innovation and Technology (EIT), a body of the European Union, under the Horizon 2020, the EU Framework Programme for Research and Innovation

1. INTRODUCTION

Bauxite has been renowned for its importance in the industry of aluminium, followed by the usage of bauxite raw materials in cement, chemical and industry of abrasives. Geological background behind bauxite deposits and their formation proved to be crucial for many bauxite occurrences, which contain significant abundances of critical raw materials (CRM). These relatively newly discovered potential applications of bauxite still need to find their way to the raw material market, since technological procedures to be applied are temporarily under development.

EIT RM REEBAUX KAVA focuses to the bauxite-related resources in the ESEE region, in particular in Croatia, Hungary, Montenegro and Slovenia, with respect to their possible application for REE recovery. Thus, collection of already existing and new data together with an assessment of the REE potential is a primary scope of the project activities, particularly in 2019, the second project year.

In this report data on REE abundances in bauxite and red mud in the focus countries will be presented together with the geological background. They are starting point for a preliminary assessment of the REE potential, following current market situation and taking into account possible technological approaches for REE recovery.

This activity has received funding from the European Institute of Innovation and Technology (EIT), a body of the European Union, under the Horizon 2020, the EU Framework Programme for Research and Innovation

2. BAUXITE DEPOSITS OF THE ESEE REGION (Croatia, Hungary, Montenegro) and their REE potential

As reported in the previous report (link), past studies of bauxite deposits in the focus countries paid occasional attention to REE abundances therein, although analytics of REE was not in all cases adequately carried out due to the difficulties of REE analytics in general, especially in the earlier days of bauxite studies.

For the purposes of the analytical tasks within REEBAUX project, intention was to harmonize and standardize field sampling practices and analytical procedures as much as possible, so that collected data from various localities could be adequately compared and assessed.

2.1. Sampling procedures

The investigated bauxite samples were collected by three major sampling procedures:

a) Sampling of a representative sample from clearly observable bauxite horizons within a bauxite deposit: both groove and point sampling were applied,
b) Sampling of a representative composite sample (several samples combined into one composite sample to represent several occurrences of bauxite of the same origin and age in an area),
c) Drill core sampling – samples for analyses are collected from drilling core at certain depths (a sample per a single depth or a composite sample of a few samples at a drilling interval).

The sampling of the red mud was performed by drilling boreholes at several position around Ajka and Almásfüzítő (Hungary), and Podgorica (Montenegro) red mud accumulations (red mud). In Kidričevo (Slovenia) the sample was obtained by a corer through the earth cover used for remediation of the out-of-usage red mud landfill.

Drilling project at Mamutovac

Drilling of the bauxite deposit in Mamutovac bauxite field in Croatia was performed during September 2019. Mamutovac is located in Šibenik-Knin County, municipality Promina, near the village of Bogetić, approximately 150 m NW from the road Čitluk-Roški slap (Figure 1). Bauxite deposit Mamutovac 1A (drilling site)(Figure 2) is a part of the former bauxite exploitation field Mamutovac, with the surface of 596 ha and several bauxite deposits (Mamutovac, Mamutovac-hrasti, Uroš, Mamutovac 1A, Mamutovac-II, Mamutovac-III, Podi kod Uroša I Validžić). After exploitation in this field, bauxite remained in the following

This activity has received funding from the European Institute of Innovation and Technology (EIT), a body of the European Union, under the Horizon 2020, the EU Framework Programme for Research and Innovation

deposits: Mamutovac 1A, Mamutovac-II, Mamutovac-III and Podi kod Uroša, with exploitation bauxite reserves estimated to 290 918 tones (Mamutovac-Ia 112 000 t), from 2005.

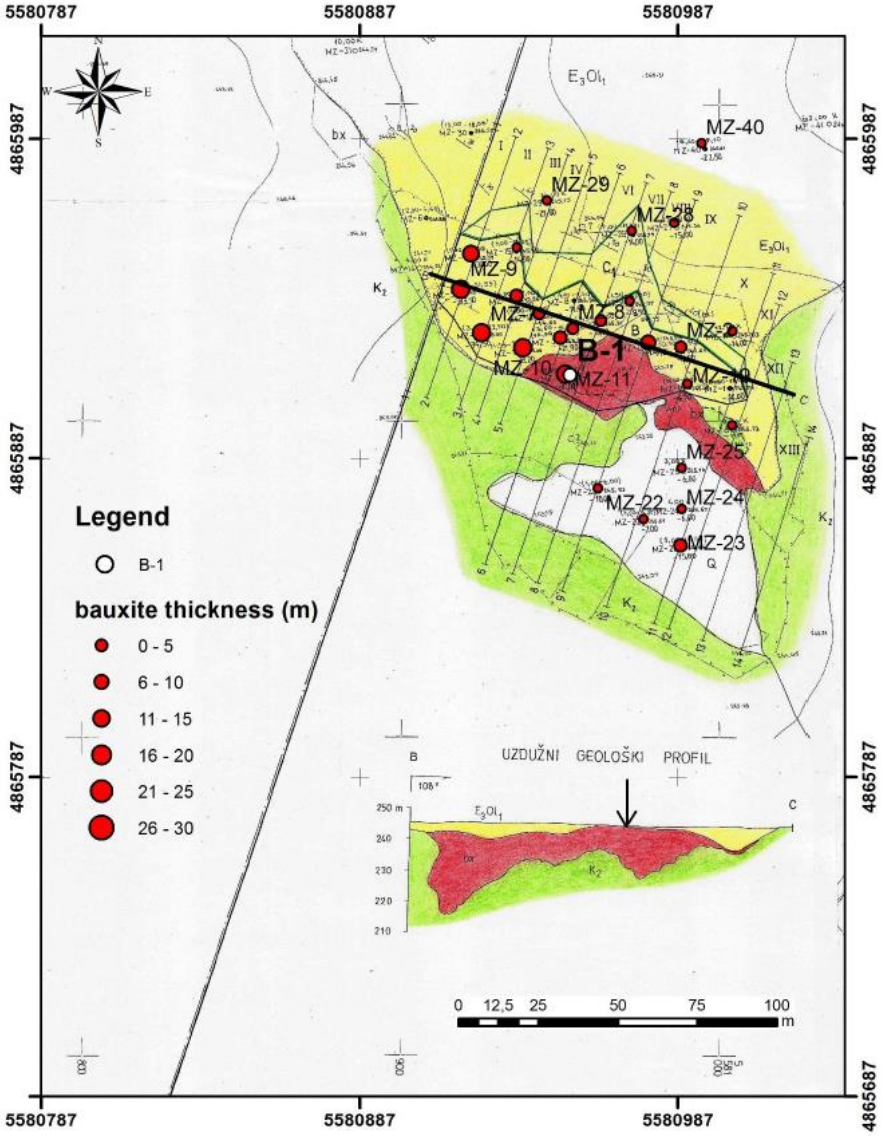

Figure 1. Drilling site and bauxite deposit profile of the Mamutovac 1A location

Due to the lower quality of the bauxite, which is not eligible for the Al industry, this bauxite is mainly used in the cement industry. It is supposed to have higher Ti content and REE, which has not been systematically investigated until now. The selection of the exact exploratory geological drilling location was done based on the literature review of previous bauxite surveys in the area, conducted mainly by the geologists from the Croatian Geological Survey, Department for mineral resources (Lukšić et al., 2004; Kruk et al., 2014). The bauxite cover at Mamutova 1A is made up of Promina deposits (conglomerates, marls, etc.), and the footwall Upper Cretaceous rudist limestones. The geological map of the bauxite deposit and geological profile was constructed based on drilling cores in

This activity has received funding from the European Institute of Innovation and Technology (EIT), a body of the European Union, under the Horizon 2020, the EU Framework Programme for Research and Innovation

Figure 2. Mamutovac 1A deposit during preliminary sampling and preparation for drilling activities

previous investigations (Lukšić et al., 2004). The ore body itself is shaped like an elongated "bed", with a thickness of almost 30 m in the central part (Figure 1). Drilling was performed approximately between the former MZ-10 and MZ-11 drilling cores, where the Promina cover is absent, and it was drilled directly into the bauxite ore body (B-1 core). The core drilling was performed with a diamond crown using double core tubes with water circulation (Figure 3). The diameter of the drilling core was 101 mm. The extracted core was in its natural state, partly solid and compact. A total of 26.4 m was drilled, however, 25.1 m of the core was preserved because of a change in lithological composition, that is, a limestone bedrock was drilled, which is permeable as opposed to bauxite.

Figure 3. Drilling at Mamutovac 1A deposit (left) and a section of the collected drilling core (right).

2.2. Analytical methods

For chemical analyses, collected samples of bauxite and red mud were crushed in the jaw mill and pulverized in agate mortar. The obtained sample powder was sieved through a set of sieves to obtain fraction with grain size < 0.02 mm. Subsequent pulverization of remained coarser fraction was carried out until all sample material passed the sieve with pore size < 0.02 mm. The prepared powdered samples were shipped to certified analytical laboratory

This activity has received funding from the European Institute of Innovation and Technology (EIT), a body of the European Union, under the Horizon 2020, the EU Framework Programme for Research and Innovation

for chemical analyses. Selected samples were also analysed by XRD (powder X-ray diffraction) to determine mineralogical composition.

The prepared samples were analysed for REE and other major and minor elements with ICP-MS and ICP-AES (inductively coupled plasma – mass/atomic emission spectroscopy). Lithium borate fusion as a sample decomposition technique was employed to prepare the samples for the analyses. The technique was selected in order to assure complete sample decomposition and to give insight into the bulk REE content of the bauxite and red mud samples. Several samples were additionally analysed by XRF (X-ray fluorescence) method for major bauxite components as this is a method used for validation of bauxite for the industrial purposes. The comparison of ICP and XRF analytical data yielded an excellent correspondence. The same analytical procedures and methods were used for the analyses of red mud samples (Chapter 3). The chemical analyses were performed in the internationally certified laboratory (Bureau Veritas Laboratory).

2.3. Country overview

The following subchapters present the obtained analytical data for the bauxite deposits in which the samples were collected within the frame of the project WP2 tasks in the focus countries (Croatia, Hungary, Montenegro).

2.3.1. Bauxite deposits in Croatia and REE potential

Bauxite deposits in Croatia vary in their origin, age, size and economical importance. They are widespread and confirmed at numerous locations in the country.

By type of formation the Croatian bauxites are divided into three groups (Marković, 2002):

1. ***Bauxite deposits including clayey bauxite, bauxitic clays and clays of Triassic, Jurassic and Neogene age.***
   Triassic deposits are found in the Slunj area and Lika (Figure 4). They are considered to have formed by bauxitic processes in situ during emersion between Ladinian and Carnian age, which was related to the beginning of the Alpine orogeny. The parent material was largely clayey (kaolinite) derived by alteration of the Ladinian clasts and pyroclasts, and then deposited in large relief depressions. As a result of long-term subaerial exposure, large deposits of clayey bauxite were formed by ferrallitic weathering of kaolinite producing mainly böhmite and diaspore. These are found in heteropic facies relation with bauxitic and kaoline clays. The origin is inferred from spatial relationship of the bauxite deposits and clastic deposits as well as from similarity of micromineralogy associations of the clastic deposits and the bauxite.
   Jurassic clayey bauxites occur at numerous localities in Istria. They are similar to the Triassic ones by their formation, however, no direct evidence for the origin of the clay material has not been presented yet. Since the Malmian mainland was characterized with a low relief, the material was unlikely to have been transported by rivers from

This activity has received funding from the European Institute of Innovation and Technology (EIT), a body of the European Union, under the Horizon 2020, the EU Framework Programme for Research and Innovation

distant areas but was rather sourced from weathering of the carbonate bedrock. Aeolian contribution has been suspected as a source of the parent material, too(references in Marković, 2002).

Neogene bauxite deposits of this type were similarly formed by in situ ferrallitic processes but from a more diverse source material. Partly this was a material derived by weathering of the carbonate bedrocks, but also from aeolian sediment derived from exposed metamorphic rocks and pyroclastics. The Neogene deposits are found in Karlovac County (Tounj) and Dalmatia (Peruča, Trilj).

Figure 4. Unexploited Triassic bauxite deposit in Rudopolje (Lika); sampling activities within WP2

2. ***"Terra rossa" type of bauxite*** – Lower Paleogene (Istria, Dalmatia and islands) and Upper Paleoegene (Dalmatia).

   Lower Paleogene bauxites were deposited after Laramian movements on paleorelief developed on the Upper Cretaceous limestones. They are preserved close or along the boundary with transgression sediments, so called Kozina deposits.

   Upper Paleogene bauxites were formed during emersion caused by Pyrenean orogenic phase in Middle Eocene, and were accumulated in the paleorelief of Upper Cretaceous and Lower Paleogene limestones, more rarely Kozina deposits. They are overlaid by transgressive Promina sediments, which were deposited during Middle and Upper Eocene as well as Lower Oligocene. Formation of both Lower and Upper Paleogene bauxites has been explained by formation of *terra rossa*-like weathering products due to alteration of carbonate bedrocks and accumulation of insoluble fraction thereof. Some contribution of aeolian material is also possible.

   Some of the sampled bauxite deposits within WP2 activities are presented in Figures 5A to 5E.

This activity has received funding from the European Institute of Innovation and Technology (EIT), a body of the European Union, under the Horizon 2020, the EU Framework Programme for Research and Innovation

Figure 5A. Bauxite deposit in Košute (Dalmatia)

Figure 5B. Bauxite deposit in Gljev (Dalmatia)

Figure 5C. Bauxite deposit in Strmendolac/Crveni klanac (Dalmatia)

This activity has received funding from the European Institute of Innovation and Technology (EIT), a body of the European Union, under the Horizon 2020, the EU Framework Programme for Research and Innovation

Figure 5D. Entrance (left) to the underground bauxite mine (abandoned) in Jukići-Đidare and contact of the hanging wall rock (limestone) with bauxite body within the mine (right).

Figure 5E. Bauxite mine near Rovinj (Istria)

3. ***Mechanically redeposited bauxite deposits***
   These deposits were formed by mechanical redeposition of already existing bauxite deposits. They are usually found within the Promina deposits and are not economically significant.

Economically the most important bauxite deposits exploited so far are those developed at the boundary of Upper Cretaceous limestones and Paleogene deposits as well as those in the contact of Upper Cretaceous/Lower Paleogene limestones with Middle Eocene/Lower Oligocene deposits (Promina). Minor quantities of Triassic (Karlovac County), Jurassic (Istria) and Neogene (Sinj) bauxites have been exploited for the industries other than aluminium production (cements, abrasives, bricks).

Mining of bauxite for aluminium industry in Croatia was continuous from 1914 till 1990. It has been evaluated that roughly 27.5 million tonnes of bauxite had been recovered in this period. After 1990 the bauxite mining gradually ceased, and today only smaller quantities are recovered for cement industry (Vujec, 1996)

This activity has received funding from the European Institute of Innovation and Technology (EIT), a body of the European Union, under the Horizon 2020, the EU Framework Programme for Research and Innovation

The samples collected within the frame of REEBAUX WP2 in Croatia are presented in Table 1 with other related information. Major components determined in the samples are presented in Table 2 whereas REE abundances in Table 3. Distribution of total REE content along drilling core from Mamutovac 1A deposit are presented in Figure 5F.

Table 1. List of bauxite sampling localities, their location, geological age and reserves (where available) for the samples collected in Croatia within REEBAUX WP2 tasks.

Locality	Sample ID	Latitude	Longitude	Age	Exploitation reserves (in tonnes)
Ćosići	COS 1-2	43°27'41.6" N	17°13'20.4" E	Middle Eocene	N/A
	COS 2-1	43°27'32.4" N	17°12'39.5" E		
Gljev	GLJ-1	43°44'17.3" N	16°43'08.6" E	Late Eocene	N/A
	GLJ-2a	43°44'30.8" N	16°43'31.4" E		
	GLJ-2b	43°44'30.8" N	16°43'31.4" E		
	G 7	43°44'13.2" N	16°43'11.6" E	Late Eocene	N/A
	G 9				
	G 12				
Jukići-Đidare	JUK-D	43°54'28.4" N	16°05'54.5" E	Late Eocene	167,650
Imotski	IMOL 8-1	43°31'12.4'' N	17°06'02.0'' E	Late Eocene	N/A
Košute	KŠ-1	43°37'14.2" N	16°41'09.5" E	Neogene	N/A
	KŠ-2	43°37'23.0" N	16°41'20.3" E		
	KS 1	43°37'14.2" N	16°41'09.5" E		
	KS 4	43°37'14.2" N	16°41'09.5" E		
Mamutovac (outcrop)	MAM-1B	43°55'59.5" N	16°00'13.7" E	Late Eocene	112,000
Mamutovac 1A borehole (B1)		43°55'59.4" N	16°00'13.0" E		
B-1 0,70-0,75 m	MAM-1				
B-1 2,70-2,75 m	MAM-2				
B-1 4,65-4,70 m	MAM-3				
B-1 6,25-6,30 m	MAM-4				
B-1 7,60-7,65 m	MAM-5				
B-1 8,90-8,95 m	MAM-6				
B-1 10,40-10,45 m	MAM-7				
B-1 11,50-11,55 m	MAM-8				
B-1 12,60-12,65 m	MAM-9				
B-1 13,75-13,80 m	MAM-10				
B-1 14,15-14,20 m	MAM-11				
B-1 15,25-15,30 m	MAM-12				
B-1 15,70-15,75 m	MAM-13				
B-1 16,30-16,35 m	MAM-14				
B-1 17,40-17,45 m	MAM-15				
B-1 18,50-18,54 m	MAM-16				

This activity has received funding from the European Institute of Innovation and Technology (EIT), a body of the European Union, under the Horizon 2020, the EU Framework Programme for Research and Innovation

Locality	Sample ID	Latitude	Longitude	Age	Exploitation reserves (in tonnes)
B-1 19,30-19,35 m	MAM-17				
B-1 20,15-20,20 m	MAM-18				
B-1 21,70-21,75 m	MAM-19				
B-1 22,30-22,35 m	MAM-20				
B-1 23,25-23,30 m	MAM-21				
B-1 24,10-24,15 m	MAM-22				
B-1 25-25,10 m	MAM-23				
Mamutovo brdo	MB-1	43°31'53.1" N	17°03'20.0" E	Late Eocene	N/A
	MB-2				
	MB-3				
	MB-4				
Mandići	MAND 1	43°28'55.4'' N	17°10'03.0'' E	Late Cretaceous/ Paleogene	N/A
	MAND 2				
	MAND 3				
	MAND 4				
Moseć	MO IS-1	43°47'31.0'' N	16°12'59.6'' E	Late Eocene	N/A
	MO IS-2				
	MO IS-3				
	MO IS-4				
	MO 1				
	MO 2				
	MO 3				
Obrovac	OB 1	44°14'17.9'' N	15°33'00.7'' E	Late Eocene	N/A
	OB 5	44°13'26.0'' N	15°35'43.8'' E		
	OB 10	44°11'36.0'' N	15°39'01.1'' E		
Ričina	RIC 1	43°30'43.0'' N	17°07'25.0'' E	Middle/Late Eocene	N/A
	RIC 2-3				
Rudopolje	RB-1	44°23'50.7" N	15°50'44.6" E	Middle/late Triassic	2,000,000
	RB-2	44°23'46.6" N	15°50'42.3" E		
	RB-3	44°23'37.5" N	15°50'42.3" E		
Strmendolac	SD-1	43°35'16.5" N	16°44'59.2" E	Neogene	N/A
	SD-2	43°35'16.5" N	16°44'59.2" E		
	SD-3	43°35'15.1" N	16°44'58.9" E		
Stari Gaj, Obrovac	SG-Tunel	44°12'39.9" N	15°38'37.2" E	Late Eocene	550,000
	SGT-1	44°12'39.9" N	15°38'37.2" E		
	SGT-2				
Tošići-Dujići	TOS-1-D	43°55'24.8" N	16°04'57.7" E	Late Eocene	14,500
	TOS-1-G	43°55'24.8" N	16°04'57.7" E		
	TOS-1-S	43°55'24.8" N	16°04'57.7" E		
	TOS-2	43°55'25.2" N	16°04'56.9" E		
	TOS-3	43°55'21.0" N	16°04'56.4" E		
	TOS-4	43°55'24.5" N	16°04'55.3" E		

This activity has received funding from the European Institute of Innovation and Technology (EIT), a body of the European Union, under the Horizon 2020, the EU Framework Programme for Research and Innovation

Locality	Sample ID	Latitude	Longitude	Age	Exploitation reserves (in tonnes)
Turban Kosa	TK 1-1	43°27'55.2" N	17°11'58.6" E	Late Cretaceous/ Paleogene	up to 10,000
	TK 2-1				
Vrace	VR-1	44°16'09.1" N	15°48'35.6" E	Middle/late Triassic	200,000
	VR-3				
Šterna	7446	45°24'29.5''N	13°46'57.9''E	Eocene	N/A
Dragozetići	7447	45°05'47.4''N	14°18'10.0''E	Eocene	N/A
	7448				
Karojba	7449	45°17'34.9''N	13°49'33.5''E	Eocene	N/A
	7450	45°17'22.4''N	13°49'48.7''E		
Kaštelir	7451	45°18'35.7''N	13°41'20.2''E	Eocen	N/A
	7452	45°19'19.7''N	13°41'24.4''E		
	7453	45°19'19.7''N	13°41'24.4''E		
	7454	45°19'20.8''N	13°42'54.2''E		
Rovinj1-1	7455	45°06'29.6''N	13°38'45.1''E	Upper Jurassic	2,000,000
	7456	45°06'29.6''N	13°38'45.1''E		
	7457	45°06'29.6''N	13°38'45.1''E		
	7458	45°06'28.3''N	13°38'43.8''E		
	7459	45°06'28.3''N	13°38'43.8''E		
	7460	45°06'28.3''N	13°38'43.8''E		
Minjera	7461	45°23'11.7''N	13°55'23.1''E	Eocene	N/A
Učka	7472	45°15'18.4''N	14°09'33''.6E	Eocene	N/A
	7473	45°15'27.2''N	14°09'12.9''E		

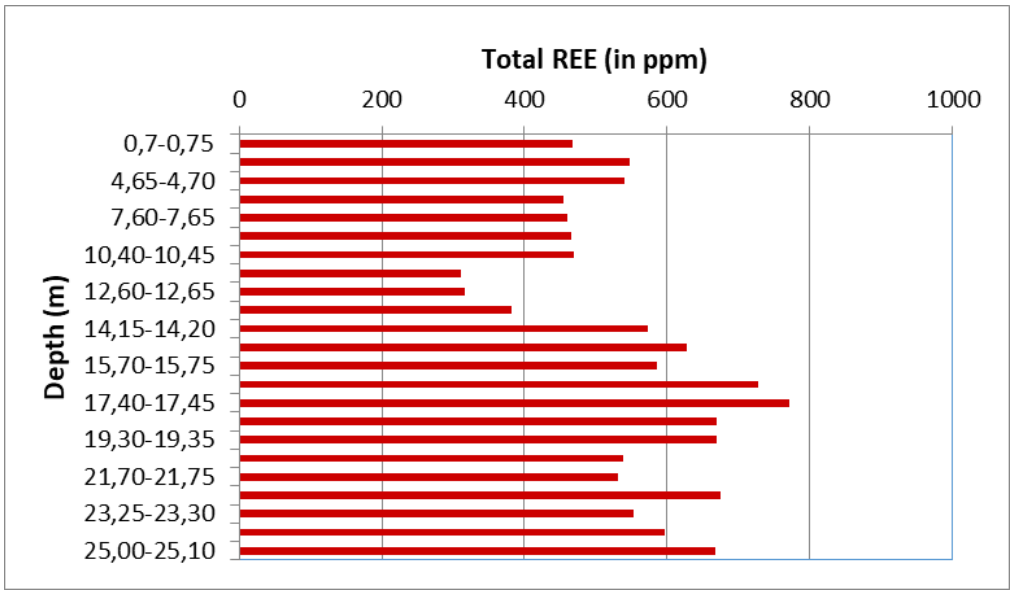

Figure 5F. Distribution of total REE content along drilling core from Mamutovac 1A deposit

This activity has received funding from the European Institute of Innovation and Technology (EIT), a body of the European Union, under the Horizon 2020, the EU Framework Programme for Research and Innovation

Table 2. Major constituents of the bauxite samples collected in Croatia within REEBAUX WP2 tasks.

Locality	Sample ID	SiO_2	Al_2O_3	Fe_2O_3	MgO	CaO	Na_2O	K_2O	TiO_2	P_2O_5	MnO	Cr_2O_3	Ba	Ni	Sc	LOI	Sum
		%	%	%	%	%	%	%	%	%	%	%	ppm	ppm	ppm	%	%
Ćosići	COS 1-2	3.57	49.96	28.64	0.06	0.12	0.01	<0,01	2.46	<0,01	0.01	0.206	13	162	47	14.6	99.67
	COS 2-1	4.92	46.17	17.81	0.17	0.11	0.01	0.03	1.99	0.03	0.72	0.171	61	875	74	27.2	99.5
Gljev	GLJ-1	11.86	44.51	18.55	0.33	0.37	0.04	0.15	2.11	0.68	0.15	0.119	82	790	57	20.4	99.4
	GLJ-2a	3	55.35	17.74	0.14	0.15	<0.01	0.01	2.46	0.43	0.03	0.201	38	553	57	19.9	99.47
	GLJ-2b	2.37	52.99	21.12	0.09	0.12	0.01	0.05	2.05	0.37	0.03	0.182	35	514	60	20.1	99.53
	G 7	2.05	55.76	18.13	0.1	0.14	0.01	0.07	2.67	0.32	0.03	0.241	39	488	59	19.9	99.51
	G 9	2.36	55.24	17.25	0.12	0.22	0.02	0.06	2.43	0.43	0.03	0.188	44	503	54	21.1	99.52
	G 12	6.16	49.18	16.24	0.15	0.34	0.03	0.12	2.57	0.69	0.07	0.081	76	517	46	23.8	99.52
Jukići-Đidare	JUK-D	3.09	49.08	21.23	0.1	0.06	0.01	<0,01	2.41	0.02	1.02	0.135	41	545	63	22.2	99.47
Imotski	IMOL 8-1	1	48.35	17.83	0.17	0.2	0.02	<0.01	2.23	0.27	1.32	0.138	92	913	64	27.8	99.45
Košute	KŠ-1	24.69	38.66	13.38	0.37	0.28	0.05	0.26	1.63	0.11	0.07	0.044	73	334	35	20.1	99.69
	KŠ-2	24.21	38.4	13.98	0.35	0.27	0.04	0.24	1.66	0.11	0.07	0.048	77	333	35	20.2	99.67
	KS 1	23.47	38.69	13.62	0.38	0.32	0.05	0.38	1.55	0.11	0.23	0.043	170	330	35	20.8	99.68
	KS 4	26.92	39.07	9.45	0.43	0.47	0.05	0.35	1.32	0.08	0.08	0.048	79	311	35	21.4	99.71
Mamutovac	MAM-1B	5.28	55.11	20.28	0.17	0.15	0.02	0.02	2.86	0.02	0.17	0.161	28	411	53	15.3	99.55
Mamutovac drilling core 1A (B1)																	
0,70-0,75 m	MAM-1	8.51	50.65	18.25	0.22	0.15	0.07	0.06	2.62	0.04	0.1	0.146	30	322	49	18.7	99.55
2,70-2,75 m	MAM-2	7.86	50.97	18.13	0.25	0.12	0.06	0.05	4.04	0.09	0.09	0.174	36	324	48	17.6	99.47
4,65-4,70 m	MAM-3	7.52	51.16	19.72	0.19	0.11	0.08	0.03	2.93	0.07	0.14	0.142	26	390	50	17.4	99.5
6,25-6,30 m	MAM-4	10.61	48.86	17.45	0.24	0.13	0.07	0.05	2.72	0.06	0.16	0.127	31	379	44	19	99.53
7,60-7,65 m	MAM-5	15.03	45.83	16.29	0.29	0.17	0.08	0.06	2.53	0.05	0.11	0.117	36	390	41	18.9	99.53
8,90-8,95 m	MAM-6	6.19	52.69	19.28	0.16	0.1	<0,01	0.02	2.74	0.04	0.12	0.147	22	357	49	18	99.53
10,40-10,45 m	MAM-7	10.26	49.89	17.37	0.24	0.13	0.03	0.05	2.44	0.04	0.11	0.144	27	382	42	18.8	99.55
11,50-11,55 m	MAM-8	18.02	43.66	16	0.35	0.19	0.04	0.09	1.62	0.03	0.07	0.138	35	444	40	19.3	99.58
12,60-12,65 m	MAM-9	19.88	42.3	16.12	0.4	0.2	0.05	0.12	1.33	0.03	0.05	0.147	35	480	43	18.9	99.6

This activity has received funding from the European Institute of Innovation and Technology (EIT), a body of the European Union, under the Horizon 2020, the EU Framework Programme for Research and Innovation

Locality	Sample ID	SiO_2	Al_2O_3	Fe_2O_3	MgO	CaO	Na_2O	K_2O	TiO_2	P_2O_5	MnO	Cr_2O_3	Ba	Ni	Sc	LOI	Sum
		%	%	%	%	%	%	%	%	%	%	%	ppm	ppm	ppm	%	%
13,75-13,80 m	MAM-10	18.49	43.46	17.04	0.38	0.2	0.06	0.11	1.36	0.03	0.1	0.168	36	550	51	18.1	99.56
14,15-14,20 m	MAM-11	5.69	54.19	20.07	0.21	0.09	0.04	0.06	2.81	0.03	0.12	0.173	31	464	57	16	99.53
15,25-15,30 m	MAM-12	6.37	52.99	20.85	0.22	0.09	0.06	0.09	2.45	0.04	0.16	0.184	37	511	57	15.9	99.5
15,70-15,75 m	MAM-13	16.41	45.28	17.37	0.42	0.19	0.07	0.12	1.56	0.07	0.14	0.127	48	580	44	17.7	99.54
16,30-16,35 m	MAM-14	17.03	45.32	16.1	0.44	0.19	0.05	0.12	1.63	0.08	0.14	0.107	42	584	39	18.3	99.55
17,40-17,45 m	MAM-15	15	44.6	16.57	0.43	0.18	0.06	0.11	2.78	0.07	0.4	0.123	54	592	41	19.1	99.46
18,50-18,54 m	MAM-16	16.34	44.07	16.57	0.47	0.19	0.06	0.12	2.75	0.08	0.22	0.12	47	560	42	18.4	99.48
19,30-19,35 m	MAM-17	17.6	41.92	15.68	0.73	0.21	0.11	0.13	4.71	0.15	0.21	0.108	65	419	41	17.7	99.34
MAM B-1 20,15-20,20 m	MAM-18	15.97	43.71	16.78	0.57	0.19	0.08	0.1	3.95	0.13	0.23	0.106	46	415	42	17.5	99.39
21,70-21,75 m	MAM-19	18.67	41.9	15.46	0.72	0.23	0.13	0.14	3.84	0.13	0.25	0.101	64	429	39	17.8	99.42
22,30-22,35 m	MAM-20	19.68	41.08	14.4	0.73	0.24	0.13	0.16	3.93	0.13	0.78	0.088	82	588	39	17.9	99.38
23,25-23,30 m	MAM-21	17.99	43.94	14.66	0.47	0.22	0.09	0.12	1.95	0.05	0.81	0.101	55	571	40	19	99.5
24,10-24,15 m	MAM-22	17.84	43.21	14.91	0.49	0.23	0.09	0.12	2.04	0.06	1.28	0.099	72	780	42	19	99.46
25-25,10 m	MAM-23	19.2	42.39	14.11	0.64	0.24	0.1	0.16	3.06	0.1	0.91	0.086	70	591	40	18.3	99.43
Mamutovo brdo	MB-1	0.93	46.69	24.11	0.07	0.12	<0,01	<0,01	2.97	0.1	0.28	0.213	30	607	81	23.9	99.45
	MB-2	1.41	48.89	22.73	0.07	0.15	0.01	0.07	2.25	0.08	0.19	0.176	38	410	71	23.5	99.58
	MB-3	3.63	47.09	21.09	0.13	0.48	0.02	0.1	2.37	0.09	0.22	0.155	46	436	73	24.1	99.52
	MB-4	3.72	47.73	21.66	0.11	0.17	0.02	0.03	2.29	0.05	0.16	0.14	37	428	57	23.4	99.54
Mandići	MAND 1	5.45	45.38	19.68	0.13	0.13	0.02	0.03	1.81	0.06	0.29	0.122	40	738	75	26.4	99.56
	MAND 2	4.59	46.19	18.55	0.13	0.12	0.01	0.01	1.94	0.05	0.83	0.129	55	1125	73	26.8	99.51
	MAND 3	2	26.4	9.91	0.27	23.08	0.01	<0,01	1.29	0.04	2.14	0.096	252	653	55	34.3	99.69
	MAND 4	3.9	29.57	12.91	0.16	18.86	0.02	0.01	1.39	0.09	0.56	0.091	101	415	45	32	99.66
Moseć	MO IS-1	11.12	43.92	20.28	0.43	0.2	0.06	0.38	2.58	0.02	0.95	0.186	116	702	55	19.3	99.56
	MO IS-2	17.3	42.27	17.56	0.47	0.22	0.08	0.45	2.28	0.01	0.28	0.149	108	545	46	18.5	99.67
	MO IS-3	8.52	45.07	20.55	0.45	0.14	0.05	0.35	2	<0,01	3.26	0.107	341	1025	60	18.8	99.53
	MO IS-4	9.17	41.69	21.05	0.51	0.21	0.06	0.36	2.03	<0,01	4.72	0.171	708	794	52	19.4	99.52

This activity has received funding from the European Institute of Innovation and Technology (EIT), a body of the European Union, under the Horizon 2020, the EU Framework Programme for Research and Innovation

Locality	Sample ID	SiO_2	Al_2O_3	Fe_2O_3	MgO	CaO	Na_2O	K_2O	TiO_2	P_2O_5	MnO	Cr_2O_3	Ba	Ni	Sc	LOI	Sum
		%	%	%	%	%	%	%	%	%	%	%	ppm	ppm	ppm	%	%
	MO 1	10.11	47.58	20.23	0.38	0.12	0.03	0.08	2.07	0.03	0.29	0.14	29	731	53	18.5	99.65
	MO 2	14.72	44.43	20.12	0.56	0.25	0.03	0.07	1.82	0.01	0.17	0.141	26	687	51	17.3	99.69
	MO 3	17.48	43.87	17.97	0.49	0.23	0.07	0.36	1.75	<0,01	0.14	0.148	71	714	51	17.1	99.68
Obrovac	OB 1	3.89	48.02	19.32	0.07	0.15	0.01	<0,01	2.09	0.08	0.07	0.17	31	298	63	25.6	99.57
	OB 5	7.48	50.19	14.99	0.13	0.19	0.02	0.03	2.76	0.11	0.06	0.164	30	316	53	23.4	99.52
	OB 10	6.96	49.64	16.73	0.11	0.19	0.01	0.01	2.21	0.09	0.09	0.168	30	344	63	23.3	99.55
Ričina	RIC 1	1.67	45.67	22.7	0.05	0.13	<0,01	<0,01	1.96	0.04	0.08	0.144	30	528	53	27	99.56
	RIC 2-3	2.8	47.65	21.06	0.09	0.14	0.02	0.03	2.37	0.03	0.15	0.146	33	373	64	24.9	99.44
Rudopolje	RB-1	8.82	64.05	10.81	0.09	0.09	0.05	0.18	2.13	0.02	<0.01	0.019	24	38	33	13.5	99.74
	RB-2	16.69	50.75	18	0.06	0.05	0.04	0.04	1.51	<0.01	0.02	0.015	18	49	37	12.6	99.79
	RB-3	10.46	57.13	16.74	0.16	0.06	0.04	0.06	1.75	0.01	0.19	0.012	29	77	42	13.1	99.73
Strmendolac	SD-1	1.71	47.4	23.23	0.08	0.18	<0.01	0.02	2.54	0.11	0.72	0.107	205	610	58	23.3	99.51
	SD-2	1.11	51.94	19.17	0.05	0.93	<0.01	<0.01	2.26	0.03	0.07	0.096	37	332	49	24	99.65
	SD-3	4.75	50.21	17.19	0.08	0.17	<0.01	0.02	2.08	0.07	0.07	0.134	33	278	53	24.8	99.62
Stari Gaj, Obrovac	SG-Tunel	20.04	40.01	15.54	0.24	0.21	0.04	0.14	2.03	0.1	0.08	0.088	61	237	31	21.1	99.69
	SGT-1	16.82	42.28	16.08	0.19	0.27	0.03	0.19	1.34	0.15	0.04	0.078	68	271	63	22.2	99.69
	SGT-2	25.96	37.25	11.87	0.39	0.98	0.06	0.29	1.64	0.14	0.2	0.048	91	300	36	20.8	99.66
Tošići-Dujići	TOS-1-D	2.21	47.12	19.05	0.12	0.32	0.02	0.01	2.3	0.2	0.9	0.112	56	397	67	27	99.44
	TOS-1-G	8.98	47.34	12.57	0.2	0.46	0.02	0.08	2.38	0.25	0.72	0.153	161	704	55	26.1	99.32
	TOS-1-S	4.14	46.43	19.65	0.13	0.33	0.02	0.03	2.22	0.22	0.3	0.125	47	393	69	25.8	99.42
	TOS-2	2.49	46.82	19.97	0.12	0.95	0.02	0.05	2.1	0.39	0.12	0.133	43	479	75	25.9	99.1
	TOS-3	6.78	33.79	35.08	0.15	0.28	0.04	0.32	1.54	0.42	0.09	0.092	80	564	67	20.6	99.2
	TOS-4	14.2	41.05	17.83	0.32	0.37	0.04	0.16	2.05	0.15	0.12	0.165	55	554	61	22.9	99.45
Turban Kosa	TK 1-1	3.81	47.23	31.42	0.09	0.1	0.02	0.05	3.14	0.02	0.08	0.164	21	270	67	13.5	99.62
	TK 2-1	3.75	45.68	19.91	0.16	0.11	0.01	0.02	1.91	0.04	0.1	0.179	36	536	76	27.6	99.58
Vrace	VR-1	12.69	51.59	20.1	0.28	0.11	0.09	0.52	1.95	0.09	0.11	0.012	145	90	40	12.1	99.66
	VR-3	21.04	46.87	16.26	0.19	0.08	0.04	0.17	1.78	0.03	0.16	0.011	61	60	36	13.1	99.77

This activity has received funding from the European Institute of Innovation and Technology (EIT), a body of the European Union, under the Horizon 2020, the EU Framework Programme for Research and Innovation

Locality	Sample ID	SiO_2	Al_2O_3	Fe_2O_3	MgO	CaO	Na_2O	K_2O	TiO_2	P_2O_5	MnO	Cr_2O_3	Ba	Ni	Sc	LOI	Sum
		%	%	%	%	%	%	%	%	%	%	%	ppm	ppm	ppm	%	%
Šterna	7446	17.41	42.51	20.67	0.15	0.23	0.05	0.11	1.96	0.09	0.13	0.07	32	192.1		15.5	98.88
Dragozetići	7447	7.93	56.38	18.89	0.21	0.12	0.07	0.08	2.68	0.04	0.15	0.07	21	176.6		12.8	99.42
	7448	6.64	59.57	15.4	0.16	0.09	0.03	0.06	3.32	0.05	0.03	0.08	22	108.7		13.5	98.93
Karojba	7449	1.91	56.52	23.94	0.13	0.05	0.03	0.05	3.15	0.05	0.14	0.05	65	139.2		12.2	98.22
	7450	1.95	54.36	26.75	0.12	0.06	0.04	0.04	3.22	0.05	0.1	0.06	35	103.2		12.4	99.15
Kaštelir	7451	12.18	50.38	16.03	0.21	0.16	0.13	0.21	2.45	0.16	0.03	0.06	85	81.3		17	99
	7452	4.13	49.4	30.41	0.16	0.12	0.04	0.13	2.91	0.09	0.16	0.05	36	133.2		11.3	98.9
	7453	10.3	37.94	31.8	0.22	0.16	0.06	0.17	2.26	0.15	0.05	0.07	45	98.3		15.9	99.08
	7454	1.98	44.78	37.37	0.09	0.08	0.04	0.03	2.72	0.05	0.1	0.08	20	91		12.1	99.42
Rovinj	7455	14.24	49.69	19.86	0.65	0.2	0.07	0.38	2.36	0.04	0.23	0.03	65	39.8		11.6	99.35
	7456	18.21	60.03	1.78	0.83	0.25	0.07	0.47	2.79	0.03	0.08	0.09	112	37.9		14.2	98.83
	7457	14.48	47.99	21.68	0.68	0.23	0.09	0.31	2.17	0.04	0.19	0.03	54	43.8		11.5	99.39
	7458	14.36	48.03	21.85	0.69	0.32	0.07	0.28	2.06	0.04	0.18	0.03	45	40.2		11.6	99.51
	7459	16.77	47.01	19.61	0.69	0.2	0.07	0.32	1.94	0.04	0.16	0.03	46	37.8		11.6	98.44
	7460	29.23	34.25	10.18	2.5	0.92	0.09	1.3	1.43	0.04	0.03	0.03	75	272.7		16.6	96.6
Minjera	7461	1.79	49.84	19.95	0.11	0.24	0.08	0.01	3.21	0.07	0.03	0.06	13	79.8		24.1	99.49
Učka	7472	10.56	40.17	25.85	0.19	0.31	0.1	0.14	1.98	0.1	0.05	0.11	43	210.9		18.9	98.46
	7473	5.27	48.08	27.87	0.12	0.16	0.04	0.04	2.93	0.08	0.03	0.13	25	98.5		14.6	99.35

Table 3. REE abundances (in ppm) in bauxite samples collected in Croatia within REEBAUX WP2 tasks.

Locality	Sample ID	Y	La	Ce	Pr	Nd	Sm	Eu	Gd	Tb	Dy	Ho	Er	Tm	Yb	Lu	ΣLREE	ΣHREE	ΣREE
Ćosići	COS 1-2	53.4	69.9	134.6	15.26	55.5	10.94	2.36	9.71	1.66	10.32	2.13	6.51	0.98	6.37	1.01	288.56	92.09	380.65
	COS 2-1	248.5	221	321	45.32	181.1	39.36	9.8	45.22	7.42	45.14	9.63	26.87	3.54	21.52	3.3	817.58	411.14	1228.72
Gljev	GLJ-1	565.7	341.1	303.8	54.06	226	44.93	11.56	60.14	9.65	63.89	15.19	45.78	6.23	37.2	5.73	981.45	809.51	1790.96
	GLJ-2a	343.1	253.1	461.4	51.69	224.8	51.38	12.69	57.45	8.67	51.74	11	31.95	4.36	26.56	4.09	1055.06	538.92	1593.98
	GLJ-2b	268.9	229.8	267.8	42.96	175.3	36.23	8.8	41.92	6.42	39.59	8.68	25.55	3.43	20.15	3.02	760.89	417.66	1178.55

This activity has received funding from the European Institute of Innovation and Technology (EIT), a body of the European Union, under the Horizon 2020, the EU Framework Programme for Research and Innovation

Locality	Sample ID	Y	La	Ce	Pr	Nd	Sm	Eu	Gd	Tb	Dy	Ho	Er	Tm	Yb	Lu	ΣLREE	ΣHREE	ΣREE
	G 7	214.1	239	337.3	46.57	187.8	37.44	8.39	36.83	5.6	34.77	7.42	22.42	3	18.46	2.8	856.5	345.4	1201.9
	G 9	252.6	243.7	311.8	48.43	203.2	40.87	9.22	41.53	6.02	35.69	7.55	21.4	2.87	17.16	2.67	857.22	387.49	1244.71
	G 12	250.7	232.5	307.5	41.89	160.9	30.5	7.2	34.08	4.97	29.74	6.35	18.22	2.44	14.67	2.29	780.49	363.46	1143.95
Jukići-Đidare	JUK-D	169.1	195.7	335.4	37.14	152.1	29.18	6.44	21.46	3.9	24.82	5.38	16.33	2.44	16.87	2.55	755.96	262.85	1018.81
Imotski	IMOL 8-1	87.5	123.3	374.5	25.32	98.9	19.26	4.48	20.87	2.98	17.16	3.38	9.72	1.43	9.31	1.46	645.76	153.81	799.57
Košute	KŠ-1	49.9	118.4	195.5	20.3	71	13.6	2.72	11.12	1.81	10.9	2.21	6.48	1	7.19	1.01	421.52	91.62	513.14
	KŠ-2	52.3	122	188.9	21.18	74.7	14.17	2.79	11.58	1.91	11.42	2.31	7.05	1.05	7.31	1.07	423.74	96	519.74
	KS 1	42.3	88.8	173.3	18.37	66.4	12.54	2.47	10.42	1.59	9.39	1.85	5.42	0.85	5.63	0.85	361.88	78.3	440.18
	KS 4	82.2	115.5	187.4	31.46	121.7	24.71	5	20.89	3.27	18.95	3.64	10.82	1.57	10.46	1.68	485.77	153.48	639.25
Mamutovac (MAM)	MAM-1B	65.9	87	204.2	19.9	74	15.49	3.3	13.42	2.12	12.34	2.54	7.61	1.12	7.55	1.17	403.89	113.77	517.66
Mamutovac drilling core 1A (B1)																			
0,70-0,75 m	MAM-1	54.5	84.7	207.8	15.4	56.5	10.61	2.24	9.42	1.5	9.32	1.96	6.06	0.93	6.35	0.97	377.25	91.01	468.26
2,70-2,75 m	MAM-2	72.3	102.2	224.5	18.3	66.7	12.9	2.71	11.45	1.97	12.87	2.67	8.13	1.29	8.62	1.33	427.31	120.63	547.94
4,65-4,70 m	MAM-3	68.4	84.4	245	15.5	58.7	13.54	2.96	11.93	2.07	13.28	2.75	8.85	1.35	9.37	1.43	420.1	119.43	539.53
6,25-6,30 m	MAM-4	58.6	77.9	193.5	14.55	55.2	11.63	2.55	9.78	1.71	10.53	2.27	6.98	1.14	7.82	1.14	355.33	99.97	455.3
7,60-7,65 m	MAM-5	53.3	74.3	211.6	14.75	54	11.18	2.36	9.17	1.57	9.8	2	6.55	1.02	7.36	1.11	368.19	91.88	460.07
8,90-8,95 m	MAM-6	60.6	75.5	200.1	14.28	55.3	12.71	2.8	10.78	1.86	11.43	2.38	7.29	1.2	7.76	1.22	360.69	104.52	465.21
10,40-10,45 m	MAM-7	48.4	61.5	253.6	12.09	46.2	9.91	2.15	8.68	1.47	9.33	1.96	6.24	0.99	6.6	1.04	385.45	84.71	470.16
11,50-11,55 m	MAM-8	35.5	50	149.3	9.41	33.8	7.02	1.5	6.07	1.02	6.26	1.36	4.4	0.67	4.81	0.72	251.03	60.81	311.84
12,60-12,65 m	MAM-9	33.2	46.6	163.8	8.95	32.2	6.29	1.38	5.76	0.96	5.93	1.27	4.27	0.65	4.39	0.68	259.22	57.11	316.33
13,75-13,80 m	MAM-10	38.1	51	203.2	10.39	38.9	8.54	1.92	7.08	1.25	7.67	1.62	5.19	0.86	6.04	0.92	313.95	68.73	382.68
14,15-14,20 m	MAM-11	62.5	85.3	264.9	17.52	66.2	15.69	3.54	12.97	2.42	14.97	2.87	9.44	1.58	10.99	1.71	453.15	119.45	572.6
15,25-15,30 m	MAM-12	78.4	102	190.7	25.72	104.8	28.48	6.74	25.31	4.46	25.53	4.76	13.64	2.04	13.05	1.99	458.44	169.18	627.62
15,70-15,75 m	MAM-13	65	120.7	156.1	26.64	102.9	26.06	6.29	23.88	4.21	23.48	4.29	11.85	1.7	10.66	1.59	438.69	146.66	585.35
16,30-16,35 m	MAM-14	70.3	176.8	180.9	42.06	153	27.49	6.05	23.98	3.55	19.34	3.51	9.64	1.29	8.01	1.17	586.3	140.79	727.09
17,40-17,45 m	MAM-15	101.6	147.8	296.7	30.22	110.4	18.85	4.12	19.33	2.7	15.8	3.32	9.73	1.34	8.61	1.33	608.09	163.76	771.85
18,50-18,54 m	MAM-16	99.6	145.4	183.7	30.31	114.8	21.51	4.89	22.11	3.21	18.36	3.73	10.97	1.42	8.69	1.36	500.61	169.45	670.06
19,30-19,35 m	MAM-17	98.4	161.8	206.7	27.31	96.4	15.97	3.32	15.26	2.44	15.32	3.34	9.98	1.46	9.91	1.53	511.5	157.64	669.14
20,15-20,20 m	MAM-18	85.4	123.9	152.7	23.35	83.6	14.49	2.95	13.38	2.19	13.74	2.96	9.07	1.32	8.6	1.39	400.99	138.05	539.04
21,70-21,75 m	MAM-19	76.8	114.4	178.4	21.71	75.8	13.08	2.66	11.69	1.92	12.5	2.63	8.11	1.23	8.13	1.24	406.05	124.25	530.3
22,30-22,35 m	MAM-20	79	115.2	301.7	23.41	85.3	14.78	3.1	13.33	2.17	13.49	2.93	8.67	1.28	8.72	1.32	543.49	130.91	674.4
23,25-23,30 m	MAM-21	63	87.4	254.3	18.08	67.2	13.19	3.02	12.67	2.02	11.97	2.44	7.61	1.09	7.29	1.11	443.19	109.2	552.39

This activity has received funding from the European Institute of Innovation and Technology (EIT), a body of the European Union, under the Horizon 2020, the EU Framework Programme for Research and Innovation

Locality	Sample ID	Y	La	Ce	Pr	Nd	Sm	Eu	Gd	Tb	Dy	Ho	Er	Tm	Yb	Lu	ΣLREE	ΣHREE	ΣREE
24,10-24,15 m	MAM-22	73	96.2	247.1	21.28	80.5	17.43	3.75	15.23	2.55	15.34	3.13	9.37	1.38	9.12	1.38	466.26	130.5	596.76
25-25,10 m	MAM-23	83.3	109.6	285.7	23.72	86.9	16.98	3.61	15.37	2.52	15.09	3.16	9.44	1.42	9.32	1.43	526.51	141.05	667.56
Mamutovo brdo	MB-1	138.4	132.3	580.5	33.84	142.5	30.21	7.27	36.86	5.35	29.88	5.8	16.13	2.38	15.92	2.46	926.62	253.18	1179.8
	MB-2	98.6	104.6	295.5	25	105.7	23.74	5.82	26.95	4.01	22.5	4.32	12.3	1.83	12.42	1.99	560.36	184.92	745.28
	MB-3	123.9	128.2	453.5	34.3	150.8	34.87	8.29	36.47	5.22	27.23	5.12	14.93	2.17	14.63	2.38	809.96	232.05	1042.01
	MB-4	141.7	165.8	251.1	28.5	104.1	20.88	4.66	21.06	3.49	22.04	4.74	14.76	2.11	13.53	2.09	575.04	225.52	800.56
Mandići	MAND 1	116.1	92.4	226.7	24.85	105.8	28.28	6.95	27.22	4.99	30.73	6.23	19	3.06	20.64	3.11	484.98	231.08	716.06
	MAND 2	156.1	109.6	443.7	32.29	135.8	37.71	9.65	41.41	7.75	48.56	10.04	30.71	4.31	26.72	4.22	768.75	329.82	1098.57
	MAND 3	103.4	73.9	208.9	20.9	83.3	19.66	4.79	20.74	3.42	20.96	4.42	13.25	1.98	13.08	1.92	411.45	183.17	594.62
	MAND 4	141.8	121.3	179.8	20.57	81.7	17.13	4.35	20.74	3.4	21.12	4.57	13.59	1.85	11.77	1.78	424.85	220.62	645.47
Moseć	MO IS-1	179.6	103.5	273.2	30.46	123.8	26	5.91	27.45	4.14	24.35	5.06	15.27	2.06	12.45	1.95	562.87	272.33	835.2
	MO IS-2	60.6	58.6	142.5	11.86	43.6	7.89	1.65	7.45	1.3	8.7	2.03	6.46	0.95	6.29	1.05	266.1	94.83	360.93
	MO IS-3	102.3	110.5	299.4	26.33	98.6	21.55	4.99	20.76	3.39	19.92	4.09	11.89	1.65	10.73	1.59	561.37	176.32	737.69
	MO IS-4	128.9	151.2	287.4	30.41	113.5	22.29	4.91	22.46	3.43	19.56	4.01	11.49	1.52	9.5	1.51	609.71	202.38	812.09
	MO 1	99.6	81.6	132.9	21.63	84.1	18.47	4.15	17.45	2.76	16.28	3.41	10.17	1.45	9.37	1.44	342.85	161.93	504.78
	MO 2	82.6	54.9	104.8	14.21	56	13.63	3.21	13.27	2.28	14.1	2.89	8.95	1.3	8.45	1.36	246.75	135.2	381.95
	MO 3	84.6	57.4	132.4	14.94	60.2	15.61	3.55	14.69	2.64	16.17	3.37	10.24	1.52	9.94	1.54	284.1	144.71	428.81
Obrovac	OB 1	59.2	70.5	234.8	13.93	53	12.5	2.88	11.52	2.08	13	2.61	8.24	1.37	10	1.51	387.61	109.53	497.14
	OB 5	136.8	141	314.6	37.41	147.7	30.69	6.79	27.44	4.24	25.12	5.03	14.79	2.07	13.1	2.01	678.19	230.6	908.79
	OB 10	142.5	158.2	313.9	39.47	151	30.06	6.53	27.27	4.29	25.33	5.14	15.69	2.17	13.65	2.1	699.16	238.14	937.3
Ričina	RIC 1	66.5	91.8	220.2	18.56	69.2	14	3.14	13.78	2.13	13.02	2.76	8.2	1.21	8.4	1.3	416.9	117.3	534.2
	RIC 2-3	194.4	207.9	365.2	44.96	179.9	36.16	8.71	41.93	6.12	35.12	6.84	18.18	2.46	15.14	2.3	842.83	322.49	1165.32
Rudopolje	RB-1	79.3	45.5	184.6	12.87	48.6	10.25	1.96	10.08	1.83	12.29	2.74	8.72	1.33	9.04	1.43	303.78	126.76	430.54
	RB-2	79.3	27.1	226.3	8.89	36.4	9.25	1.75	9.71	1.79	11.68	2.57	8.1	1.24	8.42	1.27	309.69	124.08	433.77
	RB-3	188.2	141.5	270.4	27.39	101.4	20.29	3.87	21.85	3.75	23.88	5.47	17.09	2.52	16.07	2.49	564.85	281.32	846.17
Strmendolac	SD-1	34.2	112	266.4	15.52	49.7	9.24	1.79	6.67	1.09	6.79	1.33	4.22	0.64	4.62	0.67	454.65	60.23	514.88
	SD-2	115.4	158.5	212.8	36.28	137.3	26.91	5.62	24.13	3.61	20.1	3.94	11.24	1.59	10.32	1.5	577.41	191.83	769.24
	SD-3	34.5	68.2	228.3	11.71	41.5	7.41	1.39	5.98	0.97	6.08	1.29	4.08	0.64	4.43	0.65	358.51	58.62	417.13
Stari Gaj, Obrovac	SG-Tunel	59.1	93.7	409.1	19.51	71.2	18.47	3.93	13.75	2.52	15.19	2.86	9.02	1.54	11.48	1.65	615.91	117.11	733.02
	SGT-1	46.1	61.7	178.9	13.25	49.2	11.1	2.53	9.77	1.7	10.24	2.12	6.56	1.11	7.59	1.21	316.68	86.4	403.08
	SGT-2	53.10	77.40	322.90	16.79	63.50	14.10	3.15	12.43	2.12	12.07	2.49	7.47	1.23	8.53	1.30	497.84	100.74	598.58
Tošići-Dujići	TOS-1-D	127.3	197.4	364.4	32.98	118	24.13	5.51	22.73	3.88	23.61	4.95	15.12	2.27	14.64	2.25	742.42	216.75	959.17
	TOS-1-G	353.9	228.7	368.5	45.57	203.3	49.54	11.85	55.66	7.99	46.27	9.87	28.2	3.73	22.74	3.38	907.46	531.74	1439.2

This activity has received funding from the European Institute of Innovation and Technology (EIT), a body of the European Union, under the Horizon 2020, the EU Framework Programme for Research and Innovation

Locality	Sample ID	Y	La	Ce	Pr	Nd	Sm	Eu	Gd	Tb	Dy	Ho	Er	Tm	Yb	Lu	ΣLREE	ΣHREE	ΣREE
	TOS-1-S	179.1	214	361.4	38.94	144.3	27.75	6.67	28.7	4.67	29.5	6.07	18.33	2.67	17.51	2.62	793.06	289.17	1082.23
	TOS-2	1346	465.2	347.8	113.06	523.6	109.69	29.42	182.12	24.92	149.25	35.82	95.43	10.7	54.64	8.1	1588.77	1907.08	3495.85
	TOS-3	1328	158.5	253.4	37.81	199.3	59.83	15.69	82.03	11.6	70.48	17.08	52.9	6.8	38.69	6.15	724.53	1613.73	2338.26
	TOS-4	408.1	191.7	283.4	36.84	148.9	37.25	9.61	48.79	7.86	49.31	10.98	32.17	4.41	26.43	4	707.7	592.05	1299.75
Turban Kosa	TK 1-1	61.5	69.2	145.4	16.04	61.6	13.48	2.99	12.46	2.11	12.97	2.73	8.45	1.21	8.01	1.27	308.71	110.71	419.42
	TK 2-1	125.9	124.3	317.8	23.22	89.5	20.63	5.17	22.63	4.09	26.18	5.53	16.04	2.31	14.95	2.25	580.62	219.88	800.5
Vrace	VR-1	69.9	159.8	379.7	37.13	141.3	23.03	3.86	16.3	2.43	13.57	2.66	8.01	1.13	8.03	1.22	744.82	123.25	868.07
	VR-3	63.1	82	176.7	17.67	61.4	12.15	2.47	12.51	2.1	12.58	2.68	8.26	1.26	8.48	1.33	352.39	112.3	464.69
Šterna	7446	53	78.6	297.1	17.94	64.6	12.75	2.75	11.56	1.86	10.63	2.07	6.05	0.9	5.74	0.85	473.74	92.66	566.4
Dragozetići	7447	54	85.2	635.4	12.2	39.9	7.24	1.57	8.13	1.3	8.55	1.96	6.37	1.04	6.91	1.08	781.51	89.34	870.85
	7448	79.4	114.9	231.2	19.27	65.8	12.61	2.74	11.95	2.15	14.8	3.25	9.88	1.51	10.06	1.53	446.52	134.53	581.05
Karojba	7449	62.8	107.4	132.5	17.34	58.2	9.6	1.95	8.62	1.49	9.78	2.23	6.97	1.12	7.48	1.16	326.99	101.65	428.64
	7450	64.2	109	134.8	17.5	58.4	10.04	2.05	8.73	1.62	10.86	2.31	7.75	1.14	7.7	1.23	331.79	105.54	437.33
Kaštelir	7451	49.3	174.2	221.9	17.91	45.8	6.99	1.46	6.57	1.23	8.71	1.99	6.46	1.05	7.02	1.08	468.26	83.41	551.67
	7452	53.4	102.9	144.4	16.35	52.1	8.86	1.91	8.14	1.42	9.16	2.01	6.23	0.99	6.42	1.01	326.52	88.78	415.3
	7453	66.2	69.1	139.7	14.07	51	10.54	2.31	9.89	1.8	11.87	2.54	7.52	1.15	7.65	1.15	286.72	109.77	396.49
	7454	48.1	88	100.1	13.74	43.6	7.26	1.49	6.57	1.17	7.67	1.73	5.3	0.84	5.75	0.9	254.19	78.03	332.22
Rovinj	7455	81.1	106.5	590.9	21.76	74.6	14.41	2.97	14.14	2.43	15.38	3.18	9.67	1.37	8.99	1.37	811.14	137.63	948.77
	7456	94.2	163.2	289.5	40.95	152.9	26.14	4.95	21.82	2.83	15.85	3.14	8.95	1.36	9.16	1.41	677.64	158.72	836.36
	7457	111.7	254.1	499.9	62.24	234.3	40.46	7.68	32.81	4.03	20.38	3.71	10.27	1.44	9.09	1.4	1098.68	194.83	1293.51
	7458	89.2	148	322.6	36.74	135.2	25.64	5.11	21.61	3.18	17.41	3.31	9.88	1.41	9.17	1.39	673.29	156.56	829.85
	7459	77.2	160.7	283.1	35.47	126.6	22.11	4.36	17.73	2.64	15.32	2.98	8.93	1.33	8.53	1.3	632.34	135.96	768.3
	7460	47.4	83.8	211.9	24.07	87.6	15.59	2.85	10.54	1.57	8.76	1.79	5.36	0.82	5.51	0.84	425.81	82.59	508.4
Minjera	7461	61.5	128.3	238.7	18.87	49.1	5.61	1.15	5.03	1.16	9.55	2.44	8.38	1.31	8.74	1.32	441.73	99.43	541.16
Učka	7472	74.7	93.5	163.7	17.5	60.7	11.49	2.71	11.72	1.95	12.41	2.56	7.39	1.1	6.87	1.07	349.6	119.77	469.37
	7473	69.1	102	250.3	17.05	53.9	9.14	2.05	9.13	1.68	11.68	2.66	8.99	1.39	9.35	1.43	434.44	115.41	549.85

This activity has received funding from the European Institute of Innovation and Technology (EIT), a body of the European Union, under the Horizon 2020, the EU Framework Programme for Research and Innovation

2.3.2. Bauxite deposits in Hungary and REE potential

Hungary's Transdanubian Range is well known for its Cretaceous-Tertiary bauxites. They all belong to the group of karst bauxites (overlying karstified carbonate rocks) and occur at major regional unconformities of Albian, Turonian/Senonian, early Eocene and Oligocene age. Additionally there is a fifth (mid-Miocene) likewise subaerial unconformity characterized by kaolinitic red soils and redeposited bauxite-pebbles, however, no real economy-grade deposits are associated with this youngest horizon. There are also some early Cretaceous (Berriasian) bauxite indications in South Hungary in the Villány hills. Their REE concentration is slightly higher than that of all the other Hungarian occurrences, however, they have never been exploited on the large scale and were not processed to alumina either.

1. ***Transdanubian Range (TR)***

   Lithofacies and micromineralogy of the three bauxite horizons are different. Albian and Senonian bauxites, though both displaying distinct oolitic-pisolitic textures are different in terms of porosity (Albian: 6%, Senonian: 25 to 28 %, Eocene: 33 to 43 %). Eocene bauxites are either pelitomorphic or intraclastic to gravelly with pseudo-ooids only. Their micromineralogy substantially changes with time (Mindszenty et al, 1991). In the scarce (0.01%) acid-insoluble residue of Albian bauxites titanite, amphibole, kyanite and some calc-alkaline igneous rock-fragments were detected, whereas in the Senonian ones only the ultrastables (zircon, rutile, tourmaline), some calc-alkaline igneous and very few anchimetamorphic rock-fragments could be identified. Eocene bauxites are an order of magnitude richer in detrital minerals, in addition to the ultrastables they abound in higher metamorphic minerals and rock fragments (garnet, staurolite, sillimanite, kyanite), euhedral volcanogenic zircon and ilmenite grains and even some volcanic rock fragments of trachytic texture were identified in them. Zircon grains were fission-track dated as Eocene by Dunkl (1992) pointing to contemporaneous volcanic activity contributing to the pre-bauxitic material. Latest results of Kelemen et al. (2017) provided an insight not only into the nature of the parent rocks of the bauxitic weathering products but - by single crystal dating zircons from the micromineralogical residue of Cretaceous and Eocene bauxites – also into the whereabouts of the possible source terrains of bauxites having accumulated on the then exposed karst surface of the TR. They showed that at the time of the formation of the Cretaceous deposits only Jurassic and older rocks were exposed in the wider surroundings of the TR. Carboniferous and Permian siliciclastics, Ladinian „Pietra verde"-type volcanoclastics of probably South Alpine origin and perhaps also windborn tephra of some distant CAMP origin could be supposed as the source for the pre-bauxitic material. In the case of the Eocene bauxites the contribution of contemporaneous ashfalls were proved already by Dunkl (1990, 1992) by fission track dating of euhedral zircon grains. Benedek et al. (2004) detected the presence of a 44 Ma volcanic edifice in the Transdanubian Range, so the volcanogenic contribution on

This activity has received funding from the European Institute of Innovation and Technology (EIT), a body of the European Union, under the Horizon 2020, the EU Framework Programme for Research and Innovation

Paleogene bauxites is a possibility, indeed. Recent (yet unpublished) results by Kelemen et al. (2017) confirm all these.

2. ***South Hungary/Villány Hills***

In South Hungary the Nagyharsány bauxite occurrs within the Late Jurassic/Early Cretaceous shallow-water carbonate platform succession at an erosional unconformity between latest Jurassic (Tithonian) and Early Cretaceous (Berriasian to Valanginian) strata. As shown by biostratigraphy of the immediate bedrock and cover the age of the bauxite is probably intra-Berriasian, i.e. the subaerial episode was relatively brief (at least the minimum apparent stratigraphic gap occurring in it is much smaller than that in the case of any of the bauxite deposits of the TR). Unlike the TR bauxites, on the outcrop scale, no appreciable angular unconformity between bedrock and cover can be observed here. Also the mineralogy is different from the bauxites of the TR: major Al-minerals of the Nagyharsány bauxite are böhmite and diaspore (as opposed to the prevailingly gibbsitic-böhmitic composition of the TR bauxites. Though at places where bauxite fills meter-scale dolines, the major Fe-minerals are hematite and goethite (reddish colour, suggesting some early diagenetic episode under vadose conditions!), at places where the underlying karst relief is shallower, the bauxite is pale-coloured and often contains chamosite, suggesting ambivalent redox conditions during early diagenesis related to the hydrological change related to submergence. The lithofacies of the bedrock and the cover together with the concordant appearance of the bauxite-filled shallow-karst relief and the relatively short apparent stratigraphic gap all point to a close-to-groundwater-table position on a temporarily exposed isolated pelagic platform as the depositional environment of the Nagyharsány bauxite. The relative isolation is also reflected by apparently rather poor detrital mineral assemblage in the micromineralogical residue (Nagy, 1989).

The source of the pre-bauxitic material is not simply the dissolution residue of the karstified bedrock but probably there was an admixture of aeolian (partly perhaps also pyroclastic) contribution also here, as was suggested already by Noszky in 1952, then more recently by Császár (2002). Noszky suggested that the contemporaneous diabase volcanism of the Mecsek Mts (currently situated to the North of Villány) could be blamed for the pyroclastics, while Császár insisted that rather the alkali (phonolitic) volcanism might have been the source of the windblown tephra supposedly deposited over the exposed carbonate platform of the Villány block. Even though at the time of bauxite formation those paleogeographic domains might have been situtated far away form the Villány unit, this seems to be supported by the results of Nagy (1989) according to whom in addition to a few heavily worn zircon and quartz grains, supposedly volcanogenic ilmenite was the only mineral which could be identified in the <0.063 and the 0,063-0,125 and 0,125-0,2 mm size-fraction of the bauxite.

No large-scale exploitation was ever undertaken in the Villány zone. During World War II between 1941 and 1944 a modest amount (in all cca 38 000 tonnes) of it excavated from

This activity has received funding from the European Institute of Innovation and Technology (EIT), a body of the European Union, under the Horizon 2020, the EU Framework Programme for Research and Innovation

former exploration adits, was shipped to the Ajka aluminium plant where it became mixed with Mid Cretaceous (Alsópere) and Eocene (Nyirád) bauxites, and was partly processed into aluminium, partly exported to Germany and allegedly also to Sweden (to be converted into alundum) (Gádori-Szepeshegyi, 1978; Nagy, 1989)

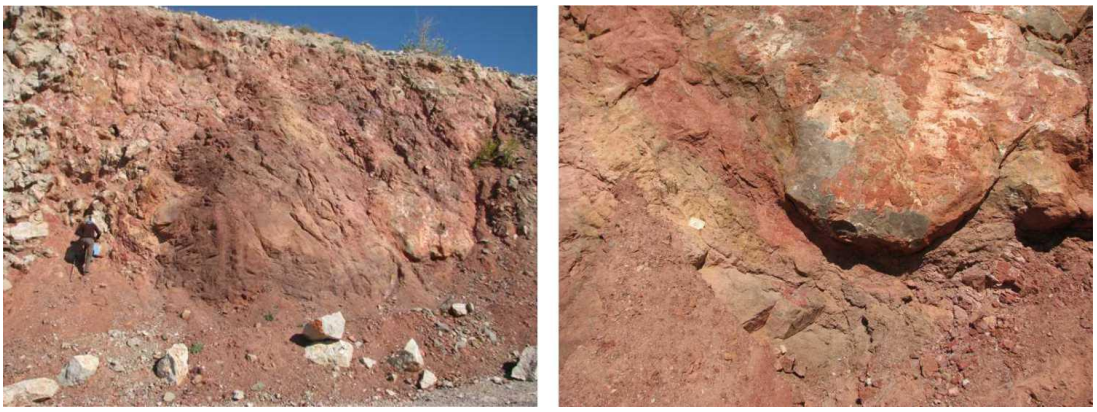

Figure 6A. Nagyharsány open-pit bauxite mine, during field visit within WP2 tasks

Figure 6B. Gánt-Bagolyhegy open-pit abandoned bauxite mine, during field visit within WP2 tasks

Figure 6C. A view to Oligocene bauxite of Óbarok during sampling within WP2 activities, with dissected karst relief underneath bauxite.

This activity has received funding from the European Institute of Innovation and Technology (EIT), a body of the European Union, under the Horizon 2020, the EU Framework Programme for Research and Innovation

Along with some open-pits the majority of the workable reserves were exploited by underground mines. Important deposits subject to mining activity were Alsópere (Albian) Halimba and Iharkút (Santonian), Nyirád, Csabpuszta, Bakonyoszlop, Fenyőfő, Iszkaszentgyörgy, Gánt, Nagyegyháza, Csordakút, Mány (Eocene) and Óbarok (Oligocene). They have been under development since 1926 with a total annual production of cca 3 million metric tons in the late 1980-ties. Since then, for economic reasons, production has gradually declined until bauxite mining came to its end in Hungary in 2013 with Halimba-II SW as the last underground mine. Since in Hungary all mining companies are obliged to recultivation, most of the former open-pits are refilled by now.

Bauxite is accessible only in some of the old pits of Nyirád Darvastó, Iszka-Kincses, Gánt and Óbarok (Eocene), and some material is available also in the form of leftover depots from the old deposits of Cretaceous bauxites of Alsópere and Iharkút. After final closure of the mines some selected core samples, originally stored by the Exploration Company, were transferred to the Geological Survey's Data Bank, and some of them are hosted by the Natural History Museum of Zirc (Transdanubia).

The bauxite deposits visited and sampled in the frames of REEBAUX WP2 are presented in Table 4. Major elements are presented in Table 5 and REE abundances in Table 6. Figures 6A-6C present some examples of the bauxite deposits visited.

This activity has received funding from the European Institute of Innovation and Technology (EIT), a body of the European Union, under the Horizon 2020, the EU Framework Programme for Research and Innovation

Table 4. Samples of bauxite collected in Hungary within REEBAUX WP2 activities, the location and age of the bauxite deposits.

Locality	Sample ID	Latitude	Longitude	Age
Nagyharsány	Nh-4	45°51'20'' N	18°24' 40''E	Early Cretaceous
	Nh-7			
	Nh-9			
	Nh-11			
	Nh-12			
	Nh-9a			
	Nh-3			
	Nh-5			
	Nh-8			
	Nh-10			
Iharkút	Ik-179/6.0-7.0 m	47°14'30.3''N	17°39'11.7''E	Late Cretaceous
	Ik-179/10.0-11.0 m			
	Ik-179/14.0-15.0 m			
Csabrendek	Cn-435/46.8-47.8 m	46°59'36.0''N	17°18'57.3''E	Late Cretaceous(Eocene
	Cn-435/54.7-55.7 m			
	Cn-435/58.8-59.8 m			
Dudar	Du-438/37.5-38.5m	47°20'07,7''N	17°57'02,6''E	Eocene
	Du-438/53.2-54.2 m			
	Du-438/68.2-69.2 m			
	Du-438/80.2-80.8 m			
	Du-487/52.6-53.1 m			
	Du-487/59.9-60.3 m			
	Du-487/74.5-75.5 m			
	Du-487/86.9-87.5 m			
Óbarok	OB-11/2	47°30'05.9"N	18°34'24.3"E	Oligocene
	OB-11/8			
	OB-11/9			
	OB-21/4			
	OB-21/8			
	Ob-11/3			
	Ob-11/4			
	Ob-11/5			
	Ob-11/6			
	Ob-11/7			
	Obfa			
	Obfabx			

This activity has received funding from the European Institute of Innovation and Technology (EIT), a body of the European Union, under the Horizon 2020, the EU Framework Programme for Research and Innovation

Table 5. Major constituents of the bauxite samples collected in Hungary within REEBAUX WP2 activities

Locality	Sample ID	SiO_2	Al_2O_3	Fe_2O_3	MgO	CaO	Na_2O	K_2O	TiO_2	P_2O_5	MnO	Cr_2O_3	Ba	Ni	LOI	SUM
		%	%	%	%	%	%	%	%	%	%	%	ppm	ppm	%	%
Nagyharsány	Nh-4	37.6	39.07	4.73	3.41	0.28	0.02	0.08	2.02	0.062	<0,01	0.022	<1	158	13.2	100.494
	Nh-7	34.85	41.6	6.6	1.31	0.26	0.02	0.02	2.23	0.098	<0,01	0.015	3	135.5	13.4	100.403
	Nh-9	6.44	60.39	16.46	0.93	0.17	0.02	<0,01	3.07	0.072	0.04	0.032	21	183.5	12.4	99.47
	Nh-11	6.57	63.93	11.76	0.57	0.11	0.02	<0,01	3.24	0.098	0.04	0.032	12	185.7	13.1	99.066
	Nh-12	6.42	62.72	11.49	0.59	0.42	0.01	<0,01	3.11	0.154	0.01	0.042	6	201.2	14.1	99.724
	Nh-9a	7.24	55.74	20.72	1.04	0.15	0.03	<0,01	2.85	0.059	0.06	0.035	23	221.2	11.8	100.071
	Nh-3	40.62	36.74	3.7	3.82	0.36	0.03	0.07	2.03	0.058	<0,01	0.013	8	178.5	12.7	100.141
	Nh-5	40.93	37.24	3.04	3.54	0.28	0.03	0.16	2.13	0.053	<0,01	0.01	7	86.3	12.8	100.213
	Nh-8	4.07	42.83	34.38	0.83	1.24	<0,01	<0,01	2.04	0.155	0.01	0.019	10	295	13.3	99.407
	Nh-10	9.12	61.37	11.33	1.15	0.21	0.02	<0,01	3.18	0.095	0.02	0.032	23	228.3	12.9	99.753
Iharkút	Ik-179/6.0-7.0 m	5.02	53.99	21.39	0.37	0.81	0.07	0.04	2.54	1.351	1.38	0.032	246	447.4	12.8	99.793
	Ik-179/10.0-11.0 m	0.66	56.58	22.93	0.23	0.63	0.03	<0,01	2.67	1.378	1.54	0.028	246	653.1	12.2	99.105
	Ik-179/14.0-15.0 m	2.48	57.61	21.54	0.2	0.39	0.03	0.02	2.77	1.173	0.48	0.032	114	181.3	12.4	99.125
Csabrendek	Cn-435/46.8-47.8 m	1.64	51.12	22.53	0.11	0.58	0.04	0.02	2.13	0.15	0.15	0.056	19	184.5	21.4	99.926
	Cn-435/54.7-55.7 m	2.12	50.14	22.22	0.13	0.29	0.03	0.02	1.8	0.26	0.15	0.053	21	293.2	21.6	98.813
	Cn-435/58.8-59.8 m	2.95	50.34	22.04	0.09	0.21	0.03	0.03	1.87	0.28	0.15	0.053	34	253.3	21.3	99.343
Dudar	Du-438/37.5-38.5m	11.53	51.25	19.91	0.3	0.13	0.06	0.17	2.51	0.095	0.17	0.042	63	92.8	13.3	99.467
	Du-438/53.2-54.2 m	14.76	48.72	18.82	0.24	0.12	0.07	0.26	2.31	0.1	0.46	0.038	80	157.1	13.8	99.698
	Du-438/68.2-69.2 m	3.94	54.39	20.35	0.15	0.08	0.04	0.08	2.83	0.104	0.29	0.033	45	55.2	17.3	99.587
	Du-438/80.2-80.8 m	17.96	45.83	17.36	0.31	0.16	0.07	0.53	2.32	0.177	1.49	0.032	162	321.2	14	100.239
	Du-487/52.6-53.1 m	19.33	44.67	13.6	0.6	0.94	0.08	0.3	2.23	0.096	1.04	0.04	74	186	16.5	99.426
	Du-487/59.9-60.3 m	18.11	43.37	20.26	0.53	0.41	0.08	0.3	2.25	0.109	0.36	0.05	60	111.9	14	99.829
	Du-487/74.5-75.5 m	15.88	48.72	18.02	0.35	0.14	0.07	0.23	2.3	0.174	0.18	0.051	57	119.4	13.7	99.815
	Du-487/86.9-87.5 m	14.57	44.87	23.71	0.29	0.25	0.06	0.27	2.11	0.139	1.55	0.055	112	276.2	12.1	99.974
Óbarok	OB-11/2	1.46	1.18	35.59	0.32	32.31	0.02	0.05	0.05	0.086	0.35	<0,004	34	151.3	27.5	98.916
	OB-11/8	22.84	32.15	26.35	0.21	0.19	0.07	0.41	1.88	0.317	0.08	0.038	188	112	15	99.535
	OB-11/9	25.53	37.55	16.42	0.18	0.19	0.06	0.22	2.19	0.274	0.03	0.049	136	69.1	17.3	99.993

This activity has received funding from the European Institute of Innovation and Technology (EIT), a body of the European Union, under the Horizon 2020, the EU Framework Programme for Research and Innovation

Locality	Sample ID	SiO_2	Al_2O_3	Fe_2O_3	MgO	CaO	Na_2O	K_2O	TiO_2	P_2O_5	MnO	Cr_2O_3	Ba	Ni	LOI	SUM
		%	%	%	%	%	%	%	%	%	%	%	ppm	ppm	%	%
	OB-21/4	36.42	37.54	8.24	0.28	0.22	0.05	0.25	1.66	0.113	0.51	0.026	167	32.2	15	100.309
	OB-21/8	31.12	34.48	15.97	0.21	0.21	0.08	0.37	2.7	0.281	0.04	0.049	180	71.7	14.4	99.91
	Ob-11/3	33.6	30.62	19.69	0.22	0.19	0.06	0.46	1.89	0.299	0.07	0.049	183	112	11.9	99.048
	Ob-11/4	20.95	32.44	25.99	0.18	0.19	0.05	0.28	1.98	0.308	0.24	0.046	179	210	15.8	98.454
	Ob-11/5	18.95	38.77	18.4	0.15	0.21	0.04	0.11	2.79	0.415	0.08	0.065	201	82.6	18.9	98.88
	Ob-11/6	19.87	35.3	23.06	0.17	0.27	0.04	0.17	2.51	0.361	0.07	0.063	195	71	16.9	98.784
	Ob-11/7	19.43	43.03	12.3	0.16	0.22	0.04	0.19	2.61	0.426	0.03	0.074	212	62.8	20.8	99.31
	Obfa	0.64	0.55	93.26	0.07	0.12	0.03	<0.01	0.03	0.024	0.34	0.004	20	73.4	3.5	99.007
	Obfabx	8.93	45.33	16.2	0.16	0.54	0.02	0.03	2.98	0.327	0.06	0.06	193	44.3	24.4	99.037

Table 6. REE abundances (in ppm) in the bauxite samples collected in Hungary within REEBAUX WP2 activities

Locality	Sample ID	Y	La	Ce	Pr	Nd	Sm	Eu	Gd	Tb	Dy	Ho	Er	Tm	Yb	Lu	ΣLREE	ΣHREE	ΣREE
Nagyharsány																			
	Nh-4	125.1	135	157.5	22.55	84.5	15.02	3.02	13.96	2.22	15.39	3.72	12.27	1.8	11.94	1.96	417.59	188.36	605.95
	Nh-7	123.9	225.4	341.6	52.28	212.1	37.53	7.09	28.8	3.31	17.15	3.56	11.13	1.62	10.42	1.7	876	201.59	1077.59
	Nh-9	237.8	296.4	377.3	61.29	251.7	46.26	10.4	45.11	6.1	35.32	7.46	22.38	3.35	22.24	3.59	1043.35	383.35	1426.7
	Nh-11	255	252.1	320.2	45.07	166	30.75	6.83	30.32	4.99	33.19	7.62	24.95	3.61	23.19	3.67	820.95	386.54	1207.49
	Nh-12	141.9	182.9	335.7	37.58	143.9	26.32	5.13	22.71	3.3	20.36	4.5	14.8	2.28	15.53	2.52	731.53	227.9	959.43
	Nh-9a	234.3	251	298.7	46.92	189.5	34.87	7.99	36.26	5.4	33.21	7.22	22.19	3.34	21.68	3.49	828.98	367.09	1196.07
	Nh-3	91.7	147.6	184.2	23.12	84.4	13.12	2.62	11.4	1.8	12.1	2.88	9.18	1.4	9.76	1.52	455.06	141.74	596.8
	Nh-5	78.8	106.6	161.7	16.75	54.1	7.12	1.47	6.7	1.29	8.91	2.32	7.52	1.15	7.54	1.22	347.74	115.45	463.19
	Nh-8	305.4	164.1	198.7	27.16	109.1	23.41	5.88	30.91	5.43	35.76	8.34	25.14	3.56	21.58	3.41	528.35	439.53	967.88
	Nh-10	229.4	326.8	404.6	53.71	201.1	37.81	8.92	39.44	5.71	33.67	7.42	22.86	3.31	21.82	3.49	1032.94	367.12	1400.06
Iharkút																			
	Ik-179/6.0-7.0 m	245	167	264.2	38.01	150.1	28.25	6.03	27.89	4.08	25.13	5.68	18.48	2.67	17.73	2.97	653.59	349.63	1003.22
	Ik-179/10.0-11.0 m	220.3	179.1	283.5	40.62	157.3	30.41	6.49	29.7	4.57	27.4	5.98	17.89	2.52	16.43	2.56	697.42	327.35	1024.77

This activity has received funding from the European Institute of Innovation and Technology (EIT), a body of the European Union, under the Horizon 2020, the EU Framework Programme for Research and Innovation

Locality	Sample ID	Y	La	Ce	Pr	Nd	Sm	Eu	Gd	Tb	Dy	Ho	Er	Tm	Yb	Lu	ΣLREE	ΣHREE	ΣREE
Ik-179/14.0-15.0 m		224.9	180.8	283.8	41.55	162.9	31.36	6.58	30.04	4.6	27.47	6.11	18.99	2.65	16.58	2.69	706.99	334.03	1041.02
Csabrendek																			
Cn-435/46.8-47.8 m		46	66.1	202.8	13	46.8	8.99	1.83	7.15	1.19	7.83	1.7	5.45	0.8	5.69	0.86	339.52	76.67	416.19
Cn-435/54.7-55.7 m		134.1	219.4	203.6	64.74	247.6	46.84	9.12	32.98	5.08	29.68	5.6	16.59	2.51	17.31	2.63	791.3	246.48	1037.78
Cn-435/58.8-59.8 m		156	196.9	217.6	58.78	237.2	48.23	10.22	37.9	5.74	32.98	6.35	18.72	2.8	18.97	2.85	768.93	282.31	1051.24
Dudar																			
Du-438/37.5-38.5 m		64.7	141.2	765.7	25.98	88.8	14.64	2.96	12.12	1.97	11.75	2.44	7.59	1.22	8.07	1.22	1039.28	111.08	1150.36
Du-438/53.2-54.2 m		102.5	156.3	281.4	31.47	111	19.08	4.13	17.8	2.73	16.65	3.45	10.01	1.46	9.53	1.46	603.38	165.59	768.97
Du-438/68.2-69.2 m		83.7	132.2	267.4	25.43	90.3	16.36	3.41	14.03	2.24	13.49	2.76	8.64	1.27	8.76	1.34	535.1	136.23	671.33
Du-438/80.2-80.8 m		173.5	134.6	223.5	37.74	153.2	27.98	6.06	25.37	3.77	22.33	4.49	13.22	1.78	11.26	1.73	583.08	257.45	840.53
Du-487/52.6-53.1 m		125.3	154.2	200.4	42.02	164.1	32.59	6.93	29.05	4.34	24.24	4.6	13.37	1.78	11.47	1.77	600.24	215.92	816.16
Du-487/59.9-60.3 m		118.7	124.4	176.7	29.2	115.9	23.3	5.22	22.36	3.37	18.88	3.89	10.53	1.49	9.48	1.41	474.72	190.11	664.83
Du-487/74.5-75.5 m		139.1	192.1	270.9	42.05	154.9	28.75	6.08	25.18	3.82	21.92	4.43	12.68	1.8	11.78	1.79	694.78	222.5	917.28
Du-487/86.9-87.5 m		103.7	148.7	206.2	33.68	127	21.62	4.64	19.56	2.85	16.42	3.41	9.97	1.4	9.1	1.38	541.84	167.79	709.63
Óbarok																			
	OB-11/2	92.3	3.9	24.6	1.7	10.1	5.33	1.89	11.93	2.12	13.53	3.04	8.82	1.18	7.26	1.16	47.52	141.34	188.86
	OB-11/8	48.6	152.6	444.6	39.37	158.5	28.27	5.63	18.72	2.13	10.88	1.82	5.23	0.79	5.08	0.73	828.97	93.98	922.95
	OB-11/9	38.2	130.6	271.2	30.37	114.7	19.68	3.91	13.16	1.72	8.98	1.57	4.62	0.67	4.46	0.65	570.46	74.03	644.49
	OB-21/4	26.7	65.1	121.6	13.89	48.1	8.12	1.71	6.22	0.87	5.09	0.97	2.93	0.45	2.89	0.44	258.52	46.56	305.08
	OB-21/8	45.3	142.7	285.7	33.22	130.7	21.86	4.29	14.53	1.79	9.2	1.65	4.7	0.71	4.69	0.71	618.47	83.28	701.75
	Ob-11/3	82.2	172.1	379.7	40.43	164	32.79	7.6	27.75	3.66	18.19	3.39	9.71	1.32	9.07	1.36	796.62	156.65	953.27
	Ob-11/4	82.9	175.4	383	37.51	143.8	25	5.88	22.73	3.28	17.08	3.41	9.35	1.34	8.76	1.28	770.59	150.13	920.72
	Ob-11/5	55.8	215	306	41.68	152.6	24.11	5.29	16.77	2.23	11.31	2.11	6.01	0.82	5.57	0.87	744.68	101.49	846.17
	Ob-11/6	45.5	200.8	277.7	38.39	137.6	22.34	4.73	14.57	1.88	9.42	1.71	4.96	0.7	4.51	0.64	681.56	83.89	765.45
	Ob-11/7	45.7	227.7	397	44.29	160.9	26.72	5.66	17.16	2.14	10.53	1.79	5.02	0.74	4.86	0.72	862.27	88.66	950.93
	Obfa	6.3	2.3	3.3	0.36	2.1	0.71	0.21	1.13	0.19	1.16	0.24	0.57	0.07	0.39	0.06	8.98	10.11	19.09
	Obfabx	37.8	161.5	211.7	28.75	98.6	15.58	3.49	11.67	1.56	8.53	1.53	4.38	0.62	4.26	0.64	519.62	70.99	590.61

This activity has received funding from the European Institute of Innovation and Technology (EIT), a body of the European Union, under the Horizon 2020, the EU Framework Programme for Research and Innovation

2.3.3. Bauxite deposits in Montenegro and REE potential

Montenegro belongs to the area of the southeastern Dinarides. Bauxite deposits in Montenegro can be divided into: a) red karst bauxites of Triassic, Jurassic and Lower Paleogene age, and b) white karst bauxites of Lower Cretaceous age (Bešić et al., 1968; Dragović, 1988; Pajović, 2009).

Economically most significant bauxite deposits in Montenegro are Jurassic red bauxite deposits, which are widespread within structural-tectonic unit of High Karst. These were formed on the karstified paleorelief composed of Late Triassic, Early Jurassic and Middle Jurassic – Oxfordian carbonate sediments. The bauxite accumulation depressions are most prominent in Late Triassic limestones hosting the most important red bauxite deposits of Montenegro. These are discordantly overlain by thick transgressive Late Kimeridgian and Tithonian limestones.

Bauxite deposits and occurrences visited and sampled during WP2 activates (for example, Figure 7A and 7B) are listed in Table 7 with location indication, age of bauxite deposit and reserves, if available. Content of major elements in the bauxites is presented in Table 8, and REE abundances in Table 9.

This activity has received funding from the European Institute of Innovation and Technology (EIT), a body of the European Union, under the Horizon 2020, the EU Framework Programme for Research and Innovation

Figure 7A. Sampling of bauxite within WP2 activities in Montenegro

Figure 7B. Sampling of bauxite within WP2 activities in Montenegro

This activity has received funding from the European Institute of Innovation and Technology (EIT), a body of the European Union, under the Horizon 2020, the EU Framework Programme for Research and Innovation

Table 7. Samples collected in Montenegro within REEBAUX WP2 activities

Locality	Sample ID	Number of samples	Sampling interval (m)	Latitude	Longitude	Estimated geological reserves (t)	Age
PIVA, Rudinice; OUTCROP	CGBX 01	6	6	43°45'49.0'' N	18°51'17.7'' E	N/A	Triassic
BIOČKI STAN; DEPOSIT in exploatation	CGBX 02	9	9	42°45'09.2'' N	19°10'26.4'' E	7,630,000	Jurassic
ZAGRAD; DEPOSIT in exploatation	CGBX 03	12	12	42°45'47.3'' N	19°52'03.7'' E	1,730,000	Jurassic
ĐURAKOV DO; DEPOSIT in exploatation	CGBX 04	9	9	42°45'46.2'' N	19°09'35.8 E	3,910,000	Jurassic
LIVEROVIĆI; ; DEPOSIT partly exploited (1957-1993)	CGBX 05	5	5	42°45'13.6'' N	19°03'21.8'' E	5,320,000	Jurassic
GREBENICI, Crveno katunište; DEPOSIT	CGBX 06	5	5	42°41'23.9'' N	19°16'46.1'' E	610,000	Jurassic
BRŠNO; DEPOSIT	CGBX 07	16	16	42°43'33.9'' N	19°01'23.2'' E	2,580,000	Jurassic
BOROVA BRDA; DEPOSIT partly exploited (1980-2006)	CGBX 08	8	8	42°41'45.7'' N	19°10'07.7'' E	300,000	Jurassic
CRVENJACI; DEPOSIT	CGBX 09	10	10	42°42'05.4'' N	19°08'19.4'' E	2,250,000	Jurassic
CRVENO PRLO; OUTCROP	CGBX 10	4	4	42°35'15.7'' N	19°17'44.3'' E	N/A	Jurassic
ĐELOV DO; DEPOSIT	CGBX 11	5	5	42°42'51.5'' N	18°42'21.8'' E	2,940,000	Jurassic
VELJA DUBOVA GLAVA; DEPOSIT partly exploited	CGBX 12	9	8.5	42°35'05.6'' N	18°42'21.8'' E	770,000	Jurassic
MILOVIĆI; OCCURRENCE partly exploited on outcrops (1955-1966)	CGBX 13	5	5	42°05'10.9'' N	18°36'33.4'' E	N/A	Jurassic
SAVINA GRADINA; OCCURRENCE partly exploited on outcrops	CGBX 14	6	4.6	42°45'26.2'' N	18°31'30.2'' E	N/A	Jurassic
PAKLARICA; DEPOSIT partly exploited (1969-1997)	CGBX 15	8	8	42°38'57.1'' N	18°49'54.0'' E	N/A	Creteceous
STUDENAC; OCCURRENCE partly exploited on outcrops (1979-1997)	CGBX 16	8	8	42°39'41.9'' N	18°51'32.3'' E	N/A	Creteceous
TREBOVINJSKI POD; DEPOSIT partly exploited (1979-1997)	CGBX 17	7	7	42°39'58.5'' N	18°52'01.7'' E	105000	Creteceous
LAZINE; DEPOSIT partly exploited (1979-1997)	CGBX 18	10	9.8	42°40'27.9'' N	18°54'21.8'' E	274,000	Creteceous
MEĐEĐE; DEPOSIT	CGBX 19	16	15.3	42°42'45.9'' N	18°56'01.4'' E	1,260,000	Creteceous
KRUŠČICA; OCCURRENCE partly exploited on outcrops	CGBX 20	5	4.3	42°45'23.7'' N	18°46'09.8'' E	N/A	Creteceous
JELINA PEĆINA; OCCURRENCE partly exploited on outcrops	CGBX 21	7	7.3	42°40'20.0 N	18°54'36.0'' E	N/A	Creteceous
BOKA KOTORSKA AREA (4 diferent locations: (Kovači-Glavati, Ukropci, Lješevići, Petrovići); OUTCROPS	CGBX 22	9				N/A	Paleogene
ULCINJ AREA (7 diferent locations: Kunje, Kurtina, Duškići, Velja Gorana, Krute, Sveti Đorđe, Bratica); OUTCROPS	CGBX 23	18				N/A	Paleogene

This activity has received funding from the European Institute of Innovation and Technology (EIT), a body of the European Union, under the Horizon 2020, the EU Framework Programme for Research and Innovation

Locality	Sample ID	Number of samples	Sampling interval (m)	Latitude	Longitude	Estimated geological reserves (t)	Age
GORNJEPOLJSKI VIR; DEPOSIT partly exploited (1952-1958)	CGBX 24	1	0.5	42°50'57.6'' N	18°55'06.2'' E	962,000	Triassic
	CGBX 25	1	0.7				
	CGBX 26	1	1				
	CGBX 27	1	1				
	CGBX 28	1	1				
	CGBX 29	1	1				
ŠTITOVO II; DEPOSIT in exploatation	CGBX 30	1	1	42°44'12.6'' N	19°10'24.5'' E	4,140,000	Jurassic
	CGBX 31	1	1				
	CGBX 32	1	1				
	CGBX 33	1	1				
	CGBX 34	1	1				
	CGBX 35	1	1				
	CGBX 36	1	0.2				
BAJOV DO; DEPOSIT partly exploited on outcrops (1953-1958)	CGBX 37	1	1	42°44'12.0'' N	18°43'20.1 E	1,150,000	Jurassic
	CGBX 38	1	1				
	CGBX 39	1	1				
	CGBX 40	1	1				
	CGBX 41	1	1				
	CGBX 42	1	1				
	CGBX 43	1	1				
	CGBX 44	1	1				
	CGBX 45	1	1				
BIJELE POLJANE; DEPOSIT partly exploited (1948-2016)	CGBX 46	1	1	42°40'52.8'' N	18°51'40.9'' E	570,000	Creteceous
	CGBX 47	1	1				
	CGBX 48	1	1				
	CGBX 49	1	1				
	CGBX 50	1	1				
	CGBX 51	1	1				
	CGBX 52	1	1				

This activity has received funding from the European Institute of Innovation and Technology (EIT), a body of the European Union, under the Horizon 2020, the EU Framework Programme for Research and Innovation

Locality	Sample ID	Number of samples	Sampling interval (m)	Latitude	Longitude	Estimated geological reserves (t)	Age
	CGBX 53	1	1				
	CGBX 54	1	1				
	CGBX 55	1	0.1				
VELIKA GORANA; OUTCROP	CGBX 56	1	0.8	41°59'47.2'' N	19°31'07.1'' E	N/A	Paleogene
	CGBX 57	1	1				
	CGBX 58	1	1				
	CGBX 59	1	1				
	CGBX 60	1	1				

Table 8. Major constituents of the bauxite samples collected in Montenegro within REEBAUX WP2 activities

Locality	Sample ID	SiO_2	Al_2O_3	Fe_2O_3	MgO	CaO	Na_2O	K_2O	TiO_2	P_2O_5	MnO	Cr_2O_3	Ba	Ni	Sc	LOI	Sum
		%	%	%	%	%	%	%	%	%	%	%	ppm	ppm	ppm	%	%
PIVA, Rudinice;	CGBX 01	6.83	62.5	12.85	0.13	0.07	<0.01	0.07	2.31	<0.01	0.07	0.018	20	69	48	14.9	99.76
BIOČKI STAN	CGBX 02	4.93	56.07	20.43	0.28	0.15	<0.01	0.16	2.83	0.1	0.56	0.055	56	792	66	13.6	99.28
ZAGRAD; DEPOSIT	CGBX 03	1.61	61.3	19.62	0.12	0.18	<0.01	0.02	2.91	0.05	0.11	0.062	24	121	65	13.7	99.63
ĐURAKOV DO; DEPOSIT	CGBX 04	7.85	54.13	20.13	0.64	0.54	<0.01	0.41	2.67	0.01	0.12	0.071	49	120	57	13	99.63
LIVEROVIĆI; ; DEPOSIT	CGBX 05	13.34	51.52	17.97	0.37	0.14	<0.01	0.47	2.45	0.05	0.13	0.043	78	232	56	13.1	99.62
GREBENICI, Crveno katunište; DEPOSIT	CGBX 06	12.21	51.6	19.69	0.34	0.06	0.01	0.58	2.54	0.04	0.09	0.039	91	180	53	12.4	99.67
BRŠNO; DEPOSIT	CGBX 07	17.2	46.78	19.13	0.52	0.13	0.03	0.96	2.23	<0.01	0.16	0.037	144	166	50	12.5	99.68
BOROVA BRDA; DEPOSIT	CGBX 08	15.83	48.75	18.45	0.52	0.18	0.02	0.81	2.29	0.07	0.14	0.035	106	181	65	12.4	99.6
CRVENJACI; DEPOSIT	CGBX 09	18.97	46.54	17.7	0.45	0.11	0.02	0.56	2.13	0.02	0.13	0.035	79	156	53	13	99.7
CRVENO PRLO; OUTCROP	CGBX 10	16.22	47.91	18.22	0.97	0.17	0.03	0.66	2.12	0.02	0.14	0.039	78	209	53	13.1	99.63
ĐELOV DO; DEPOSIT	CGBX 11	19.65	45.56	17.76	0.37	0.17	<0.01	0.34	1.91	0.02	0.08	0.034	53	198	41	13.8	99.76
VELJA DUBOVA GLAVA; DEPOSIT	CGBX 12	14.2	51.26	17.33	0.32	0.1	<0.01	0.14	2.15	0.01	0.14	0.037	29	171	46	14	99.69
MILOVIĆI; OCCURRENCE	CGBX 13	7.24	31.41	12.01	0.49	21.32	<0.01	0.27	1.42	0.02	0.12	0.028	29	180	32	25.4	99.76
SAVINA GRADINA; OCCURRENCE	CGBX 14	9.17	34.19	13.27	0.69	17.33	<0.01	0.23	1.44	<0.01	0.07	0.031	37	231	32	23.4	99.8

This activity has received funding from the European Institute of Innovation and Technology (EIT), a body of the European Union, under the Horizon 2020, the EU Framework Programme for Research and Innovation

Locality	Sample ID	SiO_2	Al_2O_3	Fe_2O_3	MgO	CaO	Na_2O	K_2O	TiO_2	P_2O_5	MnO	Cr_2O_3	Ba	Ni	Sc	LOI	Sum
		%	%	%	%	%	%	%	%	%	%	%	ppm	ppm	ppm	%	%
PAKLARICA; DEPOSIT	CGBX 15	25.76	42.34	13	0.46	0.2	0.02	0.62	2.15	0.02	<0.01	0.045	67	201	42	15.1	99.72
STUDENAC; OCCURRENCE	CGBX 16	19.63	47.39	9.65	0.28	0.47	<0.01	0.34	2.92	0.06	<0.01	0.047	56	123	39	18.9	99.74
TREBOVINJSKI POD; DEPOSIT	CGBX 17	17.23	42.61	20.72	0.46	0.16	<0.01	0.66	1.93	0.06	0.04	0.061	72	132	61	15.8	99.72
LAZINE; DEPOSIT	CGBX 18	23.13	42.52	15.04	0.4	0.09	0.02	0.98	2.13	0.04	<0.01	0.046	77	137	39	15.3	99.73
MEĐEĐE; DEPOSIT	CGBX 19	34.18	37.23	6.88	0.64	1.95	0.04	1.09	1.77	0.02	0.01	0.04	82	160	35	15.9	99.75
KRUŠČICA; OCCURRENCE	CGBX 20	24.85	41.6	12.7	0.51	0.56	0.02	0.97	1.99	0.04	<0.01	0.057	48	69	39	16.4	99.71
JELINA PEĆINA; OCCURRENCE	CGBX 21	17.16	50.87	12.92	0.21	0.05	<0.01	0.22	2.45	0.04	<0.01	0.054	29	79	42	15.8	99.74
BOKA KOTORSKA AREA	CGBX 22	13.07	47.37	19.1	0.37	1.11	<0.01	0.74	2.77	0.06	0.08	0.093	57	289	28	14.8	99.65
ULCINJ AREA	CGBX 23	9.48	48.31	21.49	0.3	0.79	<0.01	0.21	2.79	0.09	0.09	0.122	54	348	30	15.9	99.58
GORNJEPOLJSKI VIR; DEPOSIT	CGBX 24	36.08	41.21	2.1	0.39	2.1	0.05	0.15	1.21	0.01	0.01	0.013	22	71	28	16.5	99.86
	CGBX 25	29	49.37	2.07	0.28	0.77	0.03	0.12	1.27	0.01	<0.01	0.012	27	57	34	16.9	99.84
	CGBX 26	35.98	37.9	8.85	0.24	0.25	0.03	0.16	1.09	<0.01	0.17	0.01	26	42	30	15.1	99.83
	CGBX 27	34.45	37.43	9.25	0.29	0.32	0.04	0.21	1.01	0.02	0.15	0.008	48	47	31	16.5	99.66
	CGBX 28	24.58	49.41	6.47	0.22	0.21	0.02	0.11	1.34	0.03	0.12	0.01	37	58	36	17.2	99.77
	CGBX 29	24.82	44.62	12.21	0.11	0.16	0.01	0.07	1.32	0.03	0.02	0.011	17	24	29	16.4	99.81
ŠTITOVO II; DEPOSIT	CGBX 30	4.74	57.41	20.49	0.18	0.44	<0.01	0.12	2.79	0.03	0.23	0.047	36	172	53	13.2	99.68
	CGBX 31	5.8	59.04	18.08	0.21	0.19	<0.01	0.19	2.79	0.02	0.14	0.049	43	208	54	13.1	99.67
	CGBX 32	2.71	60.94	19.28	0.1	0.41	<0.01	0.12	2.99	0.03	0.15	0.042	39	141	58	12.9	99.67
	CGBX 33	3.12	58.21	20.18	0.12	1.08	<0.01	0.12	2.91	0.04	0.17	0.045	34	177	64	13.7	99.67
	CGBX 34	3.06	59.3	20.52	0.08	0.35	<0.01	0.11	2.95	0.04	0.16	0.039	39	139	70	13	99.64
	CGBX 35	6.79	56.95	19.89	0.12	0.14	<0.01	0.25	2.76	0.08	0.13	0.039	55	217	68	12.4	99.57
	CGBX 36	10.55	17.87	20.7	0.41	21.88	<0.01	0.4	0.9	0.08	1	0.027	71	771	22	25.6	99.52
BAJOV DO; DEPOSIT	CGBX 37	15.25	50.97	16.99	0.35	0.12	<0.01	0.11	2.2	<0.01	0.13	0.039	24	255	44	13.6	99.76
	CGBX 38	16.33	47.62	19.85	0.47	0.12	<0.01	0.27	2	<0.01	0.13	0.04	41	296	46	12.9	99.76
	CGBX 39	20.27	34.89	25.8	0.67	0.29	0.02	1.04	1.86	<0.01	0.05	0.039	122	209	36	14.8	99.77
	CGBX 40	16.87	26.72	27.23	0.6	6.99	<0.01	0.91	1.36	<0.01	0.03	0.037	101	145	27	19	99.81
	CGBX 41	14.24	50.25	18.88	0.43	0.12	<0.01	0.36	2.19	<0.01	0.12	0.039	50	253	46	13	99.73
	CGBX 42	11.48	51.02	21.51	0.38	0.09	<0.01	0.09	2.24	<0.01	0.16	0.038	22	299	56	12.7	99.67
	CGBX 43	12.15	51.79	19.48	0.37	0.1	<0.01	0.1	2.23	<0.01	0.14	0.041	24	284	51	13.3	99.73
	CGBX 44	16.24	43.48	21.95	0.38	0.09	<0.01	0.18	1.77	<0.01	0.03	0.037	30	448	39	15.5	99.68
	CGBX 45	22.54	25.07	35.02	0.33	0.12	<0.01	0.19	2.02	<0.01	0.01	0.046	29	202	38	14.4	99.77
BIJELE POLJANE; DEPOSIT	CGBX 46	38.11	26.89	13.35	1.41	0.77	0.03	3	1.33	0.02	0.02	0.037	131	85	30	14.8	99.83
	CGBX 47	15.25	49.48	14.24	0.24	0.05	<0.01	0.24	2.94	0.03	<0.01	0.054	53	26	51	17.2	99.74

This activity has received funding from the European Institute of Innovation and Technology (EIT), a body of the European Union, under the Horizon 2020, the EU Framework Programme for Research and Innovation

Locality	Sample ID	SiO_2	Al_2O_3	Fe_2O_3	MgO	CaO	Na_2O	K_2O	TiO_2	P_2O_5	MnO	Cr_2O_3	Ba	Ni	Sc	LOI	Sum
		%	%	%	%	%	%	%	%	%	%	%	ppm	ppm	ppm	%	%
	CGBX 48	9.71	58.11	13.17	0.12	0.07	<0.01	0.09	3.33	0.03	<0.01	0.047	21	32	43	15.1	99.77
	CGBX 49	4.15	51.1	26.57	0.46	0.18	<0.01	0.05	2.78	0.05	0.01	0.069	81	38	59	14.3	99.7
	CGBX 50	14.45	42.13	26.16	0.29	0.04	<0.01	0.2	2.26	0.06	0.01	0.057	28	183	44	14	99.69
	CGBX 51	16.82	55.39	6.02	0.26	2.31	<0.01	0.12	2.89	0.02	0.01	0.042	47	116	46	15.9	99.77
	CGBX 52	15.39	52.36	15.24	0.12	0.06	<0.01	0.09	2.47	0.02	0.01	0.048	23	103	49	13.9	99.77
	CGBX 53	16.63	46.6	16.69	0.38	2.36	<0.01	0.17	2.27	0.02	0.02	0.051	34	139	49	14.5	99.74
	CGBX 54	20.39	43.86	18.82	0.33	0.12	0.01	0.53	2.14	0.03	0.02	0.053	69	230	48	13.4	99.7
	CGBX 55	37.45	34.14	6.24	1.94	0.98	0.09	3.56	1.77	0.08	0.02	0.03	229	716	39	12.8	99.23
VELIKA GORANA; OUTCROP	CGBX 56	10.76	49.65	20.14	0.21	0.19	0.03	0.17	2.74	0.08	0.06	0.124	53	334	39	15.4	99.59
	CGBX 57	9.9	50.37	19.65	0.24	0.07	0.02	0.2	2.63	0.07	0.2	0.127	55	489	30	16	99.53
	CGBX 58	9.99	50.34	20.77	0.23	0.08	0.02	0.18	2.85	0.09	0.08	0.138	54	349	32	14.8	99.58
	CGBX 59	7.91	51.71	20.42	0.27	0.1	<0.01	0.16	2.98	0.13	0.09	0.124	48	407	28	15.7	99.59
	CGBX 60	8.34	52.92	19.32	0.24	0.08	<0.01	0.15	2.84	0.1	0.1	0.127	42	404	29	15.3	99.6

Table 9. REE abundances (in ppm) in the bauxite samples collected in Montenegro within REEBAUX WP2 activities

Locality	Sample ID	Y	La	Ce	Pr	Nd	Sm	Eu	Gd	Tb	Dy	Ho	Er	Tm	Yb	Lu	ΣLREE	ΣHREE	ΣREE
PIVA, Rudinice;	CGBX 01	73.2	54.3	311.6	9.88	34.6	8.02	1.65	8.89	1.75	11.82	2.8	9.54	1.56	10.41	1.66	420.05	121.63	541.68
BIOČKI STAN	CGBX 02	233	257	413.8	60.82	262.6	55.45	11.83	49.25	6.97	37.06	7.48	21.05	2.9	18.04	2.86	1061.5	378.61	1440.11
ZAGRAD; DEPOSIT	CGBX 03	118.7	225.2	406.6	43.81	154.4	28.95	5.86	24.7	3.86	22.63	4.53	13.53	2.03	14.23	2.23	864.82	206.44	1071.26
ĐURAKOV DO; DEPOSIT	CGBX 04	120	146	367.5	33.47	125.5	24.5	5.13	22.07	3.42	20.04	4.46	13.42	1.97	12.8	2.04	702.1	200.22	902.32
LIVEROVIĆI; ; DEPOSIT	CGBX 05	120.9	280.5	355.5	48.11	162.2	26.69	5.4	22.36	3.64	21.24	4.45	12.95	1.94	13.08	2.01	878.4	202.57	1080.97
GREBENICI, Crveno katunište; DEPOSIT	CGBX 06	97.7	156	217.6	24.81	79	12.77	2.64	12.63	2.24	14.41	3.28	9.85	1.47	9.69	1.58	492.82	152.85	645.67
BRŠNO; DEPOSIT	CGBX 07	88	116.8	358.5	18.19	61.6	11.31	2.53	12.32	2.11	13.69	2.99	9.3	1.41	9.09	1.45	568.93	140.36	709.29

This activity has received funding from the European Institute of Innovation and Technology (EIT), a body of the European Union, under the Horizon 2020, the EU Framework Programme for Research and Innovation

Locality	Sample ID	Y	La	Ce	Pr	Nd	Sm	Eu	Gd	Tb	Dy	Ho	Er	Tm	Yb	Lu	ΣLREE	ΣHREE	ΣREE
BOROVA BRDA; DEPOSIT	CGBX 08	135.7	326.2	416.1	49.67	182.1	34.05	7.68	35.92	5.2	28.21	5.55	15.66	2.15	13.85	2.13	1015.8	244.37	1260.17
CRVENJACI; DEPOSIT	CGBX 09	93.1	156.5	352.8	25.53	91.1	16.69	3.57	16.09	2.61	16.1	3.31	10.13	1.5	9.87	1.53	646.19	154.24	800.43
CRVENO PRLO; OUTCROP	CGBX 10	170.9	313	364.6	41.89	156.7	26.19	5.66	27.25	4.28	25.83	5.65	16.77	2.47	15.27	2.39	908.04	270.81	1178.85
ĐELOV DO; DEPOSIT	CGBX 11	59.4	77.8	184.6	13.61	46.3	8.52	1.8	9.03	1.72	11.42	2.51	7.68	1.19	7.69	1.17	332.63	101.81	434.44
VELJA DUBOVA GLAVA; DEPOSIT	CGBX 12	116.6	187.7	228.6	31.86	118.3	22.2	4.54	20.85	3.28	19.8	4.1	11.86	1.79	11.93	1.84	593.2	192.05	785.25
MILOVIĆI; OCCURRENCE	CGBX 13	84.1	94.9	141	18.94	71.8	13.64	2.85	13.39	2.07	12.12	2.57	7.21	0.99	6.4	1.03	343.13	129.88	473.01
SAVINA GRADINA; OCCURRENCE	CGBX 14	61.1	83.4	177.8	16.6	61.3	11.23	2.26	10.38	1.66	9.67	2	5.9	0.89	5.59	0.87	352.59	98.06	450.65
PAKLARICA; DEPOSIT	CGBX 15	50.2	69.3	145	15.48	57.4	10.75	2.18	9	1.5	9.13	1.97	5.89	0.89	6.19	0.95	300.11	85.72	385.83
STUDENAC; OCCURRENCE	CGBX 16	49.4	58.7	126.5	9.8	31.8	5.47	1.18	5.84	1.17	8.15	1.86	5.89	0.89	5.99	0.93	233.45	80.12	313.57
TREBOVINJSKI POD; DEPOSIT	CGBX 17	54.8	51.6	143.7	10.11	36.9	7.69	1.72	8.27	1.37	8.58	1.87	5.68	0.83	5.39	0.85	251.72	87.64	339.36
LAZINE; DEPOSIT	CGBX 18	36.9	84	154.4	11.4	30.8	4.83	0.98	4.74	0.94	6.54	1.4	4.54	0.76	5.34	0.83	286.41	61.99	348.4
MEĐEĐE; DEPOSIT	CGBX 19	33.4	52.4	123.5	11.58	42.1	7.97	1.68	6.76	1.15	6.59	1.47	4.35	0.67	4.61	0.7	239.23	59.7	298.93
KRUŠČICA; OCCURRENCE	CGBX 20	30.4	29.9	61.5	5.21	17	3.35	0.74	3.53	0.75	5.14	1.24	3.96	0.62	4.09	0.66	117.7	50.39	168.09
JELINA PEĆINA; OCCURRENCE	CGBX 21	40.4	41	83.2	6.29	21.1	4.53	1.09	5.14	1.02	6.73	1.52	4.8	0.77	5.22	0.81	157.21	66.41	223.62
BOKA KOTORSKA AREA	CGBX 22	44.6	90.3	163.9	16.43	55.3	9.78	2.07	8.3	1.39	8.3	1.72	5.33	0.81	5.63	0.84	337.78	76.92	414.7
ULCINJ AREA	CGBX 23	46.5	108.4	225.8	19.91	67.1	10.82	2.3	9.21	1.51	9.2	1.86	5.57	0.9	5.8	0.88	434.33	81.43	515.76
GORNJEPOLJSKI VIR; DEPOSIT	CGBX 24	58.3	30.1	61.4	7.65	29.7	6.67	1.27	6.62	1.26	8.63	1.97	6.46	0.96	6.46	0.98	136.79	91.64	228.43
	CGBX 25	63.9	42.3	93.5	10.43	39.4	9.94	1.75	8.99	1.67	10.81	2.41	7.54	1.19	8.48	1.34	197.32	106.33	303.65
	CGBX 26	82.9	59.7	159	13.01	47.7	10.77	2.06	11.62	2.02	12.55	2.66	7.87	1.16	7.39	1.11	292.24	129.28	421.52
	CGBX 27	198.7	271.2	892.7	68.8	269.4	50.42	8.58	44.77	6.26	33.51	6.44	17.85	2.52	15.6	2.29	1561.1	327.94	1889.04

This activity has received funding from the European Institute of Innovation and Technology (EIT), a body of the European Union, under the Horizon 2020, the EU Framework Programme for Research and Innovation

Locality	Sample ID	Y	La	Ce	Pr	Nd	Sm	Eu	Gd	Tb	Dy	Ho	Er	Tm	Yb	Lu	ΣLREE	ΣHREE	ΣREE
	CGBX 28	124.8	125.8	216.4	24.95	94.7	19.17	3.49	19.37	3.17	19.11	3.95	11.94	1.74	10.79	1.68	484.51	196.55	681.06
	CGBX 29	51.3	66.8	261	13.92	50.6	9.76	1.72	9.35	1.46	8.82	1.76	5.61	0.86	5.56	0.9	403.8	85.62	489.42
ŠTITOVO II; DEPOSIT	CGBX 30	84.9	114.2	342	23.26	87.9	17.9	3.85	16.46	2.7	15.89	3.33	10.12	1.57	10.65	1.65	589.11	147.27	736.38
	CGBX 31	85.1	119	313.2	24.43	92.7	18.28	3.72	15.84	2.46	14.94	3.1	9.86	1.51	10.41	1.63	571.33	144.85	716.18
	CGBX 32	93.5	124.5	332.8	23.61	89.2	17.91	3.77	16.02	2.6	15.47	3.29	10.52	1.54	10.71	1.69	591.79	155.34	747.13
	CGBX 33	107.6	142.2	381.1	30.09	118.1	25.04	5.25	22.65	3.53	20.16	4.01	12.2	1.83	12.39	1.91	701.78	186.28	888.06
	CGBX 34	119.3	162.2	364.2	33.41	130.1	29.78	6.49	27.73	4.47	25.48	5.12	14.48	2.22	15.41	2.37	726.18	216.58	942.76
	CGBX 35	190.3	391.4	347.3	71.09	261.8	54.41	11.17	46.43	7.04	40.56	8.17	22.36	3.2	20.99	3.21	1137.17	342.26	1479.43
	CGBX 36	208.5	111.3	110	27.31	129.8	32.61	7.78	38.63	5.76	31.66	6.44	17.91	2.37	14.14	2.19	418.8	327.6	746.4
BAJOV DO; DEPOSIT	CGBX 37	49	61.6	269.5	10.19	33.8	6.78	1.43	6.6	1.27	8.5	1.9	6.16	0.97	6.78	1.05	383.3	82.23	465.53
	CGBX 38	48.4	60	297.1	10.13	34.3	6.89	1.49	6.95	1.32	8.39	1.92	6.06	0.96	6.45	0.97	409.91	81.42	491.33
	CGBX 39	42	52.7	123	8.07	26	4.82	1.02	4.97	1.03	7.02	1.67	5.41	0.83	5.69	0.84	215.61	69.46	285.07
	CGBX 40	32.9	36.8	57.7	5.49	17.8	3.35	0.71	3.6	0.76	5.39	1.24	3.94	0.58	4.11	0.63	121.85	53.15	175
	CGBX 41	58.7	81.2	256.1	16.15	58.2	11.24	2.36	10.75	1.84	11.26	2.48	7.41	1.11	7.44	1.16	425.25	102.15	527.4
	CGBX 42	61.7	135	388.1	28.2	100	20.44	4.2	17.09	2.86	16.23	3.18	9.48	1.55	10.77	1.67	675.94	124.53	800.47
	CGBX 43	57.2	113.8	289.8	20.52	70	13.46	2.85	11.82	2.13	12.85	2.64	8.4	1.32	9.33	1.49	510.43	107.18	617.61
	CGBX 44	41.8	63	93.3	9.3	30.4	6.05	1.32	6.26	1.2	8.26	1.88	6.07	0.98	6.89	1.09	203.37	74.43	277.8
	CGBX 45	46.7	73.1	68.2	11.65	41.6	8.36	1.77	7.38	1.39	9.35	2.01	6.58	1.07	7.39	1.16	204.68	83.03	287.71
BIJELE POLJANE; DEPOSIT	CGBX 46	23.2	20.9	52	4.32	16.2	3.39	0.71	3.36	0.6	3.71	0.89	2.76	0.4	2.83	0.44	97.52	38.19	135.71
	CGBX 47	40.3	25.6	69.8	5.03	18.1	3.6	0.82	4.46	0.96	6.77	1.55	4.78	0.78	5.43	0.85	122.95	65.88	188.83
	CGBX 48	50.3	30.1	57.1	5.47	19	4.11	0.96	4.98	1.08	7.87	1.83	5.99	0.94	6.5	1.01	116.74	80.5	197.24
	CGBX 49	39.9	21.1	59.9	4.21	14.7	3.15	0.74	3.92	0.89	6.55	1.52	5.08	0.76	5.15	0.86	103.8	64.63	168.43
	CGBX 50	45.1	53	171	10.04	35.1	6.77	1.43	6.85	1.27	8.57	1.89	5.89	0.93	6.33	0.97	277.34	77.8	355.14
	CGBX 51	55.5	83.7	168.1	9.71	32.8	6.91	1.54	7.29	1.4	9.24	2.03	6.72	0.98	6.93	1.04	302.76	91.13	393.89
	CGBX 52	47	44.3	196.6	8.54	30.4	6.15	1.4	6.66	1.23	8.14	1.78	5.52	0.88	6.14	0.96	287.39	78.31	365.7
	CGBX 53	52.8	58.9	337.6	11.5	43.2	9.5	2	9.05	1.54	9.6	2.08	6.15	0.97	6.62	1.02	462.7	89.83	552.53
	CGBX 54	59	92.9	216.1	20.47	75.5	15.07	3.02	12.37	2.13	12.52	2.67	8.12	1.22	8.69	1.28	423.06	108	531.06
	CGBX 55	130.2	251.6	225.6	65.17	253.7	42.26	8.22	31.3	4.24	22.89	4.26	12.15	1.68	10.85	1.63	846.55	219.2	1065.75
VELIKA GORANA; OUTCROP	CGBX 56	42.2	111	279.1	19.83	61.2	9.85	2.07	8.3	1.46	9.28	1.95	6.13	0.9	6.19	0.97	483.05	77.38	560.43
	CGBX 57	49.5	130.8	202.6	19.88	60.3	9.95	2.34	9.38	1.61	9.73	1.99	5.98	0.92	6.09	0.93	425.87	86.13	512
	CGBX 58	39.2	128.8	235.3	21	62.1	9.09	2.06	7.9	1.41	8.4	1.74	5.4	0.85	5.67	0.89	458.35	71.46	529.81
	CGBX 59	45.1	153.2	295.1	26.26	82.6	12.98	2.65	10.02	1.69	9.58	1.95	5.73	0.88	5.97	0.9	572.79	81.82	654.61
	CGBX 60	43.7	109.8	213.3	19.29	59.5	9.66	2.02	8.2	1.42	8.42	1.82	5.63	0.84	5.68	0.93	413.57	76.64	490.21

This activity has received funding from the European Institute of Innovation and Technology (EIT), a body of the European Union, under the Horizon 2020, the EU Framework Programme for Research and Innovation

2.4. Mineral composition of bauxites and leaching tests

A several number of samples was selected for mineralogical analysis using X-ray powder diffraction (XRD) and leaching tests with aqua regia. X-ray powder diffraction analysis was performed for the samples collected in Croatia at the University of Zagreb-Faculty of Science and Croatian Geological Survey, using Philips and Panalitical X-ray powder diffractometers employing CuKa radiation at 45 kV and 40 mA. The results of the related phase analysis are presented in Table 10.

Table 10. Mineral composition of the selected bauxite samples

Sample	Mineral composition							
	Boehmite	***Gibbsite***	***Hematite***	***Anatase***	***Goethite***	***Kaolinite***	***Other clay minerals***	***Other minerals***
Crveni klanac								
CK 1		+	+			+		
CK 3		+	+			+		
CK 6		+	+			+	+	
CK 7		+		+	+	+		
CK 8		+		+		+	+	calcite
CK 9		+		+	+	+	+	
CK 10		+				+	+	calcite
CK 11		+				+	+	calcite
CK 13		+				+	+	calcite
Košute								
KS 1		+				+		
KS 2		+		+		+		
KS 4		+		+		+		
Gljev								
G 7	+	+		+	+			
G 9	+	+		+	+			
G 10	+	+		+	+	+		
G 12	+	+		+	+			
Obrovac								
OB 1	+	+	+		+			
OB 2	+	+		+	+	+		
OB 3	+	+		+	+	+		
OB 4		+		+		+		
OB 5	+	+		+	+			
OB 6	+	+		+	+			
OB 9	+	+		+	+	+		
OB 10	+	+		+	+	+		
Mamutovo brdo								
MB-1	+	+	+	+	+			
MB-2	+	+	+	+	+			

This activity has received funding from the European Institute of Innovation and Technology (EIT), a body of the European Union, under the Horizon 2020, the EU Framework Programme for Research and Innovation

Sample	Mineral composition							
	Boehmite	*Gibbsite*	*Hematite*	*Anatase*	*Goethite*	*Kaolinite*	*Other clay minerals*	*Other minerals*
MB-3	+	+	+	+	+			
MB-4	+	+	+	+				
Imotski								
IMOL-8 1	+	+	+	+	+			
Ričica								
RIČ 1	+	+			+			
RIČ 2-3	+	+	+	+	+			
Mandići								
MAND 1		+		+	+			
MAND 2	+	+	+	+	+			
MAND 3		+		+	+			calcite
MAND 4		+		+	+			calcite
Turban kosa								
TK 1-1	+		+	+	+	+		
TK 2-1		+	+	+				
Ćosići								
ĆOS 1-2	+	+	+					
ĆOS 1-3	+		+	+				
ĆOS 2-1		+	+		+			
Moseć								
MO Z-1	+	+		+	+			
MO IS-1	+	+		+	+			
MO IS-2	+	+		+	+	+		
MO IS-3	+	+		+	+		+	
MO IS-4	+	+		+	+		+	
MO 1	+	+		+	+			
MO 2	+	+		+	+	+		
MO 3	+	+		+	+	+		
Jukići-Đidare*								
JUK-D		75	14	6				rutile 4
*AR insoluble***		80		2				magnetite 17 rutile 1
Tošići-Dujići*								
TOS-1-D	4	66	10	2				nordstrandite 17
*AR insoluble***	2	77		2				magnetite 16 rutile 2
TOS-1-G	4	57	4	5		30		
*AR insoluble***	4	65		3		16		magnetite 13
TOS-1-S	4	72	10	2	7			rutile 5
*AR insoluble***	2	72		1				magnetite 15 nordstrandite 9

* Semiquantitative determination applying RIR method – whole rock sample

This activity has received funding from the European Institute of Innovation and Technology (EIT), a body of the European Union, under the Horizon 2020, the EU Framework Programme for Research and Innovation

Previous studies of the bauxite deposits in Vojnik-Maganik and Prekornica region, Montenegro, indicate following mineral composition: böhmite, kaolinite, gibbsite, hematite, goethite, anatase and calcite, with accessory minerals like zircon, ilmenite, magnetite, biotite, feldspar, mottramite, monazite, xenotime, and REE carbonates (bastnäsite)(Radusinović et al., 2017).

Leaching tests

Selected samples were treated by aqua regia modified digestion (HNO_3:HCl:H_2O = 1:1:1) in order to distinguish a portion of REE strongly incorporated in the structure of refractory minerals from the part of REE adsorbed to clay minerals and Fe-Mn-Al oxyhydroxides or contained in acid-soluble mineral phases. A split of 15 g of each selected sample was used for the leaching analysis. The obtained leachates were analysed by ICP-MS in Bureau Veritas laboratories. The method could give a quick assessment of the REE occurrence in the samples as an orientation for a possible future treatment for REE recovery. The summarized results of the leaching tests are presented in Table 11 with graphic representations shown in Figures 8A (REE leaching) and 8B (major elements leaching).

Table 11. Summary of REE analytical results of the aqua regia leaching tests performed for the selected bauxite samples from Croatia and red mud from Kidričevo (Slovenia).

Locality	Sample ID	Total REE in sample (ppm)	Total REE leached by aqua regia (ppm)	Insoluble in aqua regia (%)	Soluble in aqua regia (%)
Vrace	VR-1	868.07	155.06	82.14	17.86
Mamutovac	MAM-1	517.66	330.15	36.22	63.78
Rudopolje	RB-1	430.54	93.16	78.36	21.64
	RB-2	433.77	169.68	60.88	39.12
	RB-3	846.17	468.48	44.64	55.36
Tošići-Dujići	TOS-1-D	959.17	349.37	63.58	36.42
	TOS-1-G	1439.2	614.66	57.29	42.71
	TOS-1-S	1082.23	340.31	68.55	31.45
	TOS-2	3495.85	1854.16	46.96	53.04
	TOS-3	2338.26	1076.92	53.94	46.06
	TOS-4	1299.75	760.55	41.48	58.52
Jukići-Đidare	JUK-D	1018.81	279.76	72.54	27.46
Stari gaj	SGT-1	403.08	206.08	48.87	51.13
	SGT-2	598.58	329.29	44.99	55.01
Kidričevo (red mud)	KD-1	934.9	670.88	28.24	71.76

This activity has received funding from the European Institute of Innovation and Technology (EIT), a body of the European Union, under the Horizon 2020, the EU Framework Programme for Research and Innovation

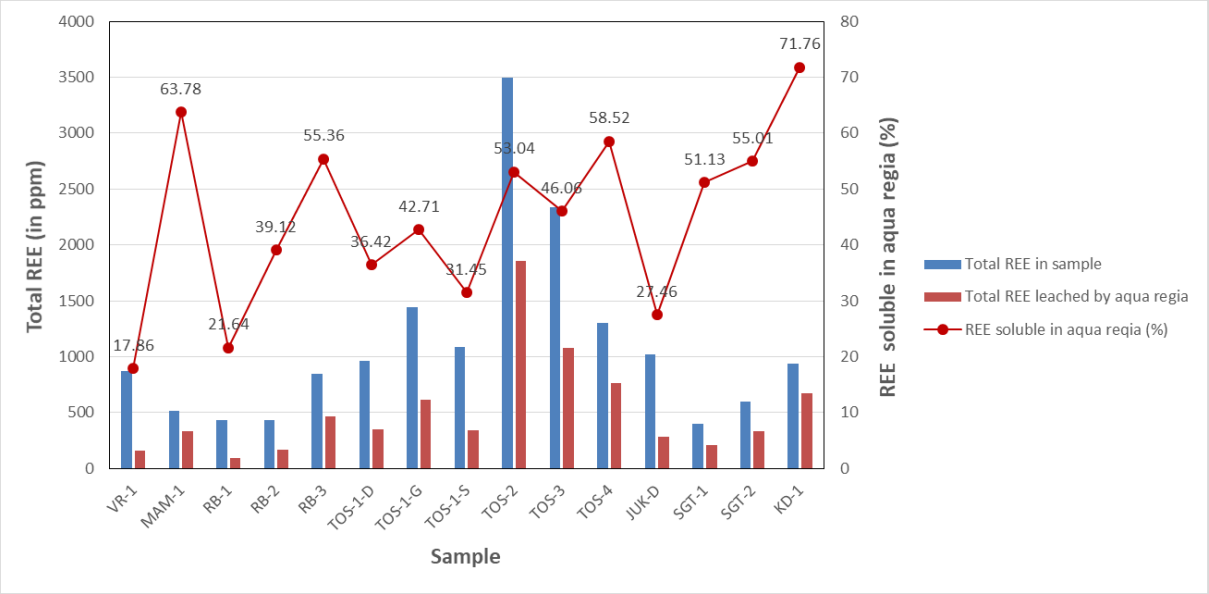

Figure 8A. Total REE content leached with aqua regia relative to the total REE content in the selected samples.

Leaching tests with aqua regia show a variable REE recovery from as low as 17% up to over 60% (Figure 8A). This variability is also observed among various bauxite horizons within single deposit. In the bauxite samples, the unleached REE are most likely contained in minerals like monazite and xenotime, which, however, usually occur at lower abundances and thus are not visible in XRD patterns. The highest recovery is achieved for the sample of red mud from Kidričevo (over 70%), indicating a significant amount of REE was converted from insoluble to acid-soluble salts during Bayer process. This is confirmed by observing recovery of the major elements (Figure 8B) that suggests their significant leaching from red mud. In the case of bauxite samples Ca and Fe are most significantly leached out. However, Ca absolute amounts are low, so only calcite is sporadically observed in XRD patterns. On the other hand, iron concentrations are significant, mostly accounting for hematite and sometimes goethite. XRD data of selected leached samples indicate disappearance of hematite and goethite, but occurrence of magnetite in some cases. On the other hand, Fe leaching rates could be also partially related to amorphous iron oxyhydroxide phases.

A previous leaching study with boiling 10% HCl of four bauxite samples from Jurassic deposit Zagrad (Nikšićka Župa) in Montenegro (Jović et al., 2009), collected at lower horizons of the deposit, showed a mass loss in a range of 37.2-40%. Regarding REE, 80% of light REE were leached (La, Ce, Pr, Nd). Sm, Eu, Gd, Tb and Dy were leached in a lesser extent, while heavier REE (Ho, Er, Tm, Yb, Lu and Y) were not leached out or were brought to the solution in very low quantities. The following mineral composition of the bauxite was determined: boehmite, hematite, kaolinite, anatase, rutile, calcite, hydoxylbastnaesite-(Nd).

This activity has received funding from the European Institute of Innovation and Technology (EIT), a body of the European Union, under the Horizon 2020, the EU Framework Programme for Research and Innovation

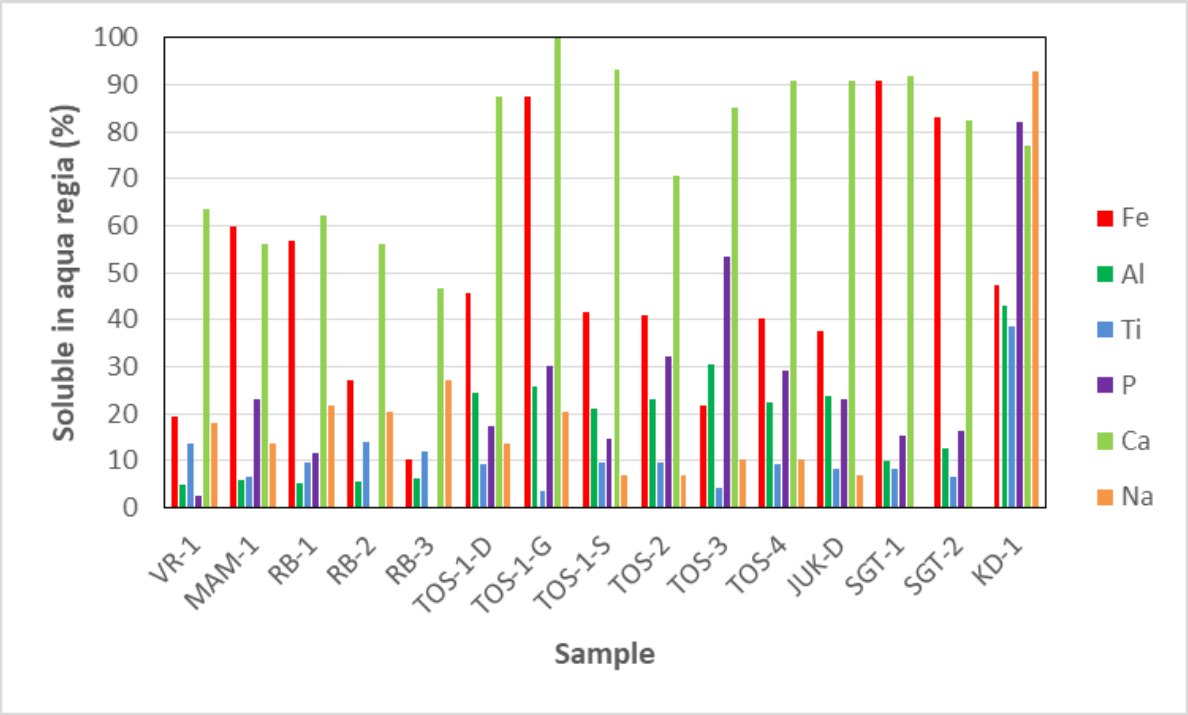

Figure 8B. Content of the selected major elements leached with aqua regia relative to their total content in the selected samples.

This activity has received funding from the European Institute of Innovation and Technology (EIT), a body of the European Union, under the Horizon 2020, the EU Framework Programme for Research and Innovation

2.5. Geological setting of the bauxite deposits in the focus countries

Bauxites have been considered as a possible viable source of rare earth elements/critical metals (REE/CRM) for a long time. The Western Tethyan Mesozoic to Palaeogene karst bauxites contain in cases significant concentrations of REE/CRM, mainly unexplored until nowadays: in general, only few data are available from the karst bauxite deposits in the "bauxite belt" of the eastern Mediterranean mountain belt, striking from the Hellenides (Greece) to the Dinarides (Serbia, Montenegro, Bosnia-Herzegovina, Croatia, Slovenia) and occurring in the different tectonic units in the Pannonian realm (Hungary, Romania, Slovakia), and with minor extent also in the Northern Calcareous Alps (Austria).

Exact data about their parent rocks and the exact age of their formation remain for most karst bauxite deposits relatively speculative due to the lack of data. The most important questions are:

1. When and why did the platforms become emerged and what can be the possible reasons? The bauxite should be the "end-product" of terra rossa: terra rossa becomes bauxitized in an alkaline fluid. Are sea-level changes or overlooked tectonic events triggering factors? In any case, due to the new results of the Triassic-Jurassic geodynamic evolution of the Inner Dinarides and the Northern Calcareous Alps (e.g., Missoni & Gawlick 2011, Gawlick & Missoni 2019) the main question is when and why these platforms became emerged and what can be the possible reasons.

2. The platform carbonates on which Mesozoic karst bauxites are normally found are extremely poor in clay minerals, thought to be a source for bauxite. Volcanic ashes thought as alternative source appear in different stratigraphic levels in comparison with the stratigraphic levels bauxites have formed. Is there overlooked volcanic activity or is the stratigraphic age of bauxite formation not exact? Volcanic ashes, which may act as the source for many bauxites, normally become rapidly eroded on shallow-water platforms and transported into adjacent basins. In the stratigraphic levels where bauxites usually have formed (e.g. "Middle" Carnian, Late Norian, late Late Jurassic, early Late Cretaceous) volcanic activity is in most cases relatively low. Intense volcanic activity is known in the Late Anisian, the Late Ladinian, and the Middle to Late Jurassic. The main question is addressed to the exact age of bauxite formation and probably overlooked volcanic activity.

3. According to all available palaeogeographic reconstructions in Triassic-Jurassic times no igneous or metamorphic rocks are exposed in the Alps or Dinarides. We question according to new own data these palaeogeographic reconstructions (Gawlick & Missoni 2019). The palaeogeographic position of the areas where the bauxites were formed in different stratigraphic levels is a crucial question for the prospection of yet undetected bauxite deposits in the nappe stack of the REEBAUX focus area. New results show that the Late Permian to Early Cretaceous sedimentary history all over the Western Tethyan realm reflects a complete Wilson cycle elsewhere (e.g. Haas et al. 2011, Kovacs et al. 2011):

This activity has received funding from the European Institute of Innovation and Technology (EIT), a body of the European Union, under the Horizon 2020, the EU Framework Programme for Research and Innovation

A) Late Permian to Middle Anisian graben infilling: from siliciclastics to carbonate ramp deposits.

B) Middle Anisian to Middle Jurassic passive margin evolution after the late Middle Anisian oceanic break-up: The complex Middle to Late Triassic shallow- to deep-water carbonate platform shelf evolution from the inner shelf (platform facies) to the outer shelf (open-marine basinal facies) and the Early to Middle Jurassic pelagic platform evolution.

C) Middle to Late Jurassic, very complex active continental margin evolution with the interplay of thrusting, trench and trench-like basin formation, mass movements, and the onset of carbonate platforms.

D) Mountain uplift from the Jurassic/Cretaceous-boundary onwards and filling of the foreland basins.

In the Mesozoic, the most important bauxite levels appear according to the literature (e.g. Timotijevic 1995, 2001; Grubic 1999, Markovic 2002, Pajovic et al. 2017) in the:

1. Middle Triassic: these deposits are overlain by Ladinian sedimentary rocks.

2. Late Triassic: these deposits are overlain by Norian sedimentary rocks.

3. Late Jurassic: these deposits are overlain by Tithonian sedimentary rocks or alternatively by Valanginian to Barremian sedimentary rocks.

4. Late Early Cretaceous: these deposits are overlain by ?Late Aptian/Albian sedimentary rocks or alternatively by Cenomanian to Santonian sedimentary rocks (Gosauic time rocks).

However, in all cases these bauxites seems to be formed during a long lasting emergence of the shallow-water carbonates between the underlying shallow-water carbonates and the overlying transgressive cycle.

In contrast, due to our new results we can draw a different picture:

Karst bauxites from Middle to Late Triassic

Karst bauxites on top of the Early Carnian Wetterstein Carbonate Platform

During the late Middle to early Late Triassic the Neo-Tethys shelf consisted of a number of isolated and attached carbonate platforms separated by intraplatform basins. The bauxite deposits are limited to the isolated carbonate platforms, mainly on those formed in the proximal shelf areas (Outer Dinarides); they are present in minor quantity on the platforms formed in outer shelf position, but are missing in the intraplatform basins. The provenance, and in several cases also the exact age of the bauxites on top of the Wetterstein Carbonate Platform remains in dispute. In addition, deposition of siliciclastic material on top of carbonate platforms representing a drowning sequence is common on top of the Wetterstein Carbonate

This activity has received funding from the European Institute of Innovation and Technology (EIT), a body of the European Union, under the Horizon 2020, the EU Framework Programme for Research and Innovation

Platform. These siliciclastics were recently detected also in the Inner Dinarides (Gawlick et al. 2017), but here they represent transported material from an unknown hinterland. Volcanic ashes as a source cannot be excluded as source material even though volcanic activity in the Late Triassic is not described in the Western Tethyan realm (Haas et al. 2011).

However, deposits situated on top of the Middle Anisian shallow-water carbonates (Steinalm carbonate ramp) could not be proven yet: existing occurrences show a deep erosion and the original (eroded) sedimentary sequence reached originally also the Wetterstein Carbonate Platform niveau. In every case the tested Middle-Late Triassic deposits rest exclusively on top of the Wetterstein Carbonate Platform, which were formed until the earliest Carnian and became drowned or emerged in the Middle Carnian. This emergence show in different regions a significant difference: whereas in most regions of the Western Tethyan realm the Wetterstein Carbonate Platform became flooded in the Middle Carnian, in other regions (mainly of Dinaridic provenance) became emerged for a long time. Flooding of these emerged platform is not contemporaneous in the different regions and differs between the late Carnian and late Norian in dependence on the palaeogeographic position.

However, intensive biostratigraphic studies are needed to verify this results in an overall manner. In addition, the provenance of the bauxite forming rocks is still unknown, but existing models about the bauxite formation cannot explain formation of bauxites in this stratigraphic position.

Samples from this stratigraphic positions, described above contain in most cases significant values of REE (Table 12).

Table 12. Geochemical results of bauxites on top of the Wetterstein Carbonate Platform (age: Middle-Late Carnian).

Locality	SiO_2	Al_2O_3	Fe_2O_3	MnO	MgO	CaO	Na_2O	K_2O	TiO_2	P_2O_5	LOI	Total
	%	%	%	%	%	%	%	%	%	%	%	%
Inner Dinarides	2.12	0.49	0.23	0.023	0.3	53.76	< 0.01	0.07	0.018	0.02	42.11	99.15
Outer Dinarides	9.98	2.81	1.21	0.021	1.36	45.04	0.03	0.92	0.14	0.08	37.31	98.90
Inner Dinarides	12.3	3.36	1.4	0.054	0.97	43.53	0.04	1.1	0.166	0.09	36.23	99.24
Inner Dinarides	92.33	0.8	5.7	0.042	0.04	0.13	< 0.01	0.07	0.025	0.01	0.9	100.1
Inner Dinarides	97.44	1.09	0.9	0.104	0.06	0.05	0.02	0.25	0.176	0.01	0.58	100.7
Outer Dinarides	39.21	32.56	14.15	0.029	0.1	0.18	0.05	0.12	1.632	0.01	12.62	100.7
Outer Dinarides	19.38	48.26	17.23	0.028	0.18	0.05	0.08	0.26	2.093	0.06	12.77	100.4
Outer Dinarides	12	47.08	25.88	0.021	0.62	0.06	0.04	0.32	2.505	0.08	11.94	100.5
Outer Dinarides	38	16.65	5.94	0.088	2.71	14.43	0.44	2.33	0.669	0.05	18.87	100.2
Outer Dinarides	38.93	15.89	5.96	0.079	3.42	14.66	0.27	2	0.652	0.05	18.99	100.9
Outer Dinarides	34.73	15.36	5.85	0.089	2.43	17.19	0.61	1.51	0.66	0.05	20.56	99.03
Outer Dinarides	12.95	54.42	18.13	0.011	0.14	0.07	0.04	0.07	2.105	0.16	12.39	100.5

Table 12. Continued

This activity has received funding from the European Institute of Innovation and Technology (EIT), a body of the European Union, under the Horizon 2020, the EU Framework Programme for Research and Innovation

Locality	Y	La	Ce	Pr	Nd	Sm	Eu	Gd	Tb	Dy	Ho	Er	Tm	Yb	Lu	ΣREE
	ppm	ppm	ppm	ppm	ppm	ppm	ppm	ppm	ppm	ppm	ppm	ppm	ppm	ppm	ppm	ppm
Inner Dinarides	11	6.9	8.4	1.54	6.2	1.4	0.29	1.5	0.2	1.4	0.3	0.8	0.12	0.8	0.12	41.0
Outer Dinarides	19	15.7	19.3	3.47	14.1	2.8	0.65	2.9	0.4	2.6	0.5	1.4	0.21	1.2	0.18	84.4
Inner Dinarides	20	15.9	20.2	3.49	14.6	3	0.67	3	0.5	2.7	0.5	1.5	0.22	1.3	0.21	87.8
Inner Dinarides	1	1.3	3.5	0.27	1	0.2	< 0.05	0.2	< 0.1	0.2	< 0.1	0.1	< 0.05	0.2	0.03	8.0
Inner Dinarides	2	2.5	8	0.63	2.3	0.5	0.11	0.5	< 0.1	0.4	< 0.1	0.3	< 0.05	0.3	0.04	17.6
Outer Dinarides	25	32.2	188	11.5	49.3	10.1	2.13	8.24	1.32	6.94	1.3	3.85	0.609	4.22	0.652	345.4
Outer Dinarides	56	61.1	206	14.8	56.3	12.5	2.75	11.3	1.9	11.9	2.4	7.3	1.17	7.8	1.29	454.5
Outer Dinarides	98	121	285	27.3	107	22.8	5.15	18.9	2.7	15.9	3.5	11	1.77	11.7	1.86	733.6
Outer Dinarides	25	31.7	71.9	7.29	27.9	5.51	1.15	4.91	0.81	4.52	0.9	2.71	0.398	2.71	0.392	187.8
Outer Dinarides	21	23.6	58.3	5.53	21.2	4.29	0.839	3.55	0.59	3.55	0.72	2.1	0.305	2.15	0.345	148.1
Outer Dinarides	28	34.3	73.9	7.91	29.9	6.11	1.18	5.27	0.88	4.89	0.94	2.84	0.419	2.72	0.448	199.7
Outer Dinarides	112	65.6	190	18.2	76.1	18.1	3.83	19.6	3.29	18.3	3.77	10.5	1.55	10.4	1.65	552.9

Karst bauxites in or on top of the Late Triassic Dachstein Carbonate Platform

Until nowadays unknown, but completely enigmatic are the latest Triassic bauxite deposits in the REEBAUX focus area. Detailed investigations on these deposits are practically missing and there is no convincing interpretation about the parent rocks. The Late Triassic is the time span of the formation of the huge Hauptdolomite/Dachstein Carbonate Platform in the Tethyan realm, commonly believed to have formed in a passive continental margin setting with continuous subsidence. Our new results show that in the Late Triassic intense strike-slip motions affected this platform. These lateral motions cut the facies belts of the platform relatively perpendicular, and new pull-apart basins with rapid subsidence were formed. Other areas became emerged and act as source for mass transport deposits in the newly formed basins. These phenomena and the formation of time-equivalent bauxite deposits have not yet been explored. Here there are a lot of basic work needed: age dating, provenance of the host rock, extend in the Western Tethyan realm.

Samples from this stratigraphic positions, described above, contain in most cases significant values of REE (Table 13).

Table 13. Geochemical results of bauxites on top of the Dachstein Carbonate Platform (age: latest Triassic)

Locality	SiO_2	Al_2O_3	Fe_2O_3	MnO	MgO	CaO	Na_2O	K_2O	TiO_2	P_2O_5	LOI	Total
	%	%	%	%	%	%	%	%	%	%	%	%
Tizia	46.19	14.03	11.24	0.156	10.86	0.84	1.81	0.12	1.164	0.11	13.83	100.4
Tizia	47.39	17.92	12.63	0.016	2.03	1.82	0.01	0.42	2.965	0.62	14.36	100.2
Tizia	49.35	12.03	4.59	0.034	6.64	7.43	0.08	4.13	0.573	0.09	15.11	100.1
Tizia	22.24	9.51	3.36	0.017	1.66	31.72	0.06	3.23	0.587	0.04	28.29	100.7

This activity has received funding from the European Institute of Innovation and Technology (EIT), a body of the European Union, under the Horizon 2020, the EU Framework Programme for Research and Innovation

Table 13. Continued

Locality	Y	La	Ce	Pr	Nd	Sm	Eu	Gd	Tb	Dy	Ho	Er	Tm	Yb	Lu	ΣREE
	ppm	ppm	ppm	ppm	ppm	ppm	ppm	ppm	ppm	ppm	ppm	ppm	ppm	ppm	ppm	ppm
Tizia	13	10	12	2.59	11.4	2.65	0.911	2.98	0.51	2.99	0.56	1.5	0.238	1.67	0.266	63.3
Tizia	27	21.5	46.7	5.98	25.7	5.63	1.94	6.21	1.02	5.83	1.13	3.13	0.441	2.81	0.427	155.4
Tizia	20	25.7	52.1	5.99	23.2	4.4	0.851	3.84	0.66	3.83	0.76	2.14	0.341	2.33	0.359	146.5
Tizia	13	22.3	39.8	4.18	14.9	2.66	0.52	2.28	0.4	2.5	0.53	1.69	0.254	1.8	0.286	107.1

Karst bauxites in the Late Jurassic

Another group of bauxite deposits were formed in the latest Jurassic. We like to relate the formation of these deposits to the emplacement of the Neo-Tethys ophiolites and their weathering products (Gawlick & Missoni 2019 with references therein), but this contrasts the actual interpretations. Detailed provenance studies have to clarify in future the controversial discussion. In addition, more detailed palaeogeographic reconstructions and a refinement of the timing of the tectonic motions in Middle-Late Jurassic times is needed for a more precise picture of formation and extend of these kind of deposits in the nappe stack of the orogens in the Circum-Pannonian realm.

Samples from this stratigraphic positions, described above contain in most cases significant values of REE (Table 14).

Table 14. Geochemical results of bauxites on top of various older shallow-water carbonates (age: Tithonian)

Locality	SiO_2	Al_2O_3	Fe_2O_3	MnO	MgO	CaO	Na_2O	K_2O	TiO_2	P_2O_5	LOI	Total
	%	%	%	%	%	%	%	%	%	%	%	%
Outer Dinarides	19.64	46.46	17.94	0.153	0.6	0.25	0.06	0.29	2.164	0.04	12.63	100.2
Outer Dinarides	21.45	8.51	3.14	0.052	0.46	34.52	0.48	0.75	0.389	0.06	30.89	100.7
Northern Calcareous Alps	12.78	45.46	25.47	0.045	1.22	0.09	0.02	0.03	2.177	0.17	12.75	100.2
Northern Calcareous Alps	5.45	4.97	4.37	0.024	0.4	46.36	< 0.01	0.03	0.251	0.03	38.02	99.92

Table 14. Continued

Locality	Y	La	Ce	Pr	Nd	Sm	Eu	Gd	Tb	Dy	Ho	Er	Tm	Yb	Lu	ΣREE
	ppm	ppm	ppm	ppm	ppm	ppm	ppm	ppm	ppm	ppm	ppm	ppm	ppm	ppm	ppm	ppm
Outer Dinarides	61	94.8	128	16.7	58.5	10.7	2.18	9.45	1.75	10.6	2.28	6.84	1.07	7.2	1.13	412.2
Outer Dinarides	46	63.2	60.3	11.7	43.4	7.74	1.59	7.23	1.01	5.42	1.08	2.99	0.394	2.42	0.362	254.8
Northern Calcareous Alps	240	183	219	35.3	138	27.7	6.23	28.8	4.5	27.6	5.9	17	2.46	15.6	2.39	953.5
Northern Calcareous Alps	14	14.2	27.3	3.72	15.3	3.03	0.687	2.82	0.44	2.31	0.46	1.3	0.187	1.24	0.183	87.2

"Middle Cretaceous" bauxites

The "Middle Cretaceous" bauxites are very common in the whole Circum-Pannonian realm for the main reason, that younger tectonic motions, i.e. nappe thrusting is limited in most of area. However, it seems that since the Late Jurassic a huge continent had become formed as result

This activity has received funding from the European Institute of Innovation and Technology (EIT), a body of the European Union, under the Horizon 2020, the EU Framework Programme for Research and Innovation

of the Middle-Late Jurassic orogen formation due to the partial closure of the Neotethys Ocean. This continental realm underwent intensive weathering and erosion, by these in certain areas bauxite deposits were formed widespread on top of different sedimentary rocks, but mainly on the Triassic-Jurassic sequences of the former passive Neotethys passive continental margin.

However, due to the fact that the "Mid-Cretaceous" and younger polyphase tectonic motions and block rotations (Csontos and Vörös, 2004; Pueyo et al., 2007; Schmid et al., 2008) draws a veil over the older Mesozoic plate configuration, several crucial and still topical questions remain (summarized in Gawlick & Misson, 2019, with references therein) and a lot of detailed studies are needed in future to elucidate formation of this bauxite "stratigraphic position".

These bauxites were since a long time studied and a lot of data are available and are therefore not in the focus of defining geological setting within REEBAUX WP2.

Samples from this stratigraphic positions, described above contain in most cases significant values of REE (Table 15).

Table 15. Geochemical results of bauxites on top of various older shallow-water carbonates (age: Mid-Cretaceous)

Locality	SiO_2	Al_2O_3	Fe_2O_3	MnO	MgO	CaO	Na_2O	K_2O	TiO_2	P_2O_5	LOI	Total
	%	%	%	%	%	%	%	%	%	%	%	%
Inner Dinarides	57.22	12.02	15.58	0.31	1.75	0.34	0.07	1.56	0.558	0.03	8.66	98.1
Inner Dinarides	50.76	17.72	6.52	1.556	2.14	1.27	0.14	2.65	0.483	0.11	15.48	98.83
Inner Dinarides	45.58	14.29	8.37	0.239	3.88	9.13	1.76	1.55	1.095	0.16	14.45	100.5
Inner Dinarides	58.77	15.28	8.51	0.161	3.58	3.08	1.58	2.11	1.191	0.14	5.73	100.1
Inner Dinarides	65.32	13.19	5.6	1.245	1.81	0.9	0.23	2.65	0.484	0.11	9.13	100.7
Northern Calcareous Alps	10.63	50.8	22.38	0.163	0.16	0.35	0.04	0.05	1.696	0.18	12.67	99.11
Northern Calcareous Alps	1.19	58.83	23.81	0.122	0.12	0.09	0.02	< 0.01	3.589	0.17	12.29	100.2
Northern Calcareous Alps	19.32	22.99	9.49	0.161	0.91	20.29	0.21	0.57	0.953	0.19	24.58	99.65
Northern Calcareous Alps	4.8	54.73	23.41	0.017	0.1	0.06	0.03	< 0.01	2.96	0.07	13.64	99.82

Table 15. Continued

Locality	Y	La	Ce	Pr	Nd	Sm	Eu	Gd	Tb	Dy	Ho	Er	Tm	Yb	Lu	ΣREE
	ppm	ppm	ppm	ppm	ppm	ppm	ppm	ppm	ppm	ppm	ppm	ppm	ppm	ppm	ppm	ppm
Inner Dinarides	17	23.8	45.5	5.28	19.4	3.9	0.9	3.5	0.6	3.3	0.7	1.9	0.28	1.9	0.28	128.2
Inner Dinarides	29	32	119	9.33	37.4	8.8	1.89	7.3	1.2	6.7	1.3	3.6	0.51	3.3	0.51	261.8
Inner Dinarides	22	14	32.2	3.65	14.9	3.7	1.1	4	0.7	4.3	0.9	2.5	0.37	2.4	0.36	107.1
Inner Dinarides	28	21.6	52.6	5.49	20.9	4.8	1.21	4.8	0.8	5.2	1.1	3.1	0.46	3.1	0.48	153.6
Inner Dinarides	20	26.8	80	6.72	26.5	5.42	1.14	4.81	0.76	4.23	0.81	2.29	0.329	2.15	0.342	182.3
Northern Calcareous Alps	228	208	314	41.2	165	34.1	7.65	33	5.39	31.7	6.59	19.7	2.91	20	3.12	1120.4
Northern Calcareous Alps	140	49.5	185	10.9	43.4	10.9	2.82	14.4	3.11	21.3	4.76	14.8	2.2	15.1	2.46	520.7
Northern Calcareous Alps	147	116	130	22.6	90.1	17.7	4.05	18.3	2.92	17	3.68	10.5	1.51	9.32	1.51	592.2
Northern Calcareous Alps	70	34.3	172	7.95	32.4	7.65	1.89	9.06	1.69	10.5	2.32	7.14	1.09	7.57	1.15	366.7

This activity has received funding from the European Institute of Innovation and Technology (EIT), a body of the European Union, under the Horizon 2020, the EU Framework Programme for Research and Innovation

Palaeogene bauxites

These bauxites were since a long time studied and a lot of data are available and are therefore not in the focus of defining geological setting within WP2 and thus were not tested.

In addition, palaeogeography and polyphase tectonic motions are still discussed controversially. Most authors still follow the multi-ocean reconstructions in the Western Tethyan realm in Triassic times, whereas others are convinced by a one-ocean reconstruction for the Triassic (see Gawlick & Missoni, 2019, for a thorough review). Pangea-breakup in the Jurassic resulted in the Western Tethys realm in the formation of a new oceanic domain related to the opening of the central Atlantic and formed in the northwest. The opening of this oceanic domain resulted in the creation of an more or less isolated continent (wider Adria) between the Alpine Atlantic to the north resp. northwest and the Neo-Tethys in the south resp. southeast. Contemporaneously with the opening of the Alpine Atlantic partial closure of the Neo-Tethys started and commenced with ophiolite obduction in Middle to early Late Jurassic times. These obducted ophiolites rest today as far-travelled allochthonous outliers everywhere and may act as source for the Late Jurassic to Palaeogene bauxites. But the formation of the Triassic bauxites are still hard to explain: their stratigraphic position does not fit to the known existing levels of volcanic activity and other sources are also not known: in a passive continental margin setting with permanent thermal subsidence long-lasting phases of emergence of carbonate platforms as dated e.g. in the Dinarides (Gawlick & Missoni, 2019) are not expectable and the reason for this phenomena is not explored.

This activity has received funding from the European Institute of Innovation and Technology (EIT), a body of the European Union, under the Horizon 2020, the EU Framework Programme for Research and Innovation

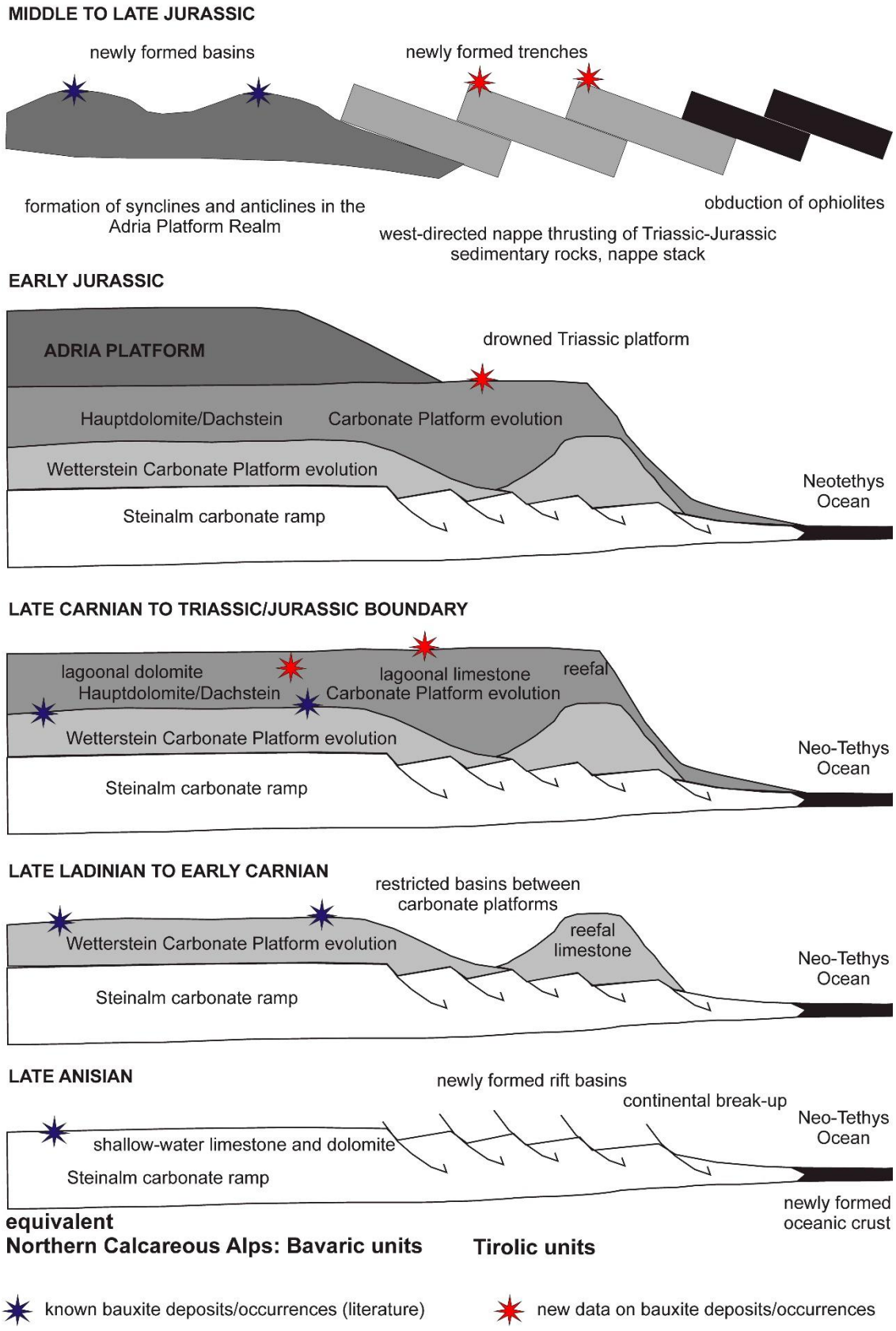

This activity has received funding from the European Institute of Innovation and Technology (EIT), a body of the European Union, under the Horizon 2020, the EU Framework Programme for Research and Innovation

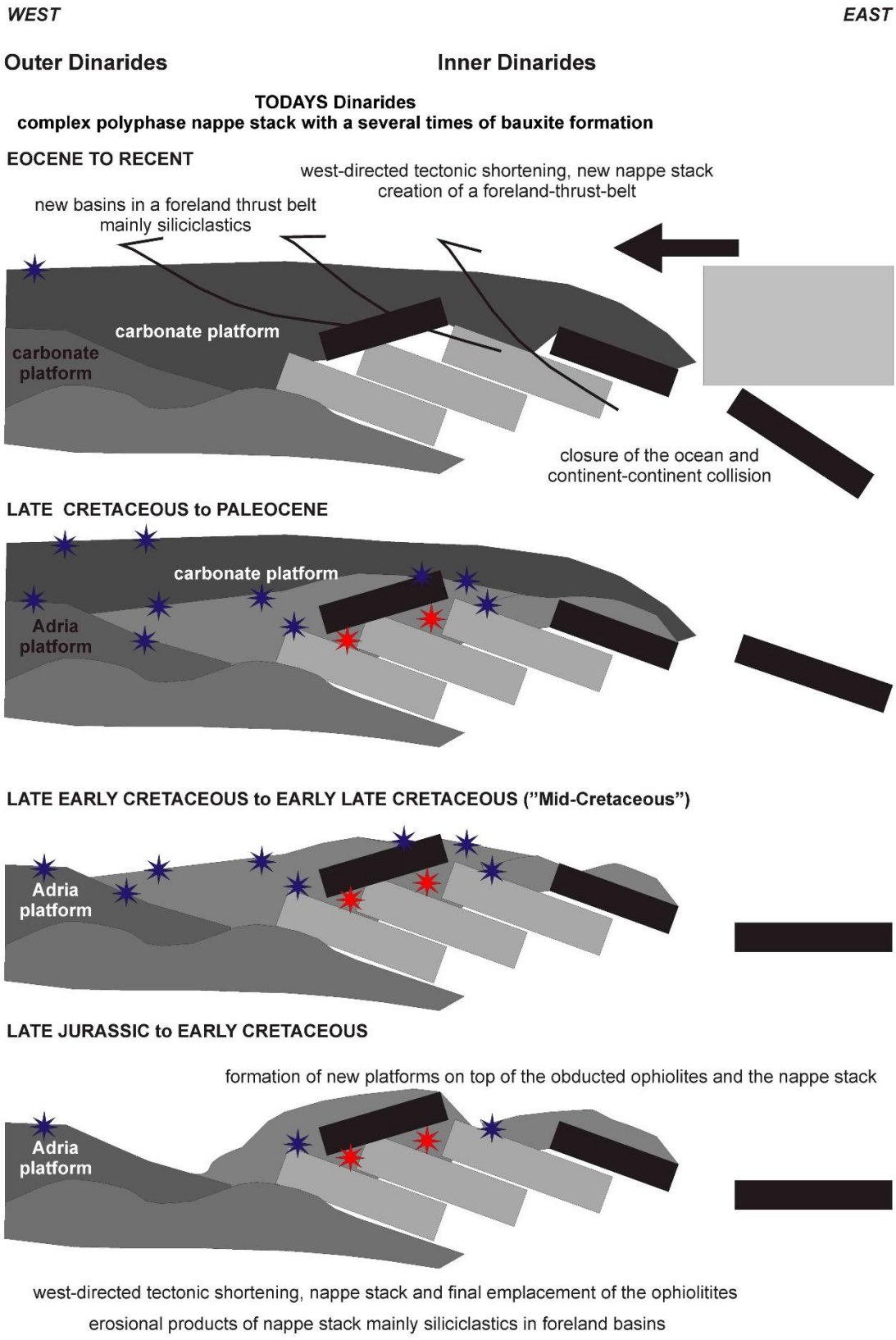

Figure 9. Sedimentological, geological and geodynamic evolution of the Dinarides and equivalent units in the Northern Calcareous Alps (after Gawlick & Missoni, 2019) with stratigraphic position of bauxites (mainly after Timotijevic, 1995, 2001; Grubić, 1999; Marković ,2002; Janković et al., 2003; Pajović et al., 2017 and own unpublished results).

This activity has received funding from the European Institute of Innovation and Technology (EIT), a body of the European Union, under the Horizon 2020, the EU Framework Programme for Research and Innovation

3. BAUXITE RESIDUE (RED MUD) ACCUMULATIONS OF THE ESEE REGION (Hungary, Montenegro, Slovenia) and their REE potential.

Red mud samples were collected at three red mud landfills in the focus countries within WP3 REEBAUX activities:

1. Slovenia – Kidričevo red mud landfill near Maribor. The ladfill has not been in use since early 1990-ties. The site of the ladfill has been remediated with complete enclosure with earth material and planting grass over it. However, the remediation has been done only on surface, and there is no insulation of the landfill basement from the underlying sediments and aquifer. The overall depth of the deposited red mud is not known, but has been estimated to be, on average, about 4 m. Currently there is a solar power plant on the premises. Thus, the sample of red mud for the analytical work had to be collected by a sample corer through the outer earth cover. The accumulation of red mud is estimated at 1,6 mil. tonnes.
2. Montenegro – Podgorica red mud landfill in Podgorica (Figure 10A and 10B). There is no deposition of new red mud since 2009 as the production of the alumina in the nearby plant has been abandoned. The landfill has not been remediated so far, and red mud is available for sampling. Altogether drilling at six boreholes was performed in order to recover the samples for the analyses. The maximum depth reached during drilling was 12 m. The accumulation of red mud is estimated at 7.5 mil. tonnes.
3. Hungary – Ajka landfill (Figure 10C). The landfill is closed for further deposition of red mud after red mud spilling accident in 2010. The samples for the analyses were recovered from three red mud accumulation cells (VII, VIII and IX) by drilling up to a depth of 15 m. The accumulation of red mud in Ajka landfill are estimated at 35 mil. tonnes.
4. Hungary – Almásfüzítő landfill (Figure 10D and 10E). Construction of the first ladfill started in 1950. The filling of the landfill ended in 1994. Altogether seven (from I to VII) accumulation cassettes were totally filled up. None of the cassettes had any kind of technological protection. Due to the environmental and health hazards of the red mud, the remediation of the ladfill started in the 1980s and several approaches have been used. Until today almost all red mud cassettes have been remediated and covered. Only a small part of the cassette VII., the largest one, is still uncovered. Within REEBAUX WP3 activities all red mud samples were collected by drilling core from the uncovered portion of the cassette VII. The total area of the landfill is 167 ha with a rage of red mud thickness of 6-11 m. The accumulated red mud is estimated at 16.85 tonnes (Naturaqua, 2014).

All red mud samples collected within REEBAUX WP3 activities are presented in Table 16.

This activity has received funding from the European Institute of Innovation and Technology (EIT), a body of the European Union, under the Horizon 2020, the EU Framework Programme for Research and Innovation

Abundances of major elements are presented in Table 17 and those of REE in Table 18.

Table 16. Red mud samples collected in Slovenia, Montenegro and Hungary within REEBAUX WP3 activities

Sample set (if applicable)	Sample ID	Sampling depth (m)	Latitude	Longitude
Slovenia (Kidričevo accumulation)				
Kidričevo	KD-1		46°23'47.4" N	15°45'46.8" E
Montenegro (Podgorica accumulation)*				
Landfil B (borehole B-1/19)	CGBR 01	0-4	42°21'01.2'' N	19°13'17.1'' E
	CGBR 02	4-7.5		
	CGBR 03	7.5-10.5		
Landfil A (borehole B-2/19)	CGBR 04	0-3	42°23'06.2'' N	19°13'14.4'' E
	CGBR 05	3-7		
	CGBR 06	7-11		
Landfil A (borehole B-3/19)	CGBR 07	0-3	42°23'12.1'' N	19°12'57.9'' E
	CGBR 08	3-6		
	CGBR 09	6-10		
Landfil A (borehole B-4/19)	CGBR 10	0-4	42°23'03.2'' N	19°12'55.3'' E
	CGBR 11	4-7		
	CGBR 12	7-10		
Landfil B (borehole B-5/19)	CGBR 13	0-3	42°22'55.7'' N	19°12'57.1'' E
	CGBR 14	3-6		
	CGBR 15	6-9		
	CGBR 16	9-12		
Landfil B (borehole B-6/19)	CGBR 17	0-3	42°22'45.9'' N	19°13'06.6'' E
	CGBR 18	3-6		
	CGBR 19	6-9		
	CGBR 20	9-12		
Hungary (Ajka accumulation)				
Cell No. IX.	A-19	2	47°05'17.2''N	17°30'30.3''E
	A-20	2.5		
	A-21	3		
	A-22	4		
	A-23	5		
	A-24	6		
	A-25	7		
	A-26	8		
	A-27	9		
	A-28	10		
	A-29	11		
	A-30	12		
	A-31	13		
	A-32	14		

This activity has received funding from the European Institute of Innovation and Technology (EIT), a body of the European Union, under the Horizon 2020, the EU Framework Programme for Research and Innovation

Sample set (if applicable)	Sample ID	Sampling depth (m)	Latitude	Longitude
	A-33	15		
Cell No. VIII.	A-50	1	47°05'19.4''N	17°30'48.2''E
	A-51	2		
	A-52	3		
	A-53	4		
	A-54	5		
	A-55	6		
	A-56	7		
	A-57	8		
	A-58	9		
	A-59	10		
	A-60	11		
	A-61	12		
	A-62	13		
	A-63	14		
	A-64	15		
	A-65	16		
Cell No. VII.	A-80	1.5	47°05'22.9''N	17°31'28.5''E
	A-81	2.5		
	A-82	3.5		
	A-83	4.5		
	A-84	5.5		
	A-85	6.5		
	A-86	7.5		
	A-87	8.5		
	A-88	9.5		
	A-89	10.2		
	A-90	10.5		
Hungary (Almásfüzítő accumulation)				
Cassette VII.	Ny 1/2	0.15-0.30	47°43'24.7''	18°16'29.9''
	Ny 1/4	0.45-0.60		
	Ny 2/2	0.15-0.30	47°43'34.7''	18°16'25.5''
	Ny 2/8	1.05-1.20		
	Ny 3/4	0.45-0.60	47°43'49.0''	18°16'26.0''

*Composite samples (3-4 subsamples per sampling interval)

This activity has received funding from the European Institute of Innovation and Technology (EIT), a body of the European Union, under the Horizon 2020, the EU Framework Programme for Research and Innovation

Figure 10A. Red mud landfill near Podgorica in Montenegro during sample collection

Figure 10B. Drilling activities in the red mud landfill near Podgorica within WP3 tasks

This activity has received funding from the European Institute of Innovation and Technology (EIT), a body of the European Union, under the Horizon 2020, the EU Framework Programme for Research and Innovation

Figure 10C. Aerial view of Ajka red mud landfill with indication of drilling positions along red mud accumulation cells No. VII., VIII. and IX.

Figure 10D. Aerial view of Almásfüzítő red mud landfill. Red mud cassettes I-II., III., IV., V., VI. are surrounded by agricultural lands (S), settlement of Almasfüzítő (E) and settlement of Nagykolónia (W) and Danube River (N). Red mud cassette VII. is located the eastern side of the settlement of Almásfüzítő, and its borderline is very close to the Danube River (N) and a narrow wetland area (SE). The studied samples are derived from the cassette VII. (Figure 10E.).

This activity has received funding from the European Institute of Innovation and Technology (EIT), a body of the European Union, under the Horizon 2020, the EU Framework Programme for Research and Innovation

Figure 10E. Sampling process in Almásfüzítő red mud cassette at Ny1 drilling point. The sampling was carried out by soil hand drill.

This activity has received funding from the European Institute of Innovation and Technology (EIT), a body of the European Union, under the Horizon 2020, the EU Framework Programme for Research and Innovation

Table 17. Major constituents in the red mud samples collected within REEBAUX WP3 activities in Slovenia, Montenegro and Hungary

Sample set (if applicable)	Sample ID	Sampling depth (m)	SiO_2	Al_2O_3	Fe_2O_3	MgO	CaO	Na_2O	K_2O	TiO_2	P_2O_5	MnO	Cr_2O_3	Ba	Ni	Sc	LOI	Sum
			%	%	%	%	%	%	%	%	%	%	%	ppm	ppm	ppm	%	%
SLOVENIA (Kidričevo red mud landfill)																		
Kidričevo	KD-1		8.61	23.72	31.39	0.56	8.34	3.92	0.13	6.86	0.19	0.14	0.188	87	283	85	15.4	99.46
MONTENEGRO (Podgorica red mud landfill)*																		
Landfil B (borehole B-1/19)	CGBR 01	0-4	9.43	29.98	27.13	0.56	5.89	4.35	0.28	3.51	0.25	0.17	0.082	76	177	81	17.9	99.54
	CGBR 02	4-7.5	13.12	22.24	26.5	0.69	11.91	4.27	0.35	3.66	0.23	0.2	0.086	77	202	81	16.2	99.5
	CGBR 03	7.5-10.5	25.17	11.27	12.25	1.19	22.9	2.1	0.7	1.65	0.08	0.11	0.06	95	141	35	22.3	99.76
Landfil A (borehole B-2/19)	CGBR 04	0-3	10.97	25.06	30.24	0.68	7.56	4.76	0.34	4.29	0.1	0.24	0.09	75	231	93	15.1	99.51
	CGBR 05	3-7	11.96	21.63	34.47	0.58	6.38	6.29	0.36	4.37	0.11	0.27	0.098	75	246	105	12.9	99.43
	CGBR 06	7-11	10.91	21.88	34.39	0.63	7.57	5.59	0.28	4.92	0.09	0.26	0.103	76	258	107	12.8	99.44
Landfil A (borehole B-3/19)	CGBR 07	0-3	8.86	31.12	29.75	0.51	4.27	5.02	0.34	4.16	0.1	0.2	0.086	72	198	92	15	99.44
	CGBR 08	3-6	10.45	25.08	32.21	0.55	4.9	6.51	0.36	4.5	0.07	0.24	0.093	78	224	100	14.5	99.48
	CGBR 09	6-10	10.49	23.3	33.77	0.65	6.02	6.5	0.28	4.72	0.08	0.25	0.101	72	244	106	13.2	99.46
Landfil A (borehole B-4/19)	CGBR 10	0-4	11.47	21.92	35.97	0.57	4.9	6.18	0.38	5.07	0.08	0.28	0.106	86	252	114	12.4	99.43
	CGBR 11	4-7	10.86	23.03	33.94	0.6	7.3	5.59	0.28	4.64	0.07	0.25	0.098	75	238	105	12.7	99.45
	CGBR 12	7-10	10.47	26.9	32.4	0.6	5.37	5.76	0.27	4.56	0.07	0.24	0.095	72	248	101	12.7	99.47
Landfil B (borehole B-5/19)	CGBR 13	0-3	10.47	17.38	31.98	0.79	12.56	5.06	0.34	3.92	0.16	0.21	0.085	71	196	95	16.5	99.47
	CGBR 14	3-6	13.35	19.04	35.22	0.61	6.1	7.67	0.35	4.8	0.11	0.32	0.099	83	250	113	11.6	99.38
	CGBR 15	6-9	11.59	19.39	39.08	0.55	4.74	6.57	0.32	5.48	0.11	0.29	0.11	83	263	124	11.1	99.36
	CGBR 16	9-12	11.94	20.42	37.67	0.56	4.53	6.96	0.34	5.26	0.12	0.29	0.11	84	257	120	11.1	99.37
Landfil B (borehole B-6/19)	CGBR 17	0-3	12.4	19.76	33.67	0.72	8.68	6.16	0.41	4.27	0.12	0.22	0.091	91	234	99	12.9	99.43
	CGBR 18	3-6	12.28	19.54	35.34	0.68	7.02	6.87	0.4	4.73	0.11	0.26	0.101	91	246	108	12	99.4
	CGBR 19	6-9	12.36	19.86	38.55	0.54	3.62	7.36	0.38	5.45	0.1	0.31	0.113	88	255	123	10.7	99.37
	CGBR 20	9-12	12.72	19.41	37.71	0.56	4.12	7.82	0.36	5.34	0.11	0.33	0.11	82	253	122	10.7	99.35
HUNGARY (Ajka red mud landfill)																		
Cell No. IX.	A-19	2	9.54	14.28	40.36	0.83	9.12	5.09	0.09	3.61	0.43	0.71						84.06
	A-20	2.5	12.6	15.96	39.34	0.78	8.04	7.22	0.1	3.94	0.79	0.76						89.53
	A-21	3	14.22	17.91	36.03	0.86	7.03	8.56	0.13	4.13	0.82	0.43						90.12
	A-22	4	12.96	17.05	39.23	0.77	6.76	7.73	0.09	4	0.75	0.3						89.64

This activity has received funding from the European Institute of Innovation and Technology (EIT), a body of the European Union, under the Horizon 2020, the EU Framework Programme for Research and Innovation

Sample set (if applicable)	Sample ID	Sampling depth (m)	SiO_2	Al_2O_3	Fe_2O_3	MgO	CaO	Na_2O	K_2O	TiO_2	P_2O_5	MnO	Cr_2O_3	Ba	Ni	Sc	LOI	Sum
			%	%	%	%	%	%	%	%	%	%	%	ppm	ppm	ppm	%	%
	A-23	5	14.06	17.27	36.96	0.75	7.22	8.44	0.13	4.2	0.71	0.37						90.11
	A-24	6	13.58	16.46	35.21	0.53	9.97	7.32	0.09	3.67	0.62	0.29						87.74
	A-25	7	12.35	15.12	35.35	0.51	10.4	6.35	0.09	3.79	0.49	0.28						84.73
	A-26	8	11.78	14.68	34.88	0.67	11.46	5.91	0.09	3.74	0.47	0.23						83.91
	A-27	9	10.26	15.4	34.77	0.69	13.88	5.2	0.06	3.35	0.43	0.21						84.25
	A-28	10	11.45	14.94	38.55	0.99	10.16	6.15	0.06	3.77	0.47	0.21						86.75
	A-29	11	12.1	15.25	35.43	0.69	12.05	6.3	0.07	3.62	0.47	0.22						86.2
	A-30	12	11.75	14.95	34.98	0.56	11.39	6.06	0.07	3.64	0.45	0.24						84.09
	A-31	13	12.05	14.87	37.4	0.66	7.99	6.63	0.08	4	0.42	0.25						84.35
	A-32	14	13.2	15.92	36.51	0.67	8.75	7.54	0.08	3.89	0.46	0.27						87.29
	A-33	15	12.98	15.68	36.49	0.69	9.51	7.24	0.08	3.89	0.54	0.28						87.38
Cell No. VIII.	A-50	1	11.39	16.18	40.61	1.5	7.62	6.27	0.13	4.01	0.79	0.39						88.89
	A-51	2	8.51	14.98	41.78	1.87	9.48	4.41	0.09	3.21	0.58	0.41						85.32
	A-52	3	13.33	16.82	37.29	0.9	8.22	7.61	0.14	3.85	0.55	0.28						88.99
	A-53	4	13.82	16.6	35.9	0.67	10.01	7.46	0.1	3.91	0.92	0.31						89.7
	A-54	5	11.76	15.99	37.56	2.39	9.22	6.77	0.09	3.76	0.43	0.27						88.24
	A-55	6	11.31	15.71	37.16	2.41	10.83	6.36	0.07	3.56	0.52	0.26						88.19
	A-56	7	13.13	17.12	37.12	1.59	8.98	7.89	0.09	3.98	0.48	0.26						90.64
	A-57	8	12.79	17.2	37.97	1.31	7.86	7.68	0.06	4.05	0.51	0.32						89.75
	A-58	9	12.57	16.33	37.26	1.43	9.47	7.24	0.07	3.91	0.47	0.25						89
	A-59	10	13.23	16.53	37.61	1.27	9.84	8.38	0.06	4.04	0.52	0.26						91.74
	A-60	11	11.69	15	37.2	1.15	9.84	6.66	0.06	3.93	0.52	0.27						86.32
	A-61	12	12.12	15.66	37.48	1.25	8.87	7.07	0.07	4.04	0.4	0.25						87.21
	A-62	13	12.44	15.66	39.28	1.01	6.28	7.64	0.07	4.26	0.34	0.24						87.22
	A-63	14	12.48	15.68	38.46	1.01	7.38	7.5	0.07	4.1	0.38	0.25						87.31
	A-64	15	12.68	15.85	38.95	0.62	6.24	7.98	0.06	4.24	0.35	0.28						87.25
	A-65	16	11.26	16.34	37.63	0.7	7.97	6.32	0.08	4.1	0.36	0.24						85
Cell No. VII.	A-80	1.5	10.84	17.36	37.41	1.2	7.91	5.84	0.25	3.91	0.34	0.2	0.09				12.7	98.05
	A-81	2.5	11.19	16.66	35.99	0.91	10.01	5.77	0.06	3.94	0.24	0.21	0.09				12.15	97.22
	A-82	3.5	12.49	16.71	36.95	0.95	8.87	6.9	0.08	3.85	0.48	0.2	0.1				11.8	99.38

This activity has received funding from the European Institute of Innovation and Technology (EIT), a body of the European Union, under the Horizon 2020, the EU Framework Programme for Research and Innovation

Sample set (if applicable)	Sample ID	Sampling depth (m)	SiO_2	Al_2O_3	Fe_2O_3	MgO	CaO	Na_2O	K_2O	TiO_2	P_2O_5	MnO	Cr_2O_3	Ba	Ni	Sc	LOI	Sum
			%	%	%	%	%	%	%	%	%	%	%	ppm	ppm	ppm	%	%
	A-83	4.5	14.11	16.38	42.07	0.6	1.85	9.28	0.07	4.69	0.17	0.23	0.1				8.96	98.51
	A-84	5.5	14.14	16.89	40.47	0.92	2.88	9.09	0.07	4.5	0.24	0.23	0.09				9.71	99.23
	A-85	6.5	13.49	16.53	37.79	0.64	7.33	7.55	0.08	3.88	0.12	0.18	0.09				11.6	99.28
	A-86	7.5	12.98	17.59	40.04	0.44	4.88	7.94	0.07	4.36	0.14	0.19	0.1				10.8	99.53
	A-87	8.5	12.26	16.46	38.85	0.5	6.52	7.05	0.06	4.19	0.18	0.18	0.09				12.1	98.44
	A-88	9.5	12.29	16.55	38.67	0.45	6.34	7.02	0.06	4.28	0.26	0.17	0.09				11.35	97.53
	A-89	10.2	12.6	16.68	38.54	0.33	6.55	7.31	0.06	4.1	0.15	0.17	0.09				11.65	98.23
	A-90	10.5	14.11	17.71	38.6	0.38	5.86	8.21	0.1	4.12	0.15	0.17	0.09				12.25	101.75
HUNGARY (Almásfüzítő red mud landfill) **																		
Casette VII.	Ny 1/2 (fg)	0.15-0.30	-	16,32	29,61	0,73	5,78	6,63	0,11	2,54	0,36	0,32	0,07					
	Ny 1/4 (fg)	0.45-0.60	-	14,58	29,29	0,91	5,57	6,65	0,07	1,94	0,36	0,31	0,06					
	Ny 2/2 (cg)	0.15-0.30	-	7,24	42,41	4,14	11,28	2,17	0,05	1,24	0,21	0,41	0,07					
	Ny 2/8 (cg)	1.05-1.20	-	7,26	33,30	4,46	15,00	2,11	0,05	0,93	0,14	0,23	0,05					
	Ny 3/4 (fg)	0.45-0.60	-	14,33	26,68	1,02	8,02	6,46	0,09	2,25	0,38	0,33	0,06					

*Composite samples (3-4 subsamples per sampling interval)

**Mass balance calculation based on the grain size fractions of samples and their masses (for sample Ny 2/2, for the calculation of major elements, values of the following three grain fractions (>2 mm, 0,5-1 mm, 0,125-0,25 mm) were used from Ny 2/8 sample). Note: SiO_2 was not analysed. fg - fine grained red mud, cg - coarse grained red mud.According to the bulk compositions, the fine grained samples (Ny1/2, 1/4, 3/4) have higher Al_2O_3 and Na_2O content and lower MgO and CaO content than the coarse grained samples (Ny 2/2, 2/8), whereas the latter ones show elevated Fe_2O_3 concentration compared to the others.

This activity has received funding from the European Institute of Innovation and Technology (EIT), a body of the European Union, under the Horizon 2020, the EU Framework Programme for Research and Innovation

Table 18. REE abundances (in ppm) in the red mud samples collected within REEBAUX WP3 activities in Slovenia, Montenegro and Hungary

Sample set (if applicable)	Sample ID	Sampling depth (m)	Y	La	Ce	Pr	Nd	Sm	Eu	Gd	Tb	Dy	Ho	Er	Tm	Yb	Lu	ΣLREE	ΣHREE	ΣREE
SLOVENIA (Kidričevo red mud landfill)																				
Kidričevo	KD-1		130.8	181.8	363.3	32.98	116.1	20.75	4.45	19.05	3.42	21.95	4.93	15.22	2.27	15.49	2.39	719.38	215.52	934.9
MONTENEGRO (Podgorica red mud landfill)*																				
Landfil B (borehole B-1/19)	CGBR 01	0-4	121.50	199.70	409.60	39.48	148.50	28.17	5.78	24.67	3.88	22.47	4.70	13.94	2.09	13.97	2.16	831.23	209.38	1040.61
	CGBR 02	4-7.5	128.60	204.40	424.70	40.52	148.40	28.34	5.93	25.19	4.10	24.04	4.97	14.97	2.23	15.30	2.31	852.29	221.71	1074
	CGBR 03	7.5-10.5	58.20	86.30	183.00	17.24	66.30	12.20	2.60	11.22	1.70	10.24	2.16	6.34	0.97	6.77	1.02	367.64	98.62	466.26
Landfil A (borehole B-2/19)	CGBR 04	0-3	153.40	239.70	491.20	46.74	174.40	32.79	6.68	28.35	4.63	27.38	5.70	17.33	2.54	17.24	2.68	991.51	259.25	1250.76
	CGBR 05	3-7	177.20	357.40	575.30	64.78	241.10	44.18	9.11	38.23	5.91	34.41	6.96	19.64	3.03	19.51	3.05	1291.87	307.94	1599.81
	CGBR 06	7-11	180.90	287.90	556.40	56.18	206.20	40.56	7.90	34.69	5.46	31.52	6.77	20.16	2.99	20.30	3.17	1155.14	305.96	1461.1
Landfil A (borehole B-3/19)	CGBR 07	0-3	166.00	275.50	487.10	52.76	195.60	36.91	7.46	32.24	5.08	29.23	6.09	18.20	2.67	18.46	2.77	1055.33	280.74	1336.07
	CGBR 08	3-6	167.90	275.20	535.80	51.99	191.80	35.52	7.35	32.34	5.06	29.46	6.21	18.57	2.80	18.43	2.90	1097.66	283.67	1381.33
	CGBR 09	6-10	172.50	273.50	554.80	55.51	208.30	40.27	8.26	35.05	5.42	32.20	6.68	20.06	2.95	19.78	3.02	1140.64	297.66	1438.3
Landfil A (borehole B-4/19)	CGBR 10	0-4	189.00	311.20	603.20	60.08	217.30	41.18	8.60	36.51	5.72	34.50	7.05	22.02	3.21	21.52	3.27	1241.56	322.8	1564.36
	CGBR 11	4-7	173.20	281.20	561.80	55.05	199.60	38.33	7.93	33.79	5.30	31.29	6.36	19.52	2.84	19.38	2.94	1143.91	294.62	1438.53
	CGBR 12	7-10	173.10	279.10	542.70	54.60	204.90	39.10	8.09	34.38	5.42	31.97	6.58	19.11	2.90	19.58	2.93	1128.49	295.97	1424.46
Landfil B (borehole B-5/19)	CGBR 13	0-3	154.10	261.70	534.30	54.22	205.50	39.24	8.13	34.39	5.06	29.24	5.98	16.85	2.44	16.57	2.51	1103.09	267.14	1370.23
	CGBR 14	3-6	208.40	408.00	583.50	74.41	283.20	51.69	10.79	47.76	7.01	40.20	8.04	23.20	3.33	22.11	3.35	1411.59	363.4	1774.99
	CGBR 15	6-9	222.50	352.70	649.20	65.17	234.50	43.95	9.38	41.27	6.47	38.29	8.13	23.46	3.64	24.18	3.58	1354.9	371.52	1726.42
	CGBR 16	9-12	223.00	366.80	619.20	68.43	254.00	46.97	9.72	43.48	6.74	40.25	8.15	24.26	3.57	23.47	3.60	1365.12	376.52	1741.64
Landfil B (borehole B-6/19)	CGBR 17	0-3	169.10	309.30	577.60	64.97	245.80	46.41	9.12	39.23	5.80	32.25	6.48	19.27	2.74	18.19	2.80	1253.2	295.86	1549.06
	CGBR 18	3-6	185.00	325.30	602.70	64.62	238.00	44.73	9.11	38.95	6.06	34.43	7.15	20.22	3.03	20.56	3.10	1284.46	318.5	1602.96
	CGBR 19	6-9	221.30	364.00	655.90	64.78	231.10	43.22	8.96	40.06	6.44	38.16	8.08	23.62	3.50	23.88	3.67	1367.96	368.71	1736.67
	CGBR 20	9-12	224.00	388.20	637.40	69.78	256.00	45.89	9.74	42.59	6.62	39.41	8.13	23.47	3.50	23.35	3.57	1407.01	374.64	1781.65
HUNGARY (Ajka red mud landfill)																				
Cell No. IX.	A-19	2	94.8	155	368	34.3	127.5	24.6	4.7	21.2	3.2	19.6	4	10.7	1.9	11.4	1.8	714.1	168.6	882.7

This activity has received funding from the European Institute of Innovation and Technology (EIT), a body of the European Union, under the Horizon 2020, the EU Framework Programme for Research and Innovation

Sample set (if applicable)	Sample ID	Sampling depth (m)	Y	La	Ce	Pr	Nd	Sm	Eu	Gd	Tb	Dy	Ho	Er	Tm	Yb	Lu	ΣLREE	ΣHREE	ΣREE
	A-20	2.5	125	191	386	44.1	164.5	33	6	27.6	3.8	22.6	4.4	12.5	2.2	12	2	824.6	212.1	1036.7
	A-21	3	137	225	419	50.3	191	35.3	7.1	30.3	4.2	24.8	5	14.2	2.4	13.2	2.2	927.7	233.3	1161
	A-22	4	137	196	411	45	174	33.8	6.3	28.4	4	24.3	5	13.9	2.3	13.8	2.1	866.1	230.8	1096.9
	A-23	5	128.5	218	420	48.9	183.5	32.8	7	29.1	4.2	24.7	4.9	14.2	2.2	13.2	2.2	910.2	223.2	1133.4
	A-24	6	170	231	438	52.7	202	37.3	7.3	32.2	4.8	27.5	5.6	16.2	2.6	15.9	2.4	968.3	277.2	1245.5
	A-25	7	158	236	460	52.8	201	38.2	6.8	30.5	4.4	26.7	5.2	14.8	2.6	14.5	2.4	994.8	259.1	1253.9
	A-26	8	160.5	227	489	51.2	193.5	36.5	7.3	30.2	4.4	27.3	5.4	16.8	2.9	16.5	2.5	1004.5	266.5	1271
	A-27	9	119.5	173	413	39.1	144	25.8	5.7	25.1	3.7	22.3	4.6	12.2	2.2	13.1	2.1	800.6	204.8	1005.4
	A-28	10	110.5	170	389	38.3	145	26	5	22.4	3.5	20.6	4	12	2.2	12.2	1.9	773.3	189.3	962.6
	A-29	11	138	216	443	48.4	182	32.7	6.6	27.9	3.9	24	4.9	14.5	2.4	14.4	2.4	928.7	232.4	1161.1
	A-30	12	151	217	451	49.7	185	32.6	6.5	30.1	4.3	25.3	5.1	15	2.5	14.8	2.5	941.8	250.6	1192.4
	A-31	13	169.5	244	490	52.8	204	36.1	7.1	32.9	4.6	27.7	5.7	16.7	2.7	16.3	2.7	1034	278.8	1312.8
	A-32	14	163.5	238	464	54.9	204	37.3	7	30	4.5	27	5.3	16.9	2.8	16.1	2.6	1005.2	268.7	1273.9
	A-33	15	163.5	239	466	52.7	197.5	35	7.4	32.6	4.7	27.7	5.6	16.2	2.8	16.3	2.6	997.6	272	1269.6
Cell No. VIII.	A-50	1	127.5	176	375	40.2	151.5	30.2	6.13	28.2	4.03	25	4.99	14.25	2.43	13.2	2.17	779.03	221.77	1000.8
	A-51	2	103	123	295	28.9	110.5	22.9	4.83	22.6	3.49	20.4	4.23	11.9	1.95	10.85	1.8	585.13	180.22	765.35
	A-52	3	143.5	210	431	47.9	179	34.4	6.89	30	4.3	26.7	5.52	15.35	2.63	14.6	2.39	909.19	244.99	1154.18
	A-53	4	166.5	239	437	53.6	203	36	7.28	32.8	4.6	28.2	5.46	15.8	2.82	15.1	2.59	975.88	273.87	1249.75
	A-54	5	131.5	200	419	44.8	170.5	31.5	6.47	28.9	4.19	24.9	4.86	14.4	2.34	13.9	2.33	872.27	227.32	1099.59
	A-55	6	120	177	372	39.1	151.5	28	5.89	25.3	3.88	22.8	4.4	13.65	2.22	12.85	2.15	773.49	207.25	980.74
	A-56	7	141	204	428	45.9	166.5	30.9	5.87	26.9	4.03	24.6	4.95	14.35	2.37	14	2.2	881.17	234.4	1115.57
	A-57	8	141	232	458	51.8	192.5	34.7	6.67	28.8	4.25	24.7	5.12	15.1	2.53	14.8	2.39	975.67	238.69	1214.36
	A-58	9	143.5	223	447	48.1	182.5	32.1	6.68	28.6	4.04	25.1	5.03	15.45	2.15	15.05	2.21	939.38	241.13	1180.51
	A-59	10																0	0	0
	A-60	11	148	225	467	50.1	187.5	33.4	6.72	28.4	4.15	24.3	4.97	14.9	2.47	14.2	2.44	969.72	243.83	1213.55
	A-61	12	173	251	534	55.9	206	39.6	7.2	33.9	4.89	30.8	6.27	18.05	3.08	17.15	2.91	1093.7	290.05	1383.75
	A-62	13	145.5	218	467	46.9	174	31.5	6.58	28.5	4.22	25.9	5.14	15.4	2.7	15.75	2.69	943.98	245.8	1189.78

This activity has received funding from the European Institute of Innovation and Technology (EIT), a body of the European Union, under the Horizon 2020, the EU Framework Programme for Research and Innovation

Sample set (if applicable)	Sample ID	Sampling depth (m)	Y	La	Ce	Pr	Nd	Sm	Eu	Gd	Tb	Dy	Ho	Er	Tm	Yb	Lu	ΣLREE	ΣHREE	ΣREE
	A-63	14	145	221	459	48.1	180.5	33.2	6.33	27.7	4.03	25	5.13	14.6	2.49	14.2	2.24	948.13	240.39	1188.52
	A-64	15	152.5	229	472	50.2	183.5	34.1	6.71	28.8	4.11	24.7	5.12	14.45	2.63	14.85	2.37	975.51	249.53	1225.04
	A-65	16	178	239	468	55.2	207	39.1	7.83	33.5	4.79	30.4	5.96	16.55	2.94	16.5	2.82	1016.13	291.46	1307.59
Cell No. VII.	A-80	1.5	141.5	203	411	44.3	171.5	35	6.9	29.2	4.3	26.3	5.2	15.6	2.1	16	2.5	871.7	242.7	1114.4
	A-81	2.5	154	230	447	50.7	192.5	38.2	6.8	28.9	4.5	26.8	5.3	15.5	2.3	16.3	2.6	965.2	256.2	1221.4
	A-82	3.5	158	219	420	49.2	187	37.1	7	30.4	4.4	26.3	5.6	16	2.3	16.3	2.6	919.3	261.9	1181.2
	A-83	4.5	122	241	494	49.7	176.5	31.7	6	24.7	3.8	24	4.7	14	2.1	14.9	2.5	998.9	212.7	1211.6
	A-84	5.5	133	231	457	50.5	180.5	33.8	6.5	26.5	4	24.5	5.1	14.7	2.1	15.3	2.5	959.3	227.7	1187
	A-85	6.5	102	226	456	45.7	163.5	28.9	5.3	21.4	3.2	19.4	3.9	10.8	1.7	11.6	1.8	925.4	175.8	1101.2
	A-86	7.5	114	206	423	42	148	26.8	5.1	21.4	3.3	19.4	4.2	12.2	1.7	12.5	2.1	850.9	190.8	1041.7
	A-87	8.5	87	181	385	35.2	120.5	20.8	3.8	16.4	2.4	15.9	3.2	9.7	1.4	10.6	1.7	746.3	148.3	894.6
	A-88	9.5	87.8	176	367	34.4	117	22.2	3.6	15.5	2.5	15.4	3.2	9.9	1.5	11.5	1.8	720.2	149.1	869.3
	A-89	10.2	86.5	173	358	32.1	107	19.5	3.5	15.9	2.4	15	3.2	9.5	1.5	10.9	1.7	693.1	146.6	839.7
	A-90	10.5	86.2	169	350	30.7	104	18.6	3.7	15.3	2.3	14.9	3	9	1.3	10.3	1.6	676	143.9	819.9
HUNGARY (Almásfüzítő red mud landfill)																				
Cassette VII.	1/2(fg)	0.15-0.30	128.2	183.4	281.3	39.0	151.7	29.2	6.0	26.8	3.7	23.1	4.0	12.1	1.7	12.2	1.7	690.7	213.5	904.2
	1/4(fg)	0.45-0.60	116.1	139.4	196.9	28.9	114.5	22.6	4.9	20.5	3.0	18.8	3.3	9.9	1.4	10.7	1.6	507.2	185.3	692.5
	2/2(cg)**	0.15-0.30	61.5	91.9	163.8	19.1	74.3	14.9	3.2	14.4	2.1	13.9	2.4	7.0	0.9	6.6	0.9	367.2	109.9	477.1
	2/8(cg)	1.05-1.20	52.9	79.7	144.2	17.0	64.6	12.7	2.8	12.0	1.8	11.4	2.0	5.9	0.8	5.7	0.8	321.0	93.3	414.3
	3/4(fg)	0.45-0.60	130.2	153.9	225.3	34.4	136.5	26.3	5.8	26.2	3.6	22.8	4.0	12.6	1.7	12.1	1.7	582.2	214.9	797.1

*Composite samples (3-4 sub-samples per sampling interval)

** Mass balance calculation (based on the grainsize fractions and their mass) was used for sample 2/2 and values of grain size fractions >2 mm, 0.5-1 mm and 0.125-0.25 mm were taken from sample 2/8. fg - fine grained red mud, cg - coarse grained red mud.

Fine grained samples (Ny 1/2, 1/4 and 3/4) show consistently and remarkably higher concentration of REE than coarse grained samples (Ny 2/2 and 2/8).

This activity has received funding from the European Institute of Innovation and Technology (EIT), a body of the European Union, under the Horizon 2020, the EU Framework Programme for Research and Innovation

Table 19. Mineral composition of red mud from Ajka landfill, Hungary, for cells VIII. and IX. (in wt%)

Cell	Sample ID	Depth in m	Hematite	Cancrinite	Gibbsite	Calcite	Dolomite	Katoite	Hibschite	Goethite	Boehmite	Quartz	Kaolinite	Cancrinite (OH)	Anatase	Diaspore	Manganosite	Aragonite	Gypsum	Nordstrandite	amorphous
VIII	50	1	35.2	17.1	5.1	6.6	0.8	2.5	0.4	16.6	1.4	0.5	1.9	2.8	0.1	0.3	0.3	0	0	0	8.4
	51	2	34.8	9.1	3	12	2	1.2	0.2	19.3	2.7	0.4	0.8	1.8	0.2	0.1	0.2	0	0	0	12
	52	3	34.9	19.9	1.7	7.5	0.9	4.2	0.6	12	1.4	0.5	0.6	1.8	0.2	0.2	0.3	0	0	0	13.3
	53	4	35.6	22.2	2.2	10.3	0	3	0.4	3.7	0.7	0.5	2.2	3.6	0.2	0.3	0.5	0	0	0	14.6
	54	5	37	18.4	1.2	9.6	1.4	2.3	0.4	7.2	2.3	0.2	0.7	2.7	0.2	0.3	0.2	0.4	0	0	15.5
	55	6	36.9	18.8	1.2	9.6	2.1	4.3	0.2	6.1	2.6	0.4	0.8	2.5	0.1	0.2	0.2	0.5	0.1	0	13.3
	56	7	37.9	25	0.9	7	0.2	4.3	0.4	5.3	2.4	0.5	1.3	3	0.3	0.2	0.4	0	0	1.6	9.4
	57	8	38.5	26.1	5.9	4.5	0.3	4.3	0.2	3.9	3.1	0.2	1.3	2	0.3	0.4	0.1	0	0	0	8.9
	58	9	39.5	22.9	3.3	7.1	0.4	4.3	0.2	4.5	1.7	0.3	1.6	3.6	0.1	0.3	0.1	0	0	0	11.2
	59	10	37.4	22.7	1.3	11.4	0.3	2	0.4	6.3	1.5	0.1	1.2	3.1	0.1	0.6	0.3	0	0	1.6	9.4
	60	11	37.6	21.6	0.7	7.6	0.5	4.9	0.3	6.5	1	0.2	0.9	3	0.2	0.3	0.2	0	0	0	14.4
	61	12	39.2	21	0.4	9.5	0.7	3.2	0.8	7.8	1.5	0.3	1	3	0.3	0.4	0.5	0	0	0	10.4
	62	13	37.8	22.1	0.6	6.8	0.1	1.7	0.9	8.9	0.7	0.1	0.6	2.5	0.1	0.4	0.3	0	0	1.6	14.9
	63	14	37	20.8	0.7	7.8	0.3	2.2	0.8	7.7	1.5	0.5	1.1	2.1	0.1	0.5	0.6	0.3	0	1	15
	64	15	40	23.8	1	7.3	0	2.3	0.6	7.3	1.5	0.6	1.1	1.7	0.2	0.6	0.5	0	0	0	11.5
	65	16	37.5	15.7	1	10.7	0	1.5	0.9	9.7	5.3	0.4	0.8	1.1	0.4	0.5	0.5	0	0	0	12.7
IX	19	2	44.9	15.1	2.8	8.6	1.4	3.6	0.2	4.9	5.5	0.2	2.1	1.8	0.3	0.9	0	0	0	0	7.7
	20	2.5	43.5	19.3	3.9	6.2	0.9	6.4	0.4	9.8	1.1	0.7	1.5	3.1	0.3	1.4	0	0	0	0	0
	21	3	30.4	15.6	7.9	4.3	0	5.3	0.3	12.2	1.1	0.5	1.9	2.9	0.5	0.2	0.1	0	0	0	16.6
	22	4	38	23.9	8.7	4.9	0	4.5	0.1	13.3	0.7	0.6	1.6	2.1	0.3	0.9	0	0	0	0	0
	23	5	36.5	20	4.2	5.5	0	5.2	0.3	11	1	0.6	1.9	3	0.6	0.2	0.2	0	0	0	9.7
	24	6	38.9	26.1	1.4	4.2	0	4.4	0.3	3.9	1.4	0.3	1.8	2.7	0.2	0.8	0.3	4.2	0	0	9
	25	7	36.9	19.8	1	5.9	0	4.3	0.6	6.6	1	0.2	2.6	2.4	0.4	0.2	0.1	4.1	0	0	13.6
	26	8	37.6	19.9	1.1	7.6	0	5.2	0.6	6.8	0.6	0.4	1.2	2.9	0.2	0.5	0.2	3.9	0	0	11.4
	27	9	37.9	16.3	3.1	7	0	9.4	0.2	3.7	1.2	0.5	1	2.8	0.1	1.1	0.2	4.2	0	0	11.2
	28	10	44.5	19.4	1.2	6.3	0.6	4.8	0.2	4	1.4	0.7	0.9	2.3	0.3	0.6	0.3	2.5	0	0	10
	29	11	39.9	21.6	0.7	7.9	0.1	5.7	0.4	4	1.2	0.3	1	2.5	0.2	0.4	0.3	3.3	0	0	10.5
	30	12	37.7	23.2	0.4	7	0.6	6.3	0.3	4.2	1.2	0.4	1.3	2.9	0.2	0.4	0.3	2.7	0	0	11
	31	13	38.7	22.7	0.2	6	0	4.2	0.6	6.7	1.1	0.1	1.4	3	0.3	1.1	0.2	0.3	0	0	13.5
	32	14	37.5	26.1	0.9	5.9	0	5.4	0.7	6.4	0.9	0.4	1.6	3.6	0.2	0.4	0.1	0	0	0	10

This activity has received funding from the European Institute of Innovation and Technology (EIT), a body of the European Union, under the Horizon 2020, the EU Framework Programme for Research and Innovation

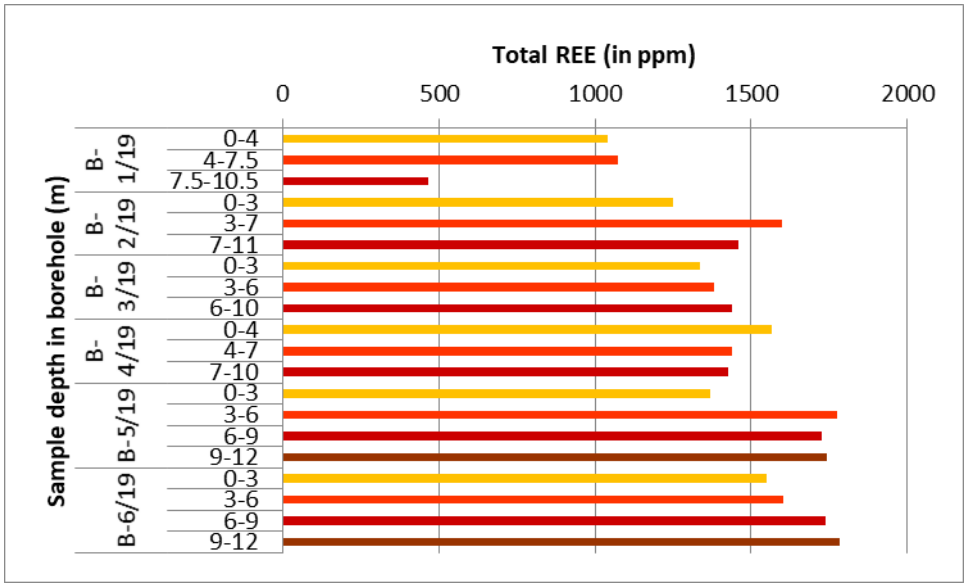

Figure 11A. Total REE distribution within six boreholes drilled at the Podgorica red mud landfill in Montenegro

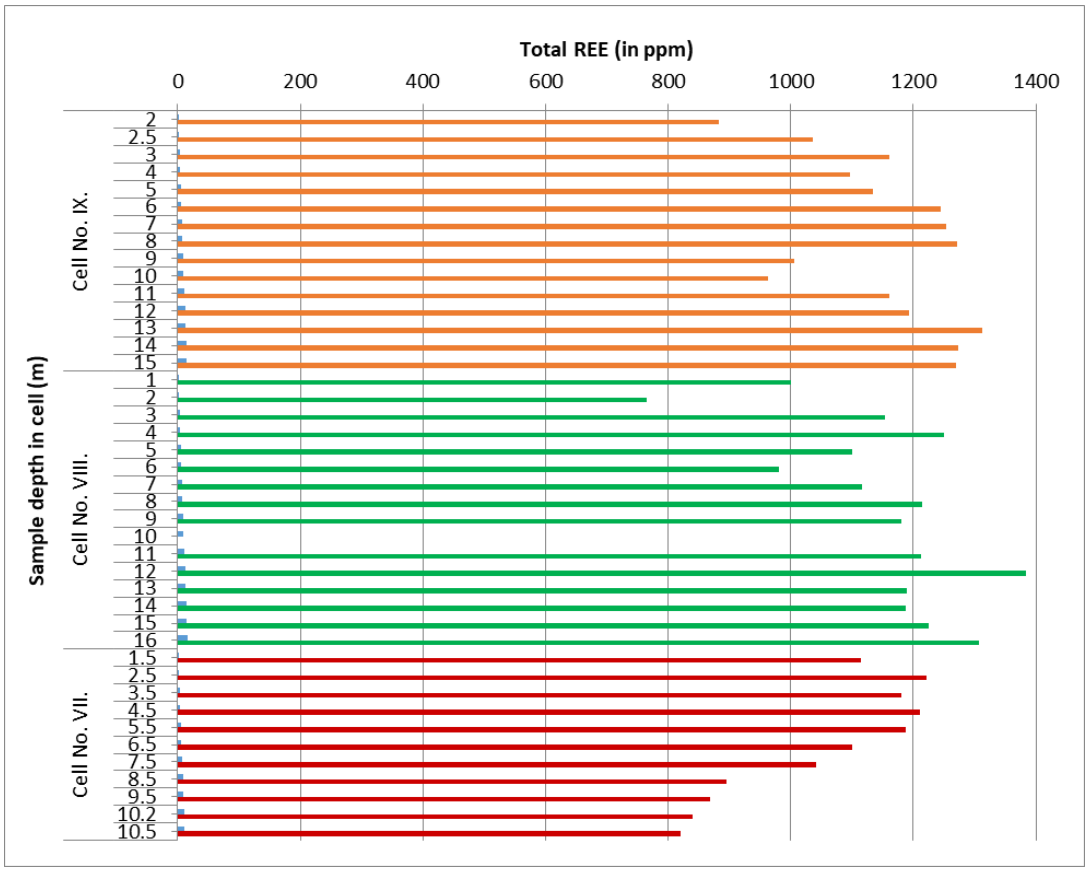

Figure 11B. Total REE distribution within boreholes drilled at the cells of Ajka red mud landfill in Hungary

This activity has received funding from the European Institute of Innovation and Technology (EIT), a body of the European Union, under the Horizon 2020, the EU Framework Programme for Research and Innovation

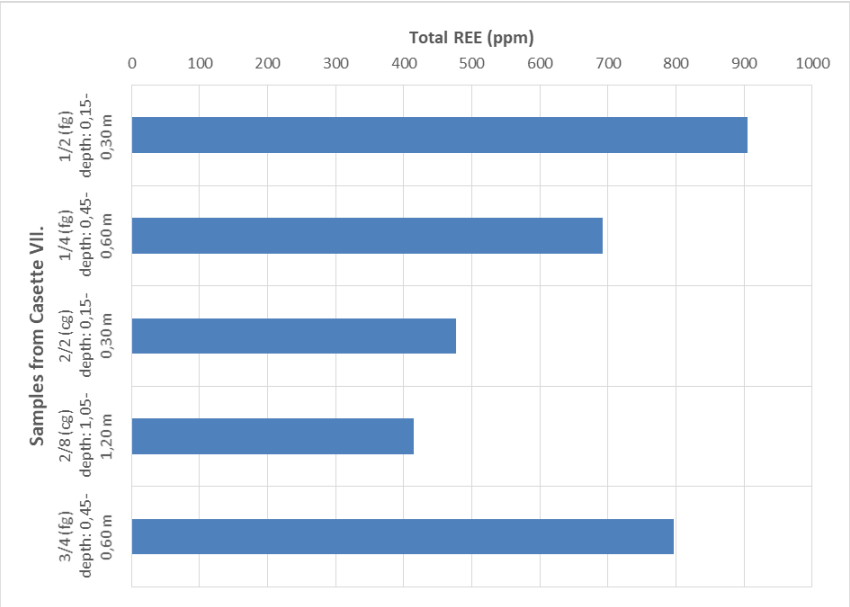

Figure 11C. Total REE distribution within the drillings of the VII. cassette of the Almásfüzítő red mud landfill in Hungary (fg – fine grained red mud, cg – course grained red mud)

Distribution of total REE values (Figures 11A, 11B and 11C) does not show a uniform pattern along the sampled boreholes. In the Podgorica landfill, in certain areas REE are more abundant closer to the red mud exposure to the surface, while for some boreholes REE concentrations increase with depth. In Ajká, a variable pattern is observed for the cells No. VIII. and IX., while in the cell No. VII. the REE values are the lowest in the bottom part of the accumulation pond. Similar trend was observed at the Almásfüzítő landfill, although mutual comparison with other landfills cannot be taken into consideration, since the hand drilling at the Almásfüzítő reached the maximal depth of just 1.2 m.

For the samples from Ajká mineral composition was determined using XRD and applying Rietveld method for quantification with results presented in Table 19. Iron oxides (hematite, goethite), cancrinite $(Na,Ca,\square)_8(Al_6Si_6O_{24})(CO_3,SO_4)_2\times 2H_2O$ and amorphous matter are present in considerable amounts. Minor phases are calcite, gibbsite, boehmite, kaolinite, cancrinite-(OH) and katoite $(Ca_3Al_2(SiO_4)_{3-x}(OH)_{4x}$, while accessory phases like dolomite, hibschite, quartz, anatase, diaspore, manganosite, aragonite, gypsum and nordstandite are found there.

Correlation analysis of REE with major constituents and mineral composition in Ajká red mud landfill

A correlation analysis has been performed on parameter changes along the drilling profiles of cell No. VIII. and IX. A distance value between two datasets was calculated based on comparing slope value changes from sampling point to sampling point along the profile. Lower distance values show better similarities between the profile pairs. In cross-correlation matrices green shaded cells show good correlation, red shaded show little correlation.

This activity has received funding from the European Institute of Innovation and Technology (EIT), a body of the European Union, under the Horizon 2020, the EU Framework Programme for Research and Innovation

Table 20. Mutual cross correlation matrix among REE along whole profile in cell No. VIII.

	La	Ce	Pr	Nd	Sm	Eu	Gd	Tb	Dy	Ho	Er	Tm	Yb	Lu
Y	0.89	0.83	0.78	0.82	0.82	0.81	0.56	0.78	0.66	0.71	0.82	0.88	0.83	0.98
La		0.75	0.28	0.36	0.75	0.92	0.92	1.17	1.28	1.17	1.28	1.19	1.20	1.34
Ce			0.81	0.85	0.68	0.76	0.70	0.81	0.96	0.79	0.85	0.97	0.75	1.03
Pr				0.28	0.55	0.94	0.85	1.12	1.23	1.13	1.27	1.06	1.20	1.21
Nd					0.48	0.79	0.78	0.98	1.09	1.03	1.11	1.06	1.13	1.18
Sm						0.74	0.61	0.80	0.87	0.74	0.89	0.90	0.92	0.93
Eu							0.54	0.68	0.76	0.85	0.73	0.91	0.66	0.70
Gd								0.45	0.41	0.47	0.45	0.68	0.53	0.64
Tb									0.58	0.56	0.39	0.73	0.60	0.56
Dy										0.38	0.36	0.84	0.56	0.84
Ho											0.44	0.92	0.64	0.91
Er												0.78	0.38	0.75
Tm													0.71	0.61
Yb														0.61

In general, it has been found from the data presented in Table 18 that there are only tiny differences among individual REE profiles. The cross-correlation calculations (Table 20) show that profiles of La-Pr-Nd-(Sm) are very similar and these comprise one group. There is another group of heavy REE (Dy-Ho-Er-Tb-Gd) where the profiles show close similarities, i.e. HREE and LREE behave in a different way, however, within the group they behave as they should.

Table 21. Cross-correlation matrix between REE and major constituents along the profile from cell No. VIII

	Y	La	Ce	Pr	Nd	Sm	Eu	Gd	Tb	Dy	Ho	Er	Tm	Yb	Lu
SiO_2	1.24	1.04	0.96	1.15	1.12	1.24	1.17	1.33	1.46	1.33	1.32	1.32	1.51	1.18	1.63
Al_2O_3	1.50	1.61	1.13	1.71	1.58	1.54	1.30	1.31	1.01	1.24	1.09	1.07	1.52	1.04	1.43
MgO	5.12	5.58	5.10	5.53	5.36	5.23	4.98	4.94	4.73	4.80	4.72	4.60	5.35	4.88	5.27
CaO	2.91	3.49	3.29	3.40	3.20	3.11	2.98	2.93	2.69	2.80	2.92	2.80	3.35	3.14	3.14
Na_2O	1.71	1.25	1.29	1.38	1.51	1.65	1.53	1.75	1.79	1.79	1.70	1.72	1.90	1.52	1.89
K_2O	2.35	2.38	2.33	2.40	2.44	2.38	2.42	2.37	2.59	2.25	2.30	2.38	2.88	2.32	2.71
Fe_2O_3	2.10	2.22	1.59	2.35	2.22	2.18	1.66	1.80	1.50	1.84	1.68	1.59	2.07	1.68	1.90
MnO	2.65	2.57	2.37	2.54	2.46	2.42	2.14	2.39	2.10	2.63	2.54	2.43	2.28	2.43	2.21
TiO_2	1.27	1.35	0.75	1.48	1.40	1.33	1.00	1.06	0.92	1.12	1.06	0.97	1.26	0.92	1.24
P_2O_5	2.87	2.88	3.02	2.84	2.74	2.93	2.96	2.91	2.83	3.09	3.11	2.98	2.90	3.23	3.04

The correlation matrix between REE and major constituents (Table 21) shows that based on similarities of concentration changes along the profile, the REE profiles have a good correlation with SiO_2, Al_2O_3, Na_2O and TiO_2. This matrix suggests also that REE are associated with the cancrinite phase. Na_2O profile shows best similarity to REE with La-Ce-Pr-Nd

Incorporated in mineral phases, REE are primarily associated with phosphates. It was approved by analysis of aggregated samples from cells No. VIII. and IX., detecting primarily xenotime and monazite grains. Total values of REE for samples from cell No. VIII. vary between 765 mg/kg (sample 51) and 1383 mg/kg (sample 61) while P_2O_5 varies from 0.34 to 0.82 %. It means that if we assume that all REE are connected to phosphate phases, this should bind at least 7-12 % of phosphate in REE-phosphates. In cell VII. this ratio increases up to 30-40%. Change of P_2O_5 along the drilling profile shows much less similarity with the REE profiles than that of SiO_2 or Na_2O as it is reflected in the above cross-correlation

This activity has received funding from the European Institute of Innovation and Technology (EIT), a body of the European Union, under the Horizon 2020, the EU Framework Programme for Research and Innovation

matrix as well. This data suggests that certain part of REE is not bound in phosphate minerals but it had been deliberated during the Bayer process, and associated with Na-Al silicate phases. This hypothesis needs support from the ongoing sequential extraction experiments.

Table 22. Cross-correlation matrix of REE and mineral composition in the whole profile in cell No. VIII.

Mineral	Range (%)	Y	La	Ce	Pr	Nd	Sm	Eu	Gd	Tb	Dy	Ho	Er	Tm	Yb	Lu
Hematite	35-40	1.77	2.02	1.41	2.13	2.05	1.99	1.42	1.55	1.33	1.53	1.55	1.28	1.82	1.28	1.66
Cancrinite	9-26	2.53	1.99	2.39	2.10	2.28	2.59	2.47	2.63	2.74	2.81	2.83	2.71	2.47	2.50	2.72
Gibbsite	1-5	7.42	7.16	7.59	7.28	7.18	7.42	7.16	7.40	7.38	7.64	7.68	7.49	7.29	7.44	7.46
Calcite	4-12	4.09	4.77	4.48	4.67	4.50	4.26	4.34	4.07	3.86	3.85	3.96	3.91	4.34	4.26	4.22
Katoite	1-4	4.62	4.36	4.55	4.42	4.44	4.51	4.61	4.78	4.91	4.90	4.81	4.85	4.74	4.92	4.99
Hibschite	0.2-1	5.80	5.68	5.57	5.68	5.80	5.76	5.82	5.78	5.89	5.60	5.65	5.78	5.80	5.64	5.73
Goethite	3-20	5.08	5.63	4.98	5.56	5.47	5.22	4.90	4.81	4.58	4.67	4.75	4.63	4.95	4.68	4.56
Boehmite	1-3	8.33	8.55	8.20	8.42	8.26	7.89	8.05	7.93	7.68	7.76	7.64	7.70	8.01	7.97	8.04
Quartz	0.1-0.5	6.42	6.96	6.64	6.94	7.02	6.73	6.96	6.63	6.78	6.48	6.41	6.53	6.77	6.59	7.10
Kaolinite	0.6-1	5.85	6.03	6.21	6.11	6.14	6.23	6.45	6.18	6.29	6.15	6.18	6.16	6.49	6.29	6.71
Cancrinite (OH)	1.8-3	3.49	3.71	3.83	3.82	3.84	4.08	3.95	3.78	3.85	3.71	3.86	3.73	4.03	3.74	4.02
Anatase	0.1-0.3	6.84	7.40	6.85	7.14	7.29	6.84	7.17	6.79	6.65	6.68	6.50	6.85	6.69	6.96	6.87
Diaspore	0.1-0.6	4.14	3.41	3.72	3.56	3.56	3.71	3.77	3.88	4.07	4.17	4.15	4.15	3.92	4.00	3.99
Manganosite	0.1-0.5	5.71	5.88	6.10	5.87	5.93	5.87	6.39	6.14	6.35	6.07	6.07	6.23	6.04	6.33	6.46

Main mineral phases based on XRD analysis with Rietveld refinement (Table 19) in cell No. VIII. are hematite, cancrinite, calcite and goethite. OH-cancrinite, katoite and boehmite amount for a few percent, while the occurrence of other detected minerals is below one percent. Phosphates were not detected by XRD in the samples due to their low abundance.

Mineral composition changes along the drilling profile and shows that REE show good correlation with cancrinite (Table 22). The best correlation values are with hematite concentration that exhibits very little changes along the profile.

Table 23. Cross-correlation matrix of REE and mineral composition for the upper 5 m of cell No. VIII.

Mineral	Range (%)	Y	La	Ce	Pr	Nd	Sm	Eu	Gd	Tb	Dy	Ho	Er	Tm	Yb	Lu
Hematite	35-40	0.93	1.19	0.69	1.12	1.09	0.86	0.77	0.72	0.52	0.65	0.60	0.56	0.78	0.61	0.66
Cancrinite	9-26	0.90	0.51	0.98	0.55	0.60	0.80	0.89	0.93	1.14	1.00	1.12	1.10	0.88	1.05	1.00
Gibbsite	1-5	1.65	1.78	2.00	1.79	1.78	1.86	1.86	1.76	1.82	1.80	1.91	1.87	1.74	1.90	1.83
Calcite	4-12	1.91	2.21	1.98	2.17	2.12	2.05	1.94	1.83	1.66	1.83	1.84	1.78	1.92	1.83	1.78
Katoite	1-4	1.78	1.49	1.77	1.52	1.58	1.65	1.76	1.87	2.03	1.87	1.85	1.91	1.78	1.87	1.92
Hibschite	0.2-1	1.91	1.50	1.51	1.54	1.58	1.57	1.65	1.78	1.88	1.78	1.74	1.76	1.81	1.69	1.78
Goethite	3-20	3.24	3.50	2.99	3.43	3.40	3.17	3.08	3.03	2.83	2.97	2.85	2.87	3.09	2.92	2.97
Boehmite	1-3	3.93	4.19	3.67	4.11	4.09	3.86	3.76	3.72	3.51	3.65	3.54	3.56	3.77	3.61	3.66
Quartz	0.1-0.5	0.89	1.24	1.00	1.17	1.15	1.00	0.94	0.88	0.92	0.85	0.85	0.87	0.82	0.91	0.93
Kaolinite	0.6-1	3.01	3.14	3.36	3.15	3.14	3.23	3.22	3.12	3.18	3.16	3.27	3.23	3.10	3.26	3.19
Cancrinite (OH)	1.8-3	1.12	1.25	1.47	1.26	1.25	1.33	1.33	1.23	1.29	1.27	1.38	1.34	1.21	1.37	1.30

This activity has received funding from the European Institute of Innovation and Technology (EIT), a body of the European Union, under the Horizon 2020, the EU Framework Programme for Research and Innovation

Mineral	Range (%)	Y	La	Ce	Pr	Nd	Sm	Eu	Gd	Tb	Dy	Ho	Er	Tm	Yb	Lu
Anatase	0.1-0.3	1.59	1.85	1.34	1.78	1.75	1.52	1.43	1.38	1.18	1.32	1.22	1.22	1.44	1.27	1.32
Diaspore	0.1-0.6	1.61	1.24	1.48	1.31	1.33	1.48	1.54	1.60	1.74	1.67	1.76	1.70	1.67	1.63	1.62
Manganosite	0.1-0.5	1.23	1.22	1.49	1.23	1.22	1.30	1.40	1.44	1.64	1.51	1.62	1.60	1.39	1.55	1.50

This correlation matrix for the upper 5 m of the cell No. VIII. (Table 23) shows very good similarity of profiles for cancrinite and light REE (La-Pr-Nd), while heavy REE show better correlation with the slight changes of hematite content. Good correlation values with quartz can be ignored due to the very little concentration of quartz, and generally not significant affinity of REE to this mineral.

Table 24. Mutual cross correlation matrix of REE along the drilling profile from cell No. IX.

	Y	La	Ce	Pr	Nd	Sm	Eu	Gd	Tb	Dy	Ho	Er	Tm	Yb	Lu
Y		1.02	1.11	0.98	0.84	0.81	1.06	0.72	0.74	0.71	0.76	0.81	0.86	0.76	0.87
La			0.92	0.37	0.38	0.75	0.55	0.87	0.90	0.82	1.01	0.88	1.06	1.20	0.67
Ce				0.99	0.98	1.09	0.98	0.85	0.66	0.46	0.64	0.86	0.81	0.69	0.44
Pr					0.26	0.59	0.67	0.78	0.83	0.81	1.03	0.74	0.85	1.19	0.70
Nd						0.46	0.72	0.72	0.81	0.75	0.96	0.66	0.81	1.12	0.69
Sm							1.14	0.93	0.99	0.91	1.06	0.73	0.76	1.15	0.88
Eu								0.69	0.85	0.81	0.81	0.96	1.16	1.08	0.69
Gd									0.51	0.50	0.58	0.95	1.07	1.00	0.56
Tb										0.33	0.55	0.67	0.72	0.68	0.58
Dy											0.43	0.62	0.63	0.57	0.37
Ho												0.68	0.82	0.56	0.50
Er													0.43	0.59	0.74
Tm														0.57	0.82
Yb															0.75

Correlation analysis of REE along drilling profile in cell No. IX. shows similar results to those ones given for cell No. VIII: strong similarity is found among La-Pr-Nd-(Eu), and among some heavy REEs as Gd-Tb-Dy-Ho-(Lu)(Table 24).

Table 25. Cross-correlation matrix between REE and major constituents along the profile from cell No. IX.

	Y	La	Ce	Pr	Nd	Sm	Eu	Gd	Tb	Dy	Ho	Er	Tm	Yb	Lu
SiO_2	1.53	1.10	1.28	0.89	0.96	1.20	1.17	1.23	1.02	1.23	1.40	1.30	1.30	1.57	1.31
Al_2O_3	1.64	1.36	1.07	1.20	1.30	1.42	1.44	1.36	1.04	1.08	1.19	1.23	1.17	1.36	1.23
MgO	3.17	2.86	2.45	2.91	2.87	2.99	2.83	2.95	2.70	2.61	2.70	2.70	2.51	2.56	2.71
CaO	2.62	2.73	2.16	2.62	2.72	2.69	2.52	2.48	2.34	2.29	2.26	2.52	2.38	2.26	2.20
Na_2O	1.95	1.41	1.71	1.27	1.29	1.54	1.48	1.65	1.47	1.65	1.80	1.66	1.74	1.98	1.73
K_2O	2.26	1.45	1.88	1.69	1.61	1.92	1.81	2.18	2.00	1.84	2.06	1.85	1.90	2.16	1.85
Fe_2O_3	1.94	1.81	1.26	1.83	1.80	1.77	2.01	1.88	1.65	1.49	1.64	1.89	1.64	1.54	1.59
MnO	2.86	2.25	2.17	2.22	2.40	2.62	2.45	2.43	2.18	2.19	2.45	2.58	2.37	2.57	2.30
TiO_2	1.67	1.23	0.85	1.35	1.26	1.37	1.52	1.39	1.18	1.04	1.27	1.42	1.32	1.42	1.03
P_2O_5	2.24	2.15	2.12	1.97	1.99	1.93	2.11	1.94	1.88	2.05	2.15	2.26	2.10	2.29	2.21

Cross-correlation matrix between REE and major constituents (Table 25) shows similar results compared to the matrix for cell No. VIII. Correlation of REE elements with SiO_2, Al_2O_3 and Na_2O is strong, while with P_2O_5 is much weaker. Correlation with TiO_2 is strong also in this case.

This activity has received funding from the European Institute of Innovation and Technology (EIT), a body of the European Union, under the Horizon 2020, the EU Framework Programme for Research and Innovation

Na_2O profile shows best similarity with La, Pr, Nd. This relationship was also detected for cell No. VIII.

Table 26. Cross-correlation of REE and mineral composition along whole profile in cell No. IX.

Mineral	Range (%)	Y	La	Ce	Pr	Nd	Sm	Eu	Gd	Tb	Dy	Ho	Er	Tm	Yb	Lu
Hematite	30-45	2.35	2.36	1.77	2.33	2.30	2.26	2.39	2.21	2.00	1.88	1.95	2.22	2.03	1.91	2.05
Cancrinite	15-26	1.88	2.56	2.37	2.26	2.29	2.16	2.57	2.17	1.91	2.06	2.21	2.19	2.01	2.06	2.37
Gibbsite	02.-9	8.51	8.71	8.41	8.53	8.59	8.58	8.28	8.41	8.29	8.38	8.29	8.43	8.42	8.34	8.50
Calcite	4-9	3.30	2.96	2.49	3.00	3.10	3.17	2.81	2.98	2.95	2.79	2.82	2.96	3.04	2.73	2.55
Katoite	3.5-9.5	3.90	3.69	3.69	3.51	3.72	3.85	3.43	3.49	3.53	3.59	3.77	3.77	3.74	3.89	3.55
Hibschite	0.1-0.7	6.22	5.61	6.20	5.64	5.68	5.60	5.81	6.10	6.25	6.19	6.44	6.10	6.21	6.57	6.02
Goethite	3.5-13.5	3.62	3.65	3.65	3.72	3.56	3.48	3.85	3.80	3.81	3.65	3.80	3.70	3.66	3.85	3.79
Boehmite	0.5-5.5	5.36	5.18	5.06	5.23	5.25	5.40	5.38	5.19	5.00	5.14	5.13	5.32	5.23	5.16	5.19
Quartz	0.1-0-7	8.20	8.46	8.06	8.18	8.24	8.16	8.29	8.08	7.87	8.02	8.18	7.99	7.95	8.05	8.20
Kaolinite	0.9-2.6	3.32	2.63	2.57	2.67	2.83	3.13	2.80	2.86	2.71	2.71	2.91	3.10	2.98	3.05	2.73
Cancrinite (OH)	1.8-3.6	2.62	2.51	2.44	2.33	2.54	2.67	2.17	2.25	2.13	2.36	2.49	2.44	2.44	2.56	2.37
Anatase	0.1-0.6	7.48	6.57	6.80	6.88	6.79	7.00	7.00	7.19	7.20	7.06	7.20	7.10	7.11	7.29	7.02
Diaspore	0.2-1.4	11.10	11.90	11.48	11.86	11.77	11.58	11.61	11.30	11.32	11.38	11.21	11.42	11.41	11.13	11.46
Amorphous	7.7-16.5	9.06	8.30	8.22	8.56	8.60	8.95	8.50	8.48	8.56	8.45	8.47	8.88	8.87	8.78	8.38

Cross-correlation matrix between REE and mineral composition (Table 26) shows the strongest similarity between REE and cancrinite and hematite. Calcite, katoite and goethite have weaker correlation with REE like for these minerals in the profile from cell No. VIII. Since there are remarkable changes in REE concentration, major element composition and mineralogy for samples 27 (9 m) and 28 (10 m), the cross-correlation was calculated also separately for the 7-12 m section (Table 27). This matrix shows similar results compared to the whole profile, the best correlation of REE is with cancrinite and calcite. Good correlation with the amorphous content is also remarkable, because it is not the case for the whole profile.

Table 27. Cross-correlation of REE and mineral composition along 7-12 m of profile section in cell No. IX.

Mineral	Range (%)	Y	La	Ce	Pr	Nd	Sm	Eu	Gd	Tb	Dy	Ho	Er	Tm	Yb	Lu
Hematite	30-45	1.02	0.92	0.75	0.93	0.92	0.96	1.01	0.95	0.79	0.82	0.87	1.01	0.91	0.94	0.92
Cancrinite	15-26	0.49	0.50	0.39	0.47	0.48	0.55	0.66	0.43	0.31	0.33	0.50	0.56	0.45	0.50	0.49
Gibbsite	02.-9	3.51	3.54	3.20	3.54	3.59	3.63	3.30	3.38	3.30	3.31	3.24	3.46	3.41	3.29	3.30
Calcite	4-9	0.69	0.70	0.56	0.71	0.75	0.79	0.52	0.58	0.65	0.62	0.50	0.63	0.71	0.50	0.47
Katoite	3.5-9.5	1.67	1.87	1.58	1.83	1.89	1.97	1.67	1.57	1.55	1.57	1.51	1.67	1.68	1.50	1.58
Hibschite	0.1-0.7	1.63	1.51	1.80	1.54	1.49	1.42	1.64	1.76	1.82	1.76	1.79	1.63	1.71	1.80	1.72
Goethite	3.5-13.5	0.72	0.75	0.74	0.72	0.68	0.66	0.91	0.87	0.73	0.70	0.84	0.67	0.59	0.79	0.84
Boehmite	0.5-5.5	2.11	1.91	1.85	1.93	1.91	1.94	2.14	2.00	1.89	1.93	1.97	2.11	2.01	2.04	2.02
Quartz	0.1-0-7	2.87	2.94	2.66	2.91	2.92	3.00	2.97	2.83	2.67	2.74	2.81	2.75	2.63	2.69	2.82
Kaolinite	0.9-2.6	1.18	1.26	1.12	1.24	1.29	1.35	1.35	1.06	1.00	1.06	1.16	1.40	1.33	1.24	1.17
Cancrinite (OH)	1.8-3.6	0.74	0.94	0.57	0.90	0.96	1.04	0.74	0.64	0.56	0.61	0.58	0.74	0.67	0.58	0.65
Anatase	0.1-0.6	2.90	2.74	2.89	2.77	2.69	2.62	3.03	3.00	2.91	2.89	3.02	2.85	2.78	2.96	3.01

This activity has received funding from the European Institute of Innovation and Technology (EIT), a body of the European Union, under the Horizon 2020, the EU Framework Programme for Research and Innovation

Mineral	Range (%)	Y	La	Ce	Pr	Nd	Sm	Eu	Gd	Tb	Dy	Ho	Er	Tm	Yb	Lu
Diaspore	0.2-1.4	3.10	3.13	2.79	3.13	3.17	3.22	2.92	2.97	2.89	2.90	2.83	2.98	2.92	2.81	2.89
Amorphous	7.7-16.5	0.72	0.72	0.55	0.69	0.74	0.81	0.77	0.53	0.50	0.53	0.53	0.86	0.78	0.69	0.61

Correlation analysis of REE and major constituents in Almásfüzítő red mud landfill

Pearson correlation analysis has been performed for REE with major constituents and minerals composition determined in Almásfüzítő red mud landfill (Tables 28. and 29.).

Table 28. Pearson correlation matrix of mutual REE concentrations in the cassette VII. of Almásfüzítő.

	La	Ce	Pr	Nd	Sm	Eu	Gd	Tb	Dy	Ho	Y	Er	Tm	Yb	Lu
La	1,00	0,97	1,00	0,99	1,00	0,98	0,97	0,98	0,97	0,97	0,96	0,95	0,96	0,97	0,97
Ce			0,97	0,96	0,96	0,93	0,94	0,93	0,93	0,91	0,87	0,90	0,89	0,90	0,88
Pr				1,00	1,00	0,99	0,99	0,99	0,99	0,98	0,96	0,97	0,97	0,98	0,97
Nd					1,00	0,99	0,99	0,99	0,99	0,99	0,97	0,98	0,98	0,98	0,97
Sm						1,00	0,99	0,99	0,99	0,99	0,97	0,98	0,98	0,99	0,98
Eu							0,99	1,00	1,00	1,00	0,99	0,99	0,99	1,00	0,99
Gd								1,00	1,00	0,99	0,97	1,00	0,99	0,98	0,96
Tb									1,00	1,00	0,98	0,99	0,99	0,99	0,98
Dy										1,00	0,98	1,00	0,99	0,99	0,97
Ho											0,99	1,00	1,00	0,99	0,98
Y												0,98	0,99	1,00	1,00
Er													1,00	0,99	0,97
Tm														1,00	0,98
Yb															1,00
Lu															

Based on Pearson correlation, only minor, but probably significant differences can be seen for the REE behaviour in Almasfüzítő red mud:

Among the LREE, group of La-Pr-Nd-Sm has a highly strong sympathetic correlation.

For the HREE, a group of Gd-Tb-Dy-Ho has even a stronger correlation. Also, within HREE, a group of Y-Er-Tm-Yb can be identified by their highly strong correlation. Note that the HREE Y, Yb and Lu have the best positive correlation.

In contrast, Eu has a highly strong correlation with its close neighbours (like the Pr, Nd and Sm, and Gd, Tb, Dy and Ho).

Ce also behaves a bit differently. It has the lowest level of positive correlation particularly for the HREE (probably because it has a different oxidation state).

The Lu unexpected lower positive correlation is likely related to its the lowest concentration values (<1.7 ppm, Table 18).

This activity has received funding from the European Institute of Innovation and Technology (EIT), a body of the European Union, under the Horizon 2020, the EU Framework Programme for Research and Innovation

Table 29. Pearson correlation matrix of REE and major elements (excluded SiO_2) from the cassette VII in Almásfüzítő.

	La	Ce	Pr	Nd	Sm	Eu	Gd	Tb	Dy	Ho	Y	Er	Tm	Yb	Lu
Al_2O_3	0,97	0,89	0,96	0,96	0,97	0,97	0,94	0,95	0,94	0,95	0,98	0,93	0,95	0,97	0,99
Fe_2O_3	-0,70	-0,58	-0,72	-0,73	-0,72	-0,75	-0,72	-0,73	-0,70	-0,73	-0,79	-0,74	-0,77	-0,77	-0,77
MgO	-0,94	-0,85	-0,94	-0,95	-0,95	-0,96	-0,93	-0,95	-0,94	-0,96	-0,99	-0,94	-0,96	-0,98	-0,99
CaO	-0,89	-0,80	-0,86	-0,87	-0,88	-0,88	-0,84	-0,87	-0,87	-0,88	-0,90	-0,84	-0,86	-0,90	-0,93
Na_2O	0,93	0,82	0,92	0,93	0,94	0,95	0,92	0,94	0,93	0,94	0,98	0,92	0,95	0,97	0,99
K_2O	0,98	0,98	0,99	0,99	0,99	0,97	0,98	0,98	0,97	0,96	0,93	0,96	0,95	0,95	0,93
TiO_2	0,99	0,96	0,99	1,00	1,00	0,99	0,99	0,99	0,99	0,99	0,97	0,97	0,98	0,98	0,98
P_2O_5	0,91	0,81	0,91	0,93	0,94	0,96	0,94	0,95	0,95	0,97	0,98	0,95	0,96	0,98	0,98
MnO	0,11	0,14	0,09	0,11	0,12	0,12	0,15	0,15	0,19	0,17	0,09	0,16	0,12	0,12	0,09
Cr_2O_3	0,52	0,58	0,46	0,45	0,46	0,41	0,40	0,42	0,43	0,40	0,36	0,35	0,34	0,40	0,42

REE have a strong positive correlation with Al_2O_3, Na_2O, K_2O, TiO_2 and P_2O_5 major elements. They show no positive correlation with the other major elements like MnO, Cr_2O_3, Fe_2O_3, MgO and CaO.

Sequential extraction test on the material from the Ajká red mud landfill

Sequential extraction analysis was carried out in order to determine which mineral phase contains REE. Based on the previously presented results on the mineralogical and chemical analysis, 5 samples were chosen from the Cell VII. of Ajká, along a vertical profile, collected from depth of 1 to 5 metres.

Similarly to earlier studies (Gu et al., 2018), a Tessier type 5-step test was carried out, which builds up from the dissolution of: 1. water soluble fraction; 2., exchangeable fraction; 3. fraction bound to carbonates; 4. fraction bound to Fe-Mn oxides; and 5. fraction bound to organic matter. In the residual of the 5^{th} step, only the quartz and the different silicates are contained. The test comprised two sets of chemical analysis, because the leachate of each step was analysed by a microwave plasma-atomic emission spectrometer (MP-AES) at the University of Miskolc, and 5 g portions from the residuals – as well as from the original material – were sent to the Bureau Veritas Laboratory for analysis with inductively coupled plasma emission spectrometer (ICP-ES) and mass spectrometry (ICP-MS), as well as with XRF method.

To the Tessier's original partitioning procedure (Tessier et al., 1979), extraction with distilled water is added as an initial step. Used reagents are listed near each step of the leaching process (Figure 12). The solid residues remaining after each extraction step were washed out with distilled water and centrifuged at 2500 rpm for 60 minutes in the first steps because of the high rate of colloidal fraction. The centrifuge time was decreased to 20 minutes at the end of the test, as the amount of the colloidal fraction significantly decreased. After decantation residue mass was measured back, and portions of 5 g were taken out for chemical analysis. The rests were sent to the next extraction steps (Figure 12). After each extraction step, the

This activity has received funding from the European Institute of Innovation and Technology (EIT), a body of the European Union, under the Horizon 2020, the EU Framework Programme for Research and Innovation

leachate was separated from the residue by centrifuge and filtered for chemical analysis with MP-AES measuring device.

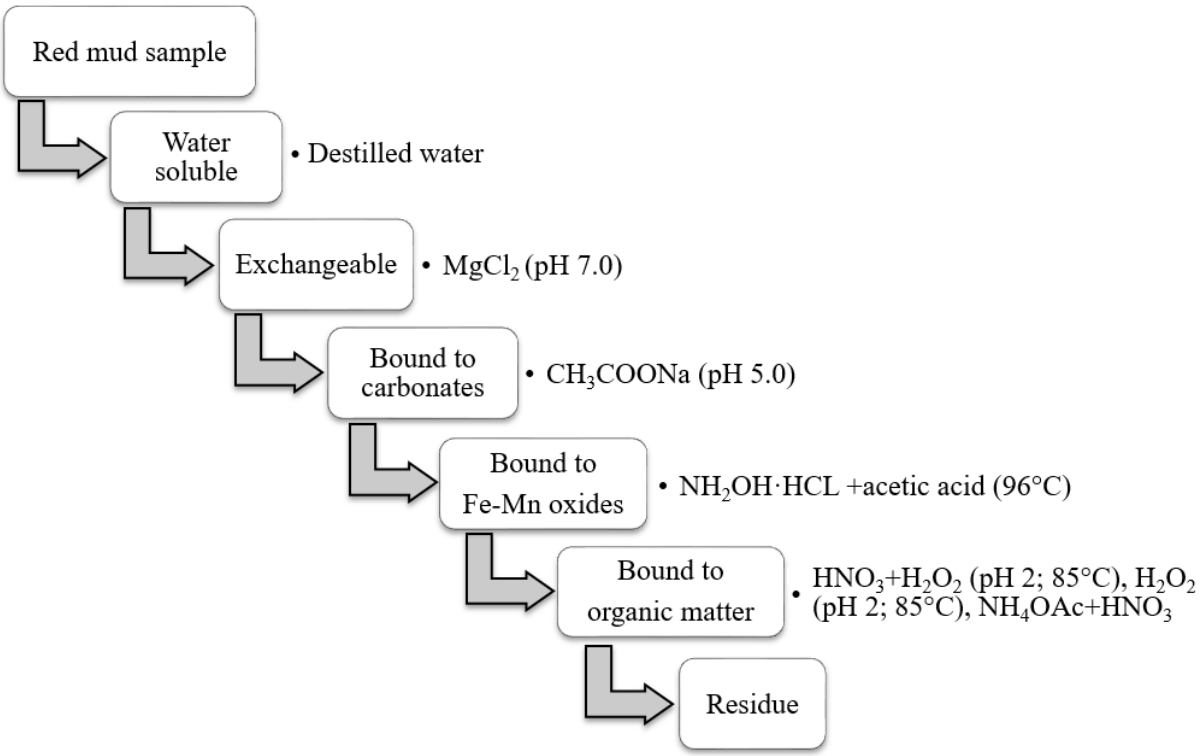

Figure 12. Sequential extraction procedure taken from Tessier et al., (1979) and modified by Gu et al., (2018).

Since in the case of each step it as necessary to take out 5 g from the dry residue, in the sequential extraction test procedure a 20-times enlarging was done, thus instead of 3 g of sample, 60 g was the initial starting weight. Amount of the reagents was also multiplied 20 times, accordingly.

Step 1st. *Water soluble fraction*

60.00 g of red mud sample was transferred into a glass beaker and the sample was shaken for 24 h with 600 mL of distilled water, then centrifuged and decanted.

Step 2nd. *Exchangeable fraction*

In this stage, the extraction solution applied was 600 mL of 1 M magnesium chloride ($MgCl_2$) solution at pH 7.0, with shaking for 24 h at room temperature, then washed, centrifuged and decanted.

Step 3rd. *Fraction bound to carbonates*

The extraction solution applied was 600 mL of 1 M sodium acetate (CH_3COONa) adjusted to pH 5.0 with acetic acid, and the residue was shaken for 24 h at room temperature, then centrifuged and decanted.

This activity has received funding from the European Institute of Innovation and Technology (EIT), a body of the European Union, under the Horizon 2020, the EU Framework Programme for Research and Innovation

Step 4th. Fraction bound to Fe–Mn oxides

The extraction solution applied was 600 mL of 0.03 M hydroxylamine hydrochloride ($NH_2OH{\cdot}HCL$) in 25% (v/v) acetic acid. Extraction was completed at 96 ± 1 °C for 6 h with occasional agitation on a magnetic stirrer provided with a heater. After cooling to room temperature, the sample was washed out, centrifuged and decanted.

Step 5th. Fraction bound to organic matter

To the residue from the previous step, 180 mL of 0.02 M HNO_3 and 300 mL of 30% H_2O_2 were added and adjusted to pH 2.0 with HNO_3. The mixture was heated to 85 ± 1 °C for 2 h with occasional agitation. A second amount of 180 mL aliquot of 30% H_2O_2 (adjusted to pH 2.0 with HNO_3) was added, and the sample was heated again to 85 ± 1 °C for 3 h with intermittent agitation. After cooling, 300 mL of 3.2 M NH_4OAc in 20% (v/v) HNO_3 was added, and the sample was diluted to 1200 mL, and agitated continuously for 30 minutes, then washed, centrifuged and decanted.

Residue

Finally, after drying the residue from the 5th step, the solid material was also washed out with distilled water, then centrifuged and decanted.

The REE content of the residuals from the sequential extraction (Table 30) show relatively high variability. Three different trend lines can be clearly observed (Figure 13). In the upper zone (sample A-50 and A-51) of the vertical sampling, the REE concentrations are decreasing, less in case of the depth of 1 metre, but significantly more in case of the sample from the depth of 2 metres. This trend line implies that the REE are partly contained in such minerals, which dissolved in the steps of the leaching. In the middle zone (sample A-52; sampling depth 3m) the trend line of the concentrations are stable, which means although the REE containing minerals are slightly dissolving, but the enriching effect – as less and less material remained for the next step – kept it in balance. In the case of the two deepest samples (A-53 and A-54; sampling depth of 4 and 5 m) a slight increase of REE concentrations is visible toward the advancing leaching steps. This proves that REE are contained in minerals, which are stable during the whole test process, and produce relative REE enrichment as other minerals are dissolved.

Based on the result of the test, it can be established that in the upper sampling zone a smaller amount of REE occur in such mineral phases, which dissolved back, so probably in carbonates, goethite or hematite, but the main part of REE is in silicates or in REE-phosphates. In the lower sampling zone – where the trend line increased – the REE are only in non-soluble mineral species, the soluble part is missing.

This activity has received funding from the European Institute of Innovation and Technology (EIT), a body of the European Union, under the Horizon 2020, the EU Framework Programme for Research and Innovation

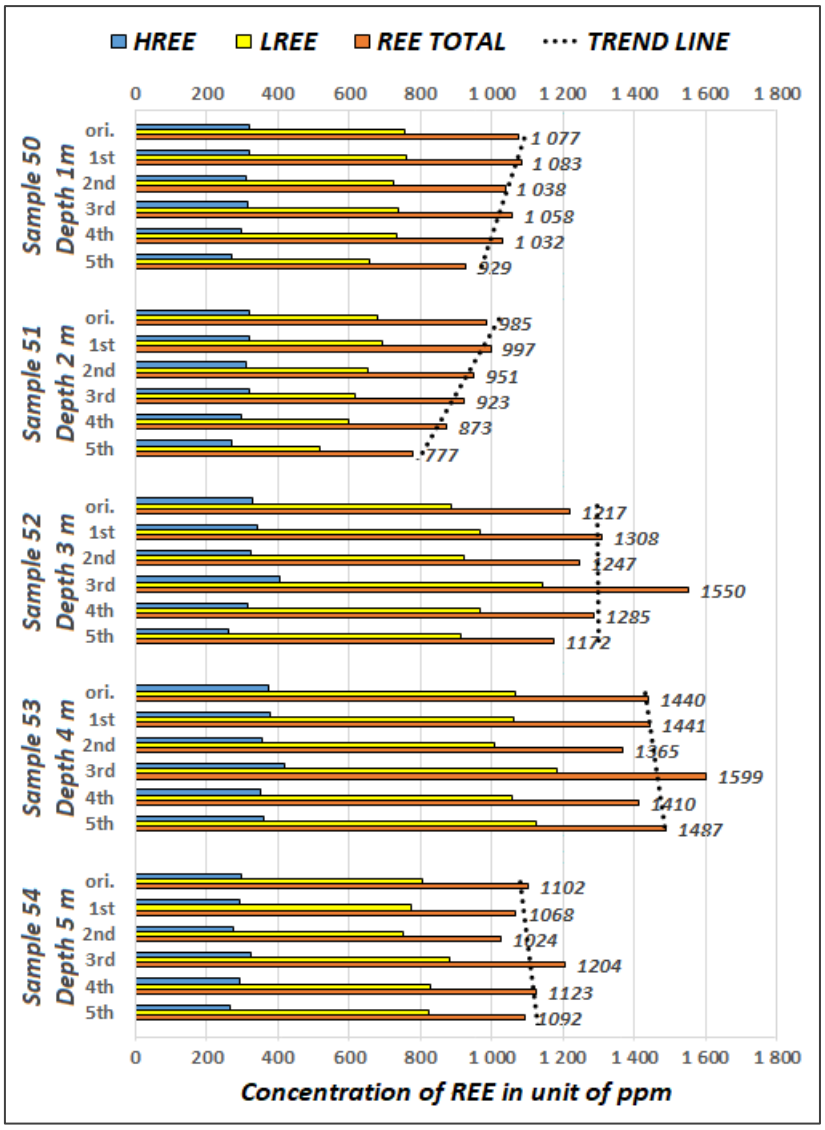

Figure 13. REE distribution in the residuals of the different steps of the sequential extraction testing on the five chosen samples from the cell No. VIII. of Ajká

This activity has received funding from the European Institute of Innovation and Technology (EIT), a body of the European Union, under the Horizon 2020, the EU Framework Programme for Research and Innovation

Table 30. REE concentrations (in ppm) in the residuals of the steps of the sequential extraction of the selected Ajká red mud samples

Sample ID	Sequential extraction step	Sc	Y	La	Ce	Pr	Nd	Sm	Eu	Gd	Tb	Dy	Ho	Er	Tm	Yb	Lu	ΣLREE	ΣHREE	ΣREE
A-50 sampling depth 1 m	original	98	128.6	174.8	364.7	38.16	142.1	29.06	6.1	27.65	4.36	25.69	5	14.75	2.12	13.92	2.04	755	322	1077
	1st	97	129.6	176.5	364.5	38.73	144.8	29.85	6.28	27.44	4.4	25.93	5.05	14.96	2.13	13.9	2.07	761	322	1083
	2nd	95	123.4	169	349.8	36.88	137	27.35	6.04	27.35	4.25	25.45	4.93	14.25	2.09	13.05	2.03	726	312	1038
	3rd	104	120.9	168	358.4	37.21	143	27.38	6	26.42	4.29	24.94	5.05	14.86	2.16	13.78	2.1	740	319	1058
	4th	109	105	169.4	375.8	34.74	126.1	23.94	5.18	23.39	3.86	21.99	4.34	13.09	1.87	12.08	1.75	735	296	1032
	5th	111	86.2	138.1	354.4	29.6	109.4	22.01	4.63	20.62	3.41	20.01	4.09	11.73	1.66	10.35	1.59	658	271	929
A-51 sampling depth 2 m	original	98	117	149.6	346.6	32.57	119.5	26.7	5.75	25.18	4.16	24.79	4.79	13.89	1.96	12.68	1.91	681	304	985
	1st	98	117.1	146.4	352.2	32.99	128.3	26.85	5.72	25.72	4.12	24.39	4.85	13.85	1.97	12.43	1.82	692	304	997
	2nd	97	114.2	142.9	324.3	32	120.3	25.77	5.6	25.03	4.08	24.72	4.86	13.89	1.95	12.67	1.82	651	300	951
	3rd	108	110.5	139.2	307.2	30.31	112	24.08	5.38	23.58	4.02	23.24	4.89	14.14	1.95	13.07	1.86	618	305	923
	4th	110	90.9	134.2	310.9	27.84	99.4	20.39	4.56	20.77	3.42	19.75	4.04	12.1	1.7	10.96	1.63	597	275	873
	5th	112	80.1	109.7	281.2	23.3	84.5	17.56	3.84	17.62	2.95	18	3.49	10.65	1.4	9.44	1.39	520	257	777
A-52 sampling depth 3 m	original	89	140.8	213.2	425.5	45.21	163.3	32.66	6.67	29.76	4.53	26.32	5.38	15.48	2.3	14.51	2.26	887	330	1217
	1st	88	146.7	237	458.6	49.37	180	33.87	7.05	31.03	4.7	28.27	5.7	16.5	2.39	16	2.36	966	342	1308
	2nd	86	137.1	221	440.8	46.93	173.3	32.5	6.83	29.99	4.53	26.68	5.39	16.15	2.36	15.05	2.35	921	326	1247
	3rd	109	172.1	278.2	545.6	59.19	211.5	40.64	8.58	36.2	5.65	33.49	6.65	19.55	2.86	18.4	2.86	1144	407	1550
	4th	106	118.9	242.3	485.9	46.63	158.9	28.04	5.69	25.84	4.14	24.66	4.97	14.91	2.08	14.31	2.12	967	318	1285
	5th	107	82.5	215.4	483.8	41.53	141.1	24.86	4.97	20.71	3.27	19.06	3.74	10.99	1.54	10.11	1.42	912	260	1172

This activity has received funding from the European Institute of Innovation and Technology (EIT), a body of the European Union, under the Horizon 2020, the EU Framework Programme for Research and Innovation

Sample ID	Sequential extraction step	Sc	Y	La	Ce	Pr	Nd	Sm	Eu	Gd	Tb	Dy	Ho	Er	Tm	Yb	Lu	ΣLREE	ΣHREE	ΣREE
A-53 sampling depth 4 m	original	86	175.2	273.3	485.3	57.74	204.7	37.4	7.74	32.85	4.98	29.17	5.91	17.47	2.52	16.78	2.55	1066	373	1440
	1st	87	179.3	272.5	481.6	57.29	205.2	37.26	7.65	33.2	5.1	29.59	5.94	17.88	2.59	16.76	2.56	1062	380	1441
	2nd	83	165.6	253.6	465.4	53.84	194.3	35.3	7.26	31.15	4.7	28.26	5.6	16.82	2.43	15.63	2.43	1010	356	1365
	3rd	98	195	297.9	543.7	63.74	225.6	41.18	8.54	35.93	5.58	33.49	6.57	19.49	2.85	18.46	2.77	1181	418	1599
	4th	101	149.8	268.6	500.7	54.65	193.9	32.76	6.74	29.07	4.57	27.08	5.5	15.88	2.37	14.97	2.27	1057	353	1410
	5th	112	147.1	282.6	544.1	56.95	199.8	34.05	7.13	29.55	4.58	26.66	5.68	16.39	2.3	15.47	2.33	1125	362	1487
A-54 sampling depth 5 m	original	83	127.7	185	397.1	40.18	147.4	28.33	5.79	25.21	3.9	23.5	4.63	13.59	2.06	12.79	2.04	804	298	1102
	1st	82	122.9	184.8	370.7	40.22	146.1	27.94	5.81	25.41	3.88	22.8	4.6	13.52	1.93	13.14	2.03	776	292	1068
	2nd	78	113.3	177.6	359.4	38.44	142.9	26.38	5.62	23.84	3.61	21.39	4.4	12.56	1.83	12.42	1.92	750	273	1024
	3rd	97	130.7	209.3	431.8	43.88	159.2	30	6.39	26.92	4.29	25.47	5.11	14.69	2.19	14.7	2.29	881	323	1204
	4th	98	110.9	198.4	420	39.75	141.2	25.46	5.34	24.01	3.77	21.51	4.47	13.43	1.92	12.63	1.9	830	293	1123
	5th	103	92	191.4	432.8	37.47	133.7	23.68	4.72	20.8	3.34	19.54	3.98	11.67	1.68	10.81	1.71	824	269	1092

This activity has received funding from the European Institute of Innovation and Technology (EIT), a body of the European Union, under the Horizon 2020, the EU Framework Programme for Research and Innovation

Supplementary MP-AES analysis was performed for the leachates of the different steps of sequential extraction. Only small concentrations (Figure 14) were measured. In the cases of all five samples, REE were detected in the 4th step. In the graph, there are no REE measured in the 1st-3rd and the 5th step, however, this is a false observation. In those steps the concentrations were lower than the detection limit, which was relatively high (usually 2.5 or 10 ppm), because a 25-times dilution was used to protect the torch of the MP-AES machine from the strong or too dense chemicals. Moreover, in the test 600 or 1200 mL of reagents were added to the samples, which was 60 g in the beginning, but decreased to 15-20 g towards the end. This caused a high rate of dilution, further decreasing the concentration of dissolved REE.

As a conclusion of this measuring, the REE started to be dissolved towards the end of the test series, in particular in the 4th step, which is designed for the dissolution of the Fe-Mn oxides. This result is confirmed by a high content of goethite and hematite (Table 19) in the samples (between 45 and 55%). Compared to the other minerals phases identified, these two phases are with highest content in the samples, so an additional effect takes place: a smaller concentration of REE in a larger portion produces a higher concentration by dissolution. Moreover, the residual of the last (5th) step – where the silicates and phosphates are contained – was not digested and measured, so it is not comparable with the set of the residuals.

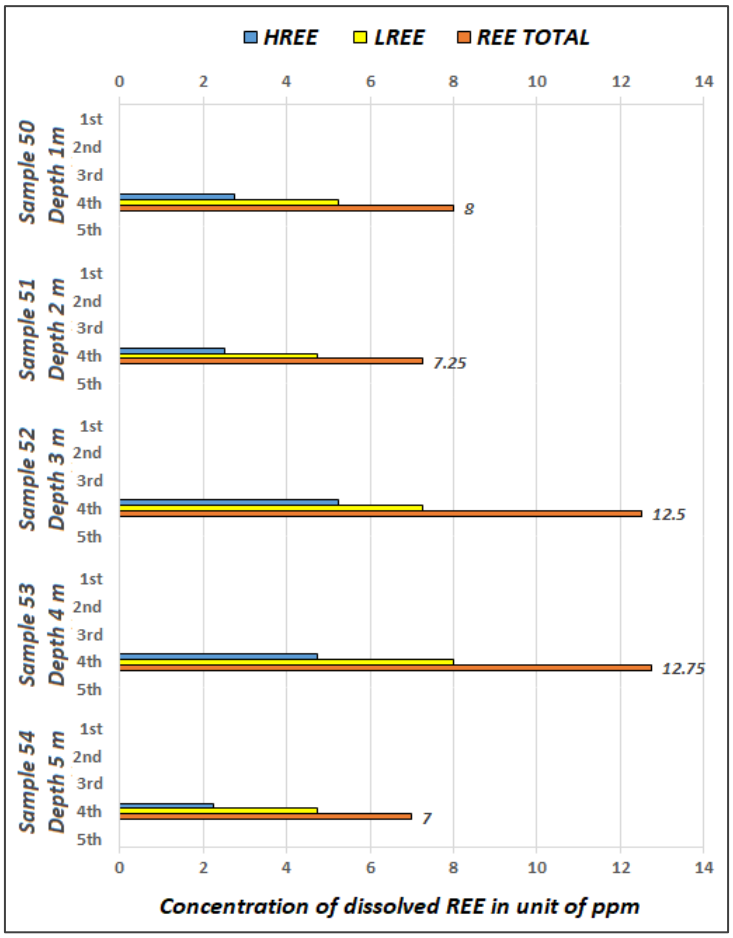

Figure 14. REE concentration in the leachates produced in the steps of the sequential extraction, measured by MP-AES technique, for selected Ajká red mud samples

This activity has received funding from the European Institute of Innovation and Technology (EIT), a body of the European Union, under the Horizon 2020, the EU Framework Programme for Research and Innovation

4. PRELIMINARY ASSESSMENT OF REE POTENTIAL IN BAUXITE – related resources; possible technological approaches

4.1. Recent technologies for recovery of the metals from REE

The recovery of REE from bauxite residue in recent, very extensive research in EU funded Horizon 2020 project RED MUD (completed in 2019) included three acid leaching methods: 1) neutralisation-leaching; 2) dry digestion-leaching; 3) high-pressure acid leaching (HPAL) preceded by reductive smelting in comparison with the direct conventional acid leaching method (Tables 31-33).

1. **CO2-neutralisation followed by acid leaching**
   - Neutralisation at room temperature
     - 2 – 4 wt% of sodium reacts with the carbonic acid formed during the dissolution of CO_2 in water,
     - Less than 5 wt% of calcium dissolved
     - pH reduced from 10.7 to 9.3
   - High-pressure neutralisation, at high temperature,
     - 27 % sodium dissolved
     - pH reduced to ca. 8.7
     - Precipitation of calcite (increase up to 8 wt%)
   - General observations for neutralisation of bauxite residue with CO_2 gas
     - Not enhanced extraction of REE from bauxite residue during acid leaching due to their association with major metals, but also as a consequence of the lack of acid caused by the transformation of $CaCO_3$ into $CaSO_4$ and the decomposition of silicate compounds.
     - Scandium remained associated to iron (hematite) and aluminium mineral phases in the untreated and neutralised bauxite residue.
     - Neodymium and lanthanum may also remain associated to hematite, as they tend to occur simultaneously in similar mineral phases as that of cerium (found associated to iron and aluminium); their extraction yields could be enhanced by increasing the acid concentration.
     - The extraction of yttrium is not affected by the neutralised with CO_2, (yttrium could remain associated to cancrinite and/or chamosite, if not completely dissolved by H_2SO_4).

This activity has received funding from the European Institute of Innovation and Technology (EIT), a body of the European Union, under the Horizon 2020, the EU Framework Programme for Research and Innovation

2. **Dry digestion with multiple-stage leaching vs. direct leaching**
   - Direct acid leaching of the non-neutralised and neutralised bauxite residue can dissolve between 50 – 65 wt% of silicon. Dry digestion process dissolves only about 5 wt% (hydrolysis of silica avoided).
   - The maximum extraction yield of REE is ca. 45 with HCl and 20 wt.% with H_2SO_4.
   - The lowest aluminium/iron leaching ratio (i.e. 2:1) under acid consumption of 788 g HCl and 412 g H_2SO_4 per kg of bauxite residue. Same acid consumptions, the dry digestion method with re-circulation of the acid leaching solution increases significantly the concentration of the REE in solution:
     - 5-stage leaching process with HCl, the REE concentration increased from 7 to ca. 19 mg/ L, (two times concentration observed by a single-stage method).
     - 5-stage leaching process with H_2SO_4, the scandium concentration increases from 5 to 14 mg/L, while the concentration of yttrium, lanthanum and neodymium increases from an average value of 3 to ca. 8 mg/L.
     - Unfortunately, the concentration of major metals also increases.
   - High consumption of bauxite residue with a substantial reduction in water consumption, i.e. a reduction ca. 60 wt% with respect to the conventional acid leaching method.
   - Simultaneous recovery of REE and titanium oxide with a H_2SO_4-based dry digestion method is crucial to ensure a positive profit margin.

3. **Smelting followed by high-pressure acid leaching of bauxite residue slags**
   - Highest extraction yields of REE:
     - The concentration of REE in the slags increases by a factor of about 1.4 compared to the concentration of REE in the bauxite residue sample.
     - The highest extraction yield of REE with an acid concentration of 3 N (with 1 N very low, beyond 3 N concentration, no further increases, can be optimized below 3N)
   - HCl-based HPAL, the lowest aluminium/iron, Al/Fe, and scandium/iron, Sc/Fe, leaching ratios (i.e. 1.1 and 0.9, respectively) at 120°C with a high REE extraction (Sc: 79 wt%; Y, Nd and La > 97 wt%) and very low concentration of titanium and silicon in the solution (< 0.5 g L-1)
   - H_2SO_4-based HPAL, the lowest Al/Fe and Sc/Fe (i.e. 0.9 and 1.1) ratios obtained at 150°C, the selectivity of scandium over other REE was the highest (i.e. 3). The treatment of the slag with H_2SO_4 allows to extract ca. 90 wt.% of scandium, while most of the other REE remain undissolved in the solid fraction after leaching (HPAL process with H_2SO_4 as a leaching reagent might cause these elements to be adsorbed on the surface of silicon/aluminium-oxides compounds and/or associated to a sodium-lanthanide-double sulfate compound (NaLn(SO4)2×*n*H2O),

This activity has received funding from the European Institute of Innovation and Technology (EIT), a body of the European Union, under the Horizon 2020, the EU Framework Programme for Research and Innovation

- Low concentration of iron in the slag (< 5 wt%), and low concentration in the leach solution (< 2 g/L) compared to the concentration in the leach solution of the bauxite residue (24 g/L with HCl, and 13 g/L with H_2SO_4).
- The extraction of aluminium from the slag is very high (14 – 17 g/L) with both mineral acids. Due to the enrichment of aluminium in the slags, its concentration in the leach solution was 3 – 4 times higher than the concentration obtained after the direct processing of the bauxite residue.
- The concentration of silicon and titanium, remained < 0.5 g/L.
- The preliminary comparative economic analysis shows that HPAL with H_2SO_4 is the most interesting method for scandium recovery from the bauxite residue, as iron is also recovered before leaching by reductive smelting. However, further studies are required to decrease the acid consumption.

Table 31. Prospective technologies for recovery of major metals and REE from bauxite residue

DLx Direct leaching

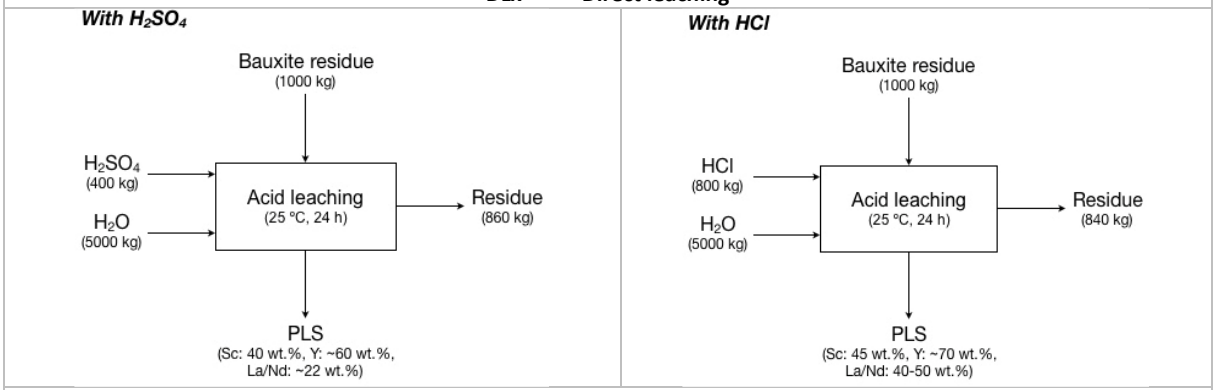

CO2 N-Lx CO2-neutralisation followed by acid leaching

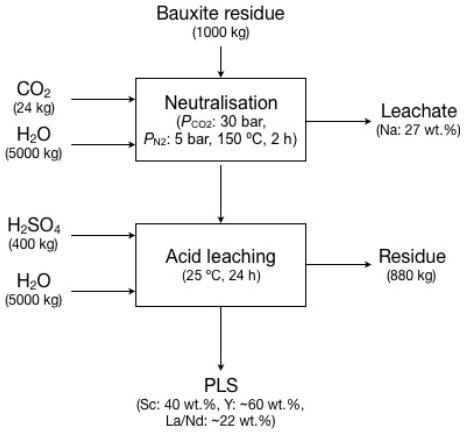

DD 1 Lx Dry digestion with single-stage leaching

This activity has received funding from the European Institute of Innovation and Technology (EIT), a body of the European Union, under the Horizon 2020, the EU Framework Programme for Research and Innovation

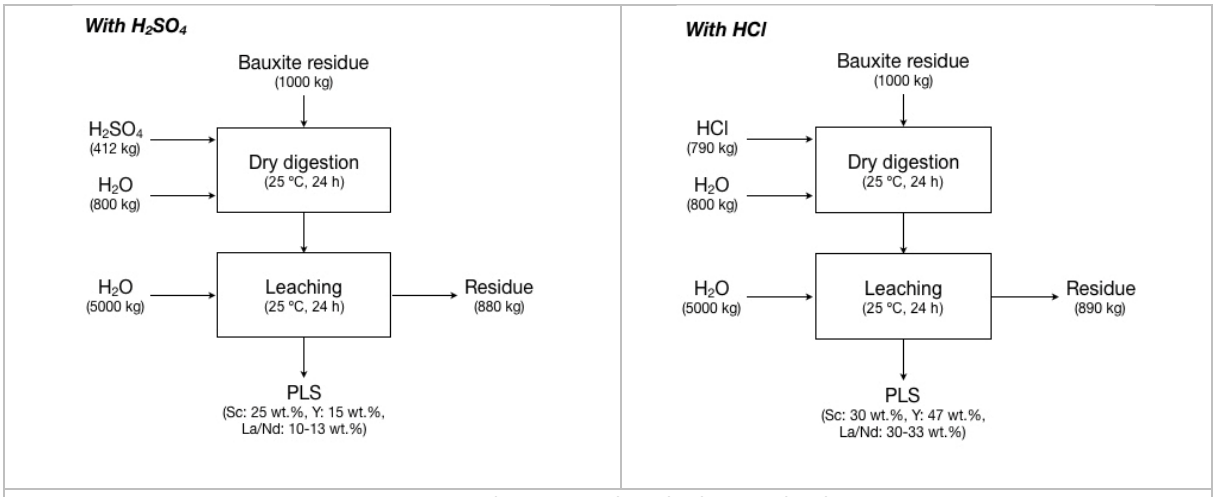

DD M Lx Dry digestion with multiple-stage leaching

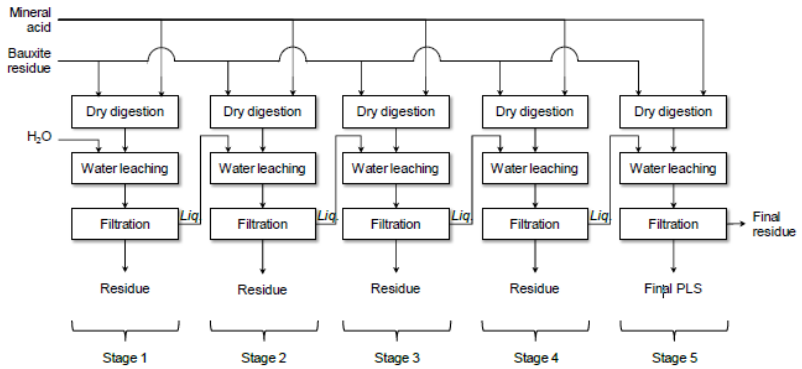

HPAL BR High-pressure acid leaching of bauxite residue

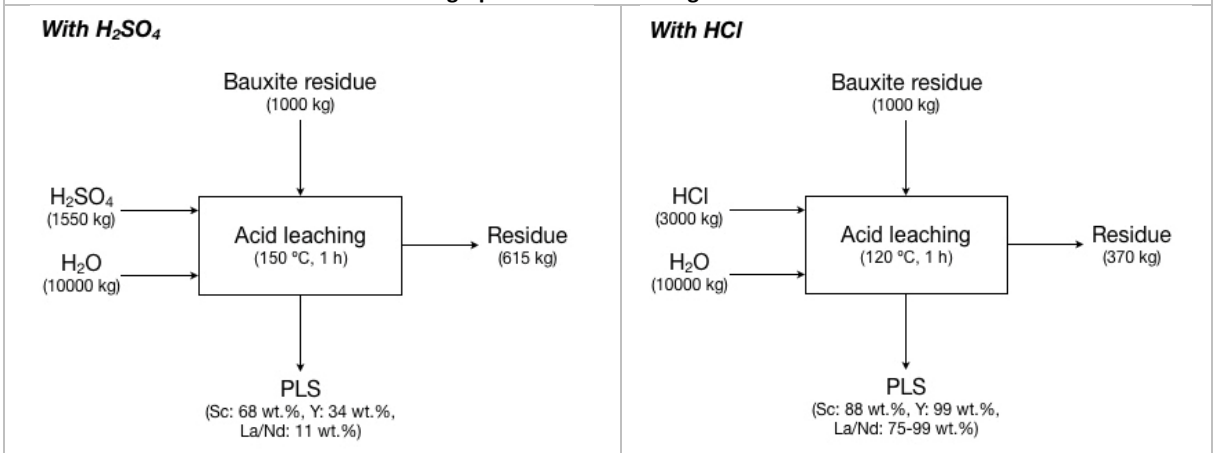

S-HPAL BRS Smelting followed by high-pressure acid leaching of bauxite residue slags

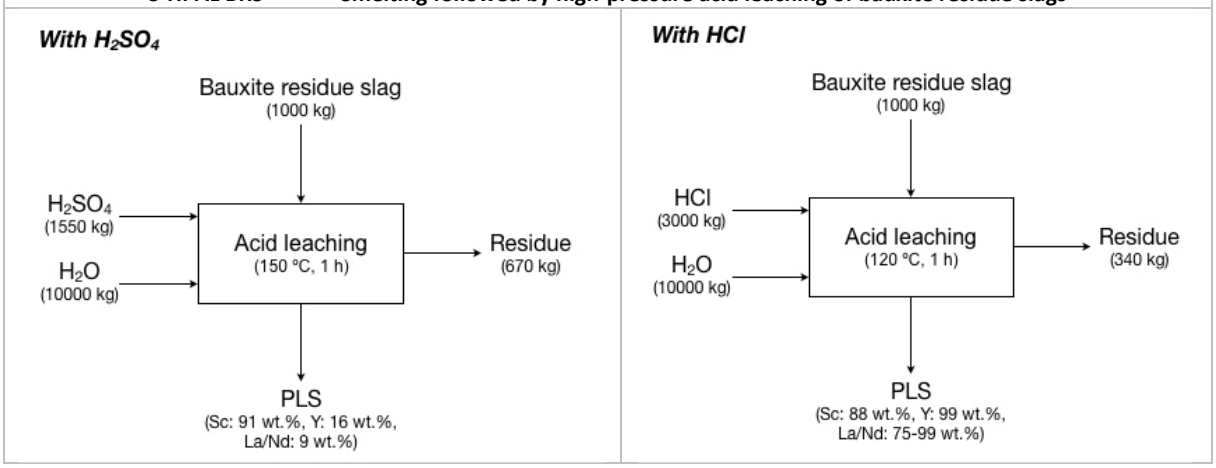

This activity has received funding from the European Institute of Innovation and Technology (EIT), a body of the European Union, under the Horizon 2020, the EU Framework Programme for Research and Innovation

Table 32. Overview of leaching processes studied by Rivera (2019) (basis: 1000 kg of bauxite residue/slag)

Prospective technology		DLx		CO_2 N-Lx		DD 1 Lx		DD M Lx		HPAL BR		S-HPAL BRS		Initial content in BR
		Direct leaching		CO_2-neutralisation followed by acid leaching		Dry digestion with single-stage leaching		Dry digestion with multiple-stage leaching		High-pressure acid leaching of bauxite residue		Smelting followed by high-pressure acid leaching of bauxite residue slags		
Lixiviant		H_2SO_4	HCl	H_2SO_4	HCl	H_2SO_4	HCl	H_2SO_4	HCl	H_2SO_4	HCl	H_2SO_4	HCl	
Fe	%	3	3	2	N/A	4	4	5	4	40	74	82	84	33 %
	g/L	1	2	1	N/A	3	3	10	7	13	24	3	3	
Al	%	26	30	21	N/A	30	23	22	24	50	40	70	91	10 %
	g/L	3	5	2	N/A	6	4	12	13	5	4	13	17	
Ti	%	28	30	29	N/A	23	2	21	3	5	7	0	0	3 %
	g/L	1	2	1	N/A	2	0	4	1	0	0	0	0	
Sc	%	39	45	36	N/A	24	30	20	32	68	88	91	79	121 mg/kg
	mg/L	5	5	4	N/A	6	7	14	19	7	9	11	12	
Y	%	58	70	56	N/A	15	47	13	50	34	99	16	99	76 mg/kg
	mg/L	4	4	4	N/A	2	7	6	19	2	7	2	11	
Nd	%	21	50	23	N/A	12	33	10	34	11	99	9	98	99 mg/kg
	mg/L	3	3	2	N/A	3	6	5	17	2	6	1	11	
La	%	23	38	20	N/A	13	30	12	32	12	77	9	98	114 mg/kg
	mg/L	2	2	2	N/A	2	7	8	18	1	11	1	17	
					N/A									

This activity has received funding from the European Institute of Innovation and Technology (EIT), a body of the European Union, under the Horizon 2020, the EU Framework Programme for Research and Innovation

Table 33. Overview of economic analysis of leaching processes studied by Rivera (2019)

Prospective technology	DLx		CO_2 N-Lx	DD 1 Lx		DD M Lx		S-HPAL BRS	
	Direct leaching		CO_2-neutralisation followed by acid leaching	Dry digestion with single-stage leaching		Dry digestion with multiple-stage leaching		Smelting followed by high-pressure acid leaching of bauxite residue slags	
Lixiviant	H_2SO_4	HCl	H_2SO_4	H_2SO_4	HCl	H_2SO_4	HCl	H_2SO_4	HCl
	PRODUCTION (in ton/year)								
Fe	-	-	-	-	-	-	-	14 850	14 850
TiO_2	335	335	335	266	23	1 214	173	0	0
Sc_2O_3	7	7	7	4	6	18	29	14	12
	COSTS (in thousand USD/year)								
	Extraction								
Capital cost	40	46	46	31	38	128	205	110	96
Acid	6 000	6 000	6 000	6 000	11 820	6 000	11 820	6 000	11 820
Operating cost	605	708	708	472	590	1 966	3 146	423	367
	Recovery								
Capital cost	45	51	40	27	34	112	180	84	73
Operating cost	6 738	7 580	6 064	4 043	5 054	16 845	26 953	12 568	10 910
	BENEFITS (in thousand USD/year)								
BR	500	500	500	500	500	500	500	500	500
TiO_2	1 174	1 214	1 174	931	81	4 251	607	0	0
Sc_2O_3	44 098	49 610	39 688	26 459	33 073	110 244	176 391	82 248	71 402
Fe	-	-	-	-	-	-		7 054	7 054
	MARGIN (in million USD / year)								
with highest prices	32.3	31.1	28.5	17.3	16.1	89.9	135.2	70.6	55.2
with lowest prices	2.9	1.7	2.4	1,2	-0.4	9.6	10.9	8.8	6.1

This activity has received funding from the European Institute of Innovation and Technology (EIT), a body of the European Union, under the Horizon 2020, the EU Framework Programme for Research and Innovation

The preliminary economic analysis by Rivera (2019) has shown that the dry digestion process with multi-stage leaching is economically the most interesting leaching alternative due to the high consumption of bauxite residue and the low consumption of water. Profit margin was four times lower to the profit margins reported in the literature (when half of the metal price is assumed). However the process did not consider the pre-treatment of bauxite residue to recover base metals, which could be done in a subsequent separation step to avoid the installation of high-temperature processes.

Main limitations of the direct treatment of bauxite residue by acid leaching are:

- the consumption of large amounts of acid during neutralisation of the alkaline bauxite residue,
- the high co-dissolution of major metals, particularly iron and aluminium, and
- the decomposition of silicate compounds that leads to the polymerisation of amorphous silica.

The HPAL and the dry digestion processes allow to suppress the silica gel formation and titanium dissolution, but the high co-dissolution of aluminium and iron may represent an offset for the downstream processing.

4.2. REE potential in bauxite related sources in the ESEE region

A comparison of the analysed red mud in the frame of REEBAUX WP3 and data from Rivera (2019)(Red Mud project) (Tables 34 and 35) has shown that both materials show similarities, with some important differences:

- the content in REE is higher in the REEBAUX materials;
- in average, the Fe content is lower in the REEBAUX materials and the Al content is the same, implying the lower consumption of acids;
- the content of the sodium is significantly higher in REEBAUX materials than in those studied by Rivera, implying the further requirements and complications for leaching of the neutralised bauxite residue;
- the silicon content is significantly higher, implying the need for dry digestion method to avoid silica-gel formation to enable REE extraction

This activity has received funding from the European Institute of Innovation and Technology (EIT), a body of the European Union, under the Horizon 2020, the EU Framework Programme for Research and Innovation

Table 34. Comparison of the main composition of the bauxite residue used in research of Rivera (2019) and the red mud samples collected within REEBAUX WP3 activities in Slovenia, Montenegro and Hungary

Compound	In Rivera (2019)	In REEBAUX Min-Max; Avg.	Comment
Fe_2O_3	46.7 wt%	12.3-42.1; 36 wt%	Lower content of Fe Lower yield and Fe margin in S-HPAL BRS
Al_3O_3	18.1 wt%	11.3-31.1; 18.1 wt%	Identical
CaO	8.5 wt%	1.9-22.9; 8.0 wt%	Similar
SiO_2	7.3 wt%	8.5-25.2; 12.2 wt%	Higher Si
TiO_2	5.8 wt%	1.7-6.9; 4.2 wt%	Somewhat lower Ti
Na_2O	2.8 wt%	2.1-9.3; 6.6 wt%	Higher sodium
Loss on ignition	8.5 wt%	N/A	
Sc	121 ±10 g/t	35-124; 100.5 ppm (g/t)	Somewhat lower Sc content.
Y	76 ±10 g/t	58.2-224; 147.7 ppm (g/t)	2X higher initial content
La	114 ±10 g/t	83.3-408; 235.9 ppm (g/t)	2X higher initial content
Nd	99 ±10 g/t	66.3-283.2; 181.9 ppm (g/t)	2X higher initial content
Total REEE	N/A	0-1781.7; 1201.7 ppm (g/t)	

Table 35. Comparison of the mineral composition of bauxite residue used in research of Rivera (2019) and of red mud from Ajká landfill, Hungary, for cells VIII. and IX. (REEBAUX)

Compound	In Rivera (2019)	In REEBAUX Min-Max; Avg.	Comment
Hematite Fe_2O_3	36 wt%	30.4-44.9; 38%	Similar
Dicalcium silicate (C2S) Ca_2SiO_4	12 wt%	N/A	
Gibbsite $Al(OH)_3$	8 wt%	0.2-8.7; 2.3%	Varies
Hydrogrossular $Ca_3Al_2(SiO_4)_{1.53}(OH)$	7 wt%	Hibschite 1.2-9.4; 4.1% Katoite 1.2-9.4; 4.1%	Observed other two minerals from the family, higher content
Diaspore AlO(OH)	7 wt%	0.1-1.4; 0.5%	Low content, as the ESEE bauxite are mostly boehmite type
Grossular $Ca_3Al_2(SiO_4)_3$	5 wt%	N/A	
Tricalcium-silicate (C_3S) Ca_3SiO_5	5 wt%	N/A	
Goethite FeO(OH)	5 wt%	3.7-19.3; 7.7%	Higher content

This activity has received funding from the European Institute of Innovation and Technology (EIT), a body of the European Union, under the Horizon 2020, the EU Framework Programme for Research and Innovation

Compound	In Rivera (2019)	In REEBAUX Min-Max; Avg.	Comment
Calcite $CaCO_3$	4 wt%	Calcite 4.2-12.0; 7.4% Aragonite 0-4.2; 0.9%	Higher content
Bayerite α-$Al(OH)_3$	4 wt%	N/A Nordstrandite 0-0.6; 0.3%	
Sodalite $Na_6(Al_6Si6O_{24})\times NaOH\times(8-2x)H_2O$	3 wt%	N/A	
Calcium phyllo-dodeca-alumotetrasilicate $Al_{12}CaO_{27}Si_4$	2 wt%	N/A	
Rutile TiO_2	2 wt%	Anatase 0.1-0.6; 0.2%	
Cancrinite $Na_6Ca_2Al_6Si_6O_{24}(CO_3)_2\cdot 2H_2O$	1 wt%	9-26; 20.5 %	High!

4.3. Next steps

Further work requires simulation of the process for the average REEBAUX materials (if possible) or careful and conservative use of market data (such as in Tables 36 and 37) and process information from Red Mud project (http://redmud.org/) to analyse the technologically probable and economically most opportune concentrate/oxides/metals mix production in an ESEE context. That step will enable modelling and important inputs for the consequential LCA in the next work package. The work already done is the Master thesis of LCA of production of bauxite in Jajce (Bosna and Herzegovina). This will enable the information on the environmental impacts of the bauxite mining in ESEE region from the underground deposits.

Table 36. Average Rare Earth Concentrate, Oxides and Metals prices (Shangai Metal Market on 6-Feb-2020)

Rare Earth Oxides			Rare Earth Metals		
Products	Avg	Unit	Products	Avg	Unit
Lanthanum Oxide	1530,945	EUR/mt	Lanthanum	4429,967	EUR/mt
Cerium Oxide	1498,371	EUR/mt	Cerium	4234,528	EUR/mt
Praseodymium Oxide	42996,74	EUR/mt	Praseodymium	84039,09	EUR/mt
Neodymium Oxide	38045,6	EUR/mt	Neodymium	47882,74	EUR/mt
Samarium Oxide	1628,664	EUR/mt	Terbium	585,6678	EUR/kg
Europium Oxide	27,36156	EUR/kg	Dysprosium	276,873	EUR/kg
Gadolinium Oxide	21172,64	EUR/mt	Yttrium	30,61889	EUR/kg
Terbium Oxide	459,2834	EUR/kg	Cerium Misch	4429,967	EUR/mt
Dysprosium Oxide	221,4984	EUR/kg	Lanthanum Cerium Metal (Battery Grade)	4625,407	EUR/mt
Erbium Oxide	20521,17	EUR/mt	Pr-Nd Alloy	46644,95	EUR/mt
Yttrium Oxide	2605,863	EUR/mt	Battery Grade Misch	18892,51	EUR/mt
Didymium Oxide	36351,79	EUR/mt	Dy-Iron Alloy	219544	EUR/mt
Holmium Oxide	40390,88	EUR/mt	Holmium Ferroalloy	42996,74	EUR/mt

This activity has received funding from the European Institute of Innovation and Technology (EIT), a body of the European Union, under the Horizon 2020, the EU Framework Programme for Research and Innovation

Concentrate			Exchange rate:	
RE Carbonate	2736,156	EUR/mt	EUR / RMB Feb.06	7.675 (-0.053 | -6.826‰)
			GBP / RMB Feb.06	9.062 (-0.054 | -5.913‰)
			HKD / RMB Feb.06	0.899 (-0.003 | -3.105‰)
			100JPY / RMB Feb.06	6.351 (-0.000 | -7.191‰)

Table 37. Average Metals prices (Shangai Metal Market on 6-Feb-2020)

Metals Products	Avg	Unit
Alumina	320,65	EUR/mt
Aluminum alloys	1760,26	EUR/mt
Aluminum fluoride	1055,37	EUR/mt
Pig iron	377,85	EUR/mt
Titanium sponge	10,42	EUR/kg

This activity has received funding from the European Institute of Innovation and Technology (EIT), a body of the European Union, under the Horizon 2020, the EU Framework Programme for Research and Innovation

4.4. In-situ value calculation (performed by DMT)

This report has been prepared by DMT GmbH & Co. KG (hereafter DMT) for the exclusive use in the research and development project REEBAUX on the basis of instructions, information and data supplied by the client or from the public domain.

No warranty or guarantee, whether expressed or implied, is made by DMT with respect to the completeness or accuracy of any aspect of this document and no party, other than the partners of REEBAUX, are authorized to or should place any reliance whatsoever on the whole or any part or parts of the document.

DMT do not undertake or accept any responsibility or liability in any way whatsoever to any person or entity in respect of the whole or any part or parts of this document, or any errors in or omissions from it, arising from negligence or any other basis in law whatsoever. This note may contain "forward looking statements" which are based on assumptions made by DMT. There is no assurance or warranty given that any of the future results or achievements expressed or implied contained will be realized.

Likewise DMT disclaim liability for any personal injury, property or other damage of any nature whatsoever, whether special, indirect, consequential or compensatory, directly or indirectly resulting from the publication, use or application, or reliance on this document.

DMT was provided with concentrations of REEs, Scandium and further elements for 250 samples taken from 158 locations in 4 countries, which are Croatia, Hungary, Montenegro and Slovenia. A total of 187 samples were taken from bauxites and 63 samples were taken from red mud, which is the bauxite residue (Table 38).

Table 38. Summary of sample amount

Country-Province	Material	Number of samples	Number of sites
Croatia-Dalmatia and Lika	Bauxite	73	54
Croatia-Istria	Bauxite	18	18
Hungary	Bauxite	36	5
Hungary	Red mud	42	3
Montenegro	Bauxite	60	58
Montenegro	Red mud	20	19
Slovenia	Red mud	1	1
SUBTOTAL	Red mud	187	135
SUBTOTAL	Bauxite	63	23
TOTAL		250	158

For each location DMT calculated the arithmetic mean of concentrations for REEs and Scandium (Table 39 and Table 40).

This activity has received funding from the European Institute of Innovation and Technology (EIT), a body of the European Union, under the Horizon 2020, the EU Framework Programme for Research and Innovation

Table 39. Concentrations of REEs and Scandium for several locations in Croatia and Hungary; Units are in ppm which equals gram of REE or Scandium per ton of bauxite or red mud

Country-Province	Material	Site	Sc ppm	Y ppm	La ppm	Ce ppm	Pr ppm	Nd ppm	Sm ppm	Eu ppm	Gd ppm	Tb ppm	Dy ppm	Ho ppm	Er ppm	Tm ppm	Yb ppm	Lu ppm	REE ppm
Croatia-Dalmatia and Lika	Bauxite	Ćosići 1	47	53	70	135	15	56	11	2	10	2	10	2	7	1	6	1	381
Croatia-Dalmatia and Lika	Bauxite	Ćosići 2	74	249	221	321	45	181	39	10	45	7	45	10	27	4	22	3	1229
Croatia-Dalmatia and Lika	Bauxite	Glijev S	46	251	233	308	42	161	31	7	34	5	30	6	18	2	15	2	1144
Croatia-Dalmatia and Lika	Bauxite	Glijev S	54	253	244	312	48	203	41	9	42	6	36	8	21	3	17	3	1245
Croatia-Dalmatia and Lika	Bauxite	Glijev S	59	214	239	337	47	188	37	8	37	6	35	7	22	3	18	3	1202
Croatia-Dalmatia and Lika	Bauxite	Gljev	57	454	297	383	53	225	48	12	59	9	58	13	39	5	32	5	1692
Croatia-Dalmatia and Lika	Bauxite	Gljev	60	269	230	268	43	175	36	9	42	6	40	9	26	3	20	3	1179
Croatia-Dalmatia and Lika	Bauxite	Imotski	64	88	123	375	25	99	19	4	21	3	17	3	10	1	9	1	800
Croatia-Dalmatia and Lika	Bauxite	Jukići-Đidar	63	169	196	335	37	152	29	6	21	4	25	5	16	2	17	3	1019
Croatia-Dalmatia and Lika	Bauxite	Košute	35	57	111	186	23	83	16	3	14	2	13	3	7	1	8	1	528
Croatia-Dalmatia and Lika	Bauxite	MAM B-1	39	75	135	220	29	105	18	4	16	3	15	3	9	1	8	1	644
Croatia-Dalmatia and Lika	Bauxite	MAM B-1	40	61	82	230	17	63	12	3	11	2	11	2	7	1	7	1	511
Croatia-Dalmatia and Lika	Bauxite	MAM B-1	41	84	128	238	24	87	15	3	15	2	14	3	9	1	9	1	634
Croatia-Dalmatia and Lika	Bauxite	MAM B-1	42	77	107	209	22	81	16	3	15	2	14	3	9	1	8	1	569
Croatia-Dalmatia and Lika	Bauxite	MAM B-1	43	33	47	164	9	32	6	1	6	1	6	1	4	1	4	1	316
Croatia-Dalmatia and Lika	Bauxite	MAM B-1	44	62	99	175	21	79	19	4	17	3	17	3	9	1	9	1	520
Croatia-Dalmatia and Lika	Bauxite	MAM B-1	48	72	102	225	18	67	13	3	11	2	13	3	8	1	9	1	548
Croatia-Dalmatia and Lika	Bauxite	MAM B-1	49	58	80	204	15	56	12	3	10	2	10	2	7	1	7	1	467
Croatia-Dalmatia and Lika	Bauxite	MAM B-1	50	68	84	245	16	59	14	3	12	2	13	3	9	1	9	1	540
Croatia-Dalmatia and Lika	Bauxite	MAM B-1	51	38	51	203	10	39	9	2	7	1	8	2	5	1	6	1	383
Croatia-Dalmatia and Lika	Bauxite	MAM B-1	57	70	94	228	22	86	22	5	19	3	20	4	12	2	12	2	600
Croatia-Dalmatia and Lika	Bauxite	Mamutovac	53	66	87	204	20	74	15	3	13	2	12	3	8	1	8	1	518
Croatia-Dalmatia and Lika	Bauxite	Mamutovo I	57	142	166	251	29	104	21	5	21	3	22	5	15	2	14	2	801
Croatia-Dalmatia and Lika	Bauxite	Mamutovo I	71	99	105	296	25	106	24	6	27	4	23	4	12	2	12	2	745
Croatia-Dalmatia and Lika	Bauxite	Mamutovo I	73	124	128	454	34	151	35	8	36	5	27	5	15	2	15	2	1042
Croatia-Dalmatia and Lika	Bauxite	Mamutovo I	81	138	132	581	34	143	30	7	37	5	30	6	16	2	16	2	1180
Croatia-Dalmatia and Lika	Bauxite	Moseć	46	61	59	143	12	44	8	2	7	1	9	2	6	1	6	1	361
Croatia-Dalmatia and Lika	Bauxite	Moseć	52	129	151	287	30	114	22	5	22	3	20	4	11	2	10	2	812
Croatia-Dalmatia and Lika	Bauxite	Moseć	55	180	104	273	30	124	26	6	27	4	24	5	15	2	12	2	835
Croatia-Dalmatia and Lika	Bauxite	Moseć	60	102	111	299	26	99	22	5	21	3	20	4	12	2	11	2	738
Croatia-Dalmatia and Lika	Bauxite	Moseć Jama	51	84	56	119	15	58	15	3	14	2	15	3	10	1	9	1	405
Croatia-Dalmatia and Lika	Bauxite	Moseć Jama	53	100	82	133	22	84	18	4	17	3	16	3	10	1	9	1	505
Croatia-Dalmatia and Lika	Bauxite	Obrovac	53	137	141	315	37	148	31	7	27	4	25	5	15	2	13	2	909
Croatia-Dalmatia and Lika	Bauxite	Obrovac	63	101	114	274	27	102	21	5	19	3	19	4	12	2	12	2	717
Croatia-Dalmatia and Lika	Bauxite	Ričina	53	67	92	220	19	69	14	3	14	2	13	3	8	1	8	1	534
Croatia-Dalmatia and Lika	Bauxite	Ričina	64	194	208	365	45	180	36	9	42	6	35	7	18	2	15	2	1165
Croatia-Dalmatia and Lika	Bauxite	Rudopolje	33	79	46	185	13	49	10	2	10	2	12	3	9	1	9	1	431
Croatia-Dalmatia and Lika	Bauxite	Rudopolje	37	79	27	226	9	36	9	2	10	2	12	3	8	1	8	1	434
Croatia-Dalmatia and Lika	Bauxite	Rudopolje	42	188	142	270	27	101	20	4	22	4	24	5	17	3	16	2	846
Croatia-Dalmatia and Lika	Bauxite	Stari Gaj, Ob	58	59	94	409	20	71	18	4	14	3	15	3	9	2	11	2	733
Croatia-Dalmatia and Lika	Bauxite	Stari Gaj, Ob	53	53	77	323	17	64	14	3	12	2	12	2	7	1	9	1	599
Croatia-Dalmatia and Lika	Bauxite	Stari Gaj, Ob	49	46	62	179	13	49	11	3	10	2	10	2	7	1	8	1	403
Croatia-Dalmatia and Lika	Bauxite	Strmendola	31	34	112	266	16	50	9	2	7	1	7	1	4	1	5	1	515
Croatia-Dalmatia and Lika	Bauxite	Strmendola	36	35	68	228	12	42	7	1	6	1	6	1	4	1	4	1	417
Croatia-Dalmatia and Lika	Bauxite	Strmendola	63	115	159	213	36	137	27	6	24	4	20	4	11	2	10	2	769
Croatia-Dalmatia and Lika	Bauxite	Tošići-Dujić	55	354	229	369	46	203	50	12	56	8	46	10	28	4	23	3	1439
Croatia-Dalmatia and Lika	Bauxite	Tošići-Dujić	61	408	192	283	37	149	37	10	49	8	49	11	32	4	26	4	1300
Croatia-Dalmatia and Lika	Bauxite	Tošići-Dujić	67	728	178	309	35	159	42	11	52	8	47	11	34	5	27	4	1649
Croatia-Dalmatia and Lika	Bauxite	Tošići-Dujić	69	179	214	361	39	144	28	7	29	5	30	6	18	3	18	3	1082
Croatia-Dalmatia and Lika	Bauxite	Tošići-Dujić	75	1346	465	348	113	524	110	29	182	25	149	36	95	11	55	8	3496
Croatia-Dalmatia and Lika	Bauxite	Turban Kosa	67	62	69	145	16	62	13	3	12	2	13	3	8	1	8	1	419
Croatia-Dalmatia and Lika	Bauxite	Turban Kosa	76	126	124	318	23	90	21	5	23	4	26	6	16	2	15	2	801
Croatia-Dalmatia and Lika	Bauxite	Vrace	36	63	82	177	18	61	12	2	13	2	13	3	8	1	8	1	465
Croatia-Dalmatia and Lika	Bauxite	Vrace	40	70	160	380	37	141	23	4	16	2	14	3	8	1	8	1	868
Croatia-Istria	Bauxite	Dragozetići-1		54	85	635	12	40	7	2	8	1	9	2	6	1	7	1	871
Croatia-Istria	Bauxite	Dragozetići-2		79	115	231	19	66	13	3	12	2	15	3	10	2	10	2	581
Croatia-Istria	Bauxite	Karojba-1		63	107	133	17	58	10	2	9	1	10	2	7	1	7	1	429
Croatia-Istria	Bauxite	Karojba-2		64	109	135	18	58	10	2	9	2	11	2	8	1	8	1	437
Croatia-Istria	Bauxite	Kaštelir-1		49	174	222	18	46	7	1	7	1	9	2	6	1	7	1	552
Croatia-Istria	Bauxite	Kaštelir-2		53	103	144	16	52	9	2	8	1	9	2	6	1	6	1	415
Croatia-Istria	Bauxite	Kaštelir-3		66	69	140	14	51	11	2	10	2	12	3	8	1	8	1	396
Croatia-Istria	Bauxite	Kaštelir-4		48	88	100	14	44	7	1	7	1	8	2	5	1	6	1	332
Croatia-Istria	Bauxite	Minjera2-1		62	128	239	19	49	6	1	5	1	10	2	8	1	9	1	541
Croatia-Istria	Bauxite	Rovinj1-1		81	107	591	22	75	14	3	14	2	15	3	10	1	9	1	949
Croatia-Istria	Bauxite	Rovinj1-2		94	163	290	41	153	26	5	22	3	16	3	9	1	9	1	836
Croatia-Istria	Bauxite	Rovinj1-3		112	254	500	62	234	40	8	33	4	20	4	10	1	9	1	1294
Croatia-Istria	Bauxite	Rovinj1-4		89	148	323	37	135	26	5	22	3	17	3	10	1	9	1	830
Croatia-Istria	Bauxite	Rovinj1-5		77	161	283	35	127	22	4	18	3	15	3	9	1	9	1	768
Croatia-Istria	Bauxite	Rovinj1-6		47	84	212	24	88	16	3	11	2	9	2	5	1	6	1	508
Croatia-Istria	Bauxite	Šterna-1		53	79	297	18	65	13	3	12	2	11	2	6	1	6	1	566
Croatia-Istria	Bauxite	Učka-1		75	94	164	18	61	11	3	12	2	12	3	7	1	7	1	469
Croatia-Istria	Bauxite	Učka-2		69	102	250	17	54	9	2	9	2	12	3	9	1	9	1	550
Hungary	Bauxite	Csabrendek		112	161	208	46	177	35	7	26	4	23	5	14	2	14	2	835
Hungary	Bauxite	Dudar		114	148	299	33	126	23	5	21	3	18	4	11	2	10	2	817
Hungary	Bauxite	Iharkút		230	176	277	40	157	30	6	29	4	27	6	18	3	17	3	1023
Hungary	Bauxite	Nagyharsány		182	209	278	39	150	27	6	27	4	25	6	17	3	17	3	990
Hungary	Bauxite	Óbarok		51	137	259	29	110	19	4	15	2	10	2	6	1	5	1	651
Hungary	Red mud	Cell No. IX.		142	212	434	48	180	33	7	29	4	25	5	14	2	14	2	1151
Hungary	Red mud	Cell No. VII.		116	205	415	42	152	28	5	22	3	21	4	12	2	13	2	1044
Hungary	Red mud	Cell No. VIII.		144	211	435	47	176	33	7	29	4	26	5	15	3	14	2	1079

This activity has received funding from the European Institute of Innovation and Technology (EIT), a body of the European Union, under the Horizon 2020, the EU Framework Programme for Research and Innovation

Table 40. Concentrations of REEs and Scandium for several locations in Montenegro and Slovenia; Units are in ppm which equals gram of REE or Scandium per ton of bauxite or red mud

Country-Province	Material	Site	Sc ppm	Y ppm	La ppm	Ce ppm	Pr ppm	Nd ppm	Sm ppm	Eu ppm	Gd ppm	Tb ppm	Dy ppm	Ho ppm	Er ppm	Tm ppm	Yb ppm	Lu ppm	REE ppm
Montenegro	Bauxite	BAJOV DO;	27	33	37	58	5	18	3	1	4	1	5	1	4	1	4	1	175
Montenegro	Bauxite	BAJOV DO;	36	42	53	123	8	26	5	1	5	1	7	2	5	1	6	1	285
Montenegro	Bauxite	BAJOV DO;	38	47	73	68	12	42	8	2	7	1	9	2	7	1	7	1	288
Montenegro	Bauxite	BAJOV DO;	39	42	63	93	9	30	6	1	6	1	8	2	6	1	7	1	278
Montenegro	Bauxite	BAJOV DO;	44	49	62	270	10	34	7	1	7	1	9	2	6	1	7	1	466
Montenegro	Bauxite	BAJOV DO;	46	54	71	277	13	46	9	2	9	2	10	2	7	1	7	1	509
Montenegro	Bauxite	BAJOV DO;	51	57	114	290	21	70	13	3	12	2	13	3	8	1	9	1	618
Montenegro	Bauxite	BAJOV DO;	56	62	135	388	28	100	20	4	17	3	16	3	9	2	11	2	800
Montenegro	Bauxite	BIJELE POLJ	30	23	21	52	4	16	3	1	3	1	4	1	3	0	3	0	136
Montenegro	Bauxite	BIJELE POLJ	39	130	252	226	65	254	42	8	31	4	23	4	12	2	11	2	1066
Montenegro	Bauxite	BIJELE POLJ	43	50	30	57	5	19	4	1	5	1	8	2	6	1	7	1	197
Montenegro	Bauxite	BIJELE POLJ	44	45	53	171	10	35	7	1	7	1	9	2	6	1	6	1	355
Montenegro	Bauxite	BIJELE POLJ	46	56	84	168	10	33	7	2	7	1	9	2	7	1	7	1	394
Montenegro	Bauxite	BIJELE POLJ	48	59	93	216	20	76	15	3	12	2	13	3	8	1	9	1	531
Montenegro	Bauxite	BIJELE POLJ	49	50	52	267	10	37	8	2	8	1	9	2	6	1	6	1	459
Montenegro	Bauxite	BIJELE POLJ	51	40	26	70	5	18	4	1	4	1	7	2	5	1	5	1	189
Montenegro	Bauxite	BIJELE POLJ	59	40	21	60	4	15	3	1	4	1	7	2	5	1	5	1	168
Montenegro	Bauxite	BIOČKI STA	66	233	257	414	61	263	55	12	49	7	37	7	21	3	18	3	1440
Montenegro	Bauxite	BOKA KOTO	28	45	90	164	16	55	10	2	8	1	8	2	5	1	6	1	415
Montenegro	Bauxite	BOROVA BR	65	136	326	416	50	182	34	8	36	5	28	6	16	2	14	2	1260
Montenegro	Bauxite	BRŠNO; DEP	50	88	117	359	18	62	11	3	12	2	14	3	9	1	9	1	709
Montenegro	Bauxite	CRVENJACI;	53	93	157	353	26	91	17	4	16	3	16	3	10	2	10	2	800
Montenegro	Bauxite	CRVENO PR	53	171	313	365	42	157	26	6	27	4	26	6	17	2	15	2	1179
Montenegro	Bauxite	ĐELOV DO;	41	59	78	185	14	46	9	2	9	2	11	3	8	1	8	1	434
Montenegro	Bauxite	ĐURAKOV D	57	120	146	368	33	126	25	5	22	3	20	4	13	2	13	2	902
Montenegro	Bauxite	GORNJEPOL	28	58	30	61	8	30	7	1	7	1	9	2	6	1	6	1	228
Montenegro	Bauxite	GORNJEPOL	29	51	67	261	14	51	10	2	9	1	9	2	6	1	6	1	489
Montenegro	Bauxite	GORNJEPOL	30	83	60	159	13	48	11	2	12	2	13	3	8	1	7	1	422
Montenegro	Bauxite	GORNJEPOL	31	199	271	893	69	269	50	9	45	6	34	6	18	3	16	2	1889
Montenegro	Bauxite	GORNJEPOL	34	64	42	94	10	39	10	2	9	2	11	2	8	1	8	1	304
Montenegro	Bauxite	GORNJEPOL	36	125	126	216	25	95	19	3	19	3	19	4	12	2	11	2	681
Montenegro	Bauxite	GREBENICI,	53	98	156	218	25	79	13	3	13	2	14	3	10	1	10	2	646
Montenegro	Bauxite	JELINA PEĆI	42	40	41	83	6	21	5	1	5	1	7	2	5	1	5	1	224
Montenegro	Bauxite	KRUŠČICA; (	39	30	30	62	5	17	3	1	4	1	5	1	4	1	4	1	168
Montenegro	Bauxite	LAZINE; DEP	39	37	84	154	11	31	5	1	5	1	7	1	5	1	5	1	348
Montenegro	Bauxite	LIVEROVIĆI;	56	121	281	356	48	162	27	5	22	4	21	4	13	2	13	2	1081
Montenegro	Bauxite	MEĐEĐE; DE	35	33	52	124	12	42	8	2	7	1	7	1	4	1	5	1	299
Montenegro	Bauxite	MILOVIĆI; C	32	84	95	141	19	72	14	3	13	2	12	3	7	1	6	1	473
Montenegro	Bauxite	PAKLARICA;	42	50	69	145	15	57	11	2	9	2	9	2	6	1	6	1	386
Montenegro	Bauxite	PIVA, Rudin	48	73	54	312	10	35	8	2	9	2	12	3	10	2	10	2	542
Montenegro	Bauxite	SAVINA GRA	32	61	83	178	17	61	11	2	10	2	10	2	6	1	6	1	451
Montenegro	Bauxite	ŠTITOVO II;	22	209	111	110	27	130	33	8	39	6	32	6	18	2	14	2	746
Montenegro	Bauxite	ŠTITOVO II;	53	85	114	342	23	88	18	4	16	3	16	3	10	2	11	2	736
Montenegro	Bauxite	ŠTITOVO II;	54	85	119	313	24	93	18	4	16	2	15	3	10	2	10	2	716
Montenegro	Bauxite	ŠTITOVO II;	58	94	125	333	24	89	18	4	16	3	15	3	11	2	11	2	747
Montenegro	Bauxite	ŠTITOVO II;	64	108	142	381	30	118	25	5	23	4	20	4	12	2	12	2	888
Montenegro	Bauxite	ŠTITOVO II;	68	190	391	347	71	262	54	11	46	7	41	8	22	3	21	3	1479
Montenegro	Bauxite	ŠTITOVO II;	70	119	162	364	33	130	30	6	28	4	25	5	14	2	15	2	943
Montenegro	Bauxite	STUDENAC;	39	49	59	127	10	32	5	1	6	1	8	2	6	1	6	1	314
Montenegro	Bauxite	TREBOVINJS	61	55	52	144	10	37	8	2	8	1	9	2	6	1	5	1	339
Montenegro	Bauxite	ULCINJ ARE	30	47	108	226	20	67	11	2	9	2	9	2	6	1	6	1	516
Montenegro	Bauxite	VELIKA GOR	28	45	153	295	26	83	13	3	10	2	10	2	6	1	6	1	655
Montenegro	Bauxite	VELIKA GOR	29	44	110	213	19	60	10	2	8	1	8	2	6	1	6	1	490
Montenegro	Bauxite	VELIKA GOR	30	50	131	203	20	60	10	2	9	2	10	2	6	1	6	1	512
Montenegro	Bauxite	VELIKA GOR	32	39	129	235	21	62	9	2	8	1	8	2	5	1	6	1	530
Montenegro	Bauxite	VELIKA GOR	39	42	111	279	20	61	10	2	8	1	9	2	6	1	6	1	560
Montenegro	Bauxite	VELJA DUBC	46	117	188	229	32	118	22	5	21	3	20	4	12	2	12	2	785
Montenegro	Bauxite	ZAGRAD; DE	65	119	225	407	44	154	29	6	25	4	23	5	14	2	14	2	1071
Montenegro	Red mud	B-1/19	35	58	86	183	17	66	12	3	11	2	10	2	6	1	7	1	466
Montenegro	Red mud	B-1/19	81	125	202	417	40	148	28	6	25	4	23	5	14	2	15	2	1057
Montenegro	Red mud	B-2/19	93	153	240	491	47	174	33	7	28	5	27	6	17	3	17	3	1251
Montenegro	Red mud	B-2/19	105	177	357	575	65	241	44	9	38	6	34	7	20	3	20	3	1600
Montenegro	Red mud	B-2/19	107	181	288	556	56	206	41	8	35	5	32	7	20	3	20	3	1461
Montenegro	Red mud	B-3/19	92	166	276	487	53	196	37	7	32	5	29	6	18	3	18	3	1336
Montenegro	Red mud	B-3/19	100	168	275	536	52	192	36	7	32	5	29	6	19	3	18	3	1381
Montenegro	Red mud	B-3/19	106	173	274	555	56	208	40	8	35	5	32	7	20	3	20	3	1438
Montenegro	Red mud	B-4/19	101	173	279	543	55	205	39	8	34	5	32	7	19	3	20	3	1424
Montenegro	Red mud	B-4/19	105	173	281	562	55	200	38	8	34	5	31	6	20	3	19	3	1439
Montenegro	Red mud	B-4/19	114	189	311	603	60	217	41	9	37	6	35	7	22	3	22	3	1564
Montenegro	Red mud	B-5/19	95	154	262	534	54	206	39	8	34	5	29	6	17	2	17	3	1370
Montenegro	Red mud	B-5/19	113	208	408	584	74	283	52	11	48	7	40	8	23	3	22	3	1775
Montenegro	Red mud	B-5/19	120	223	367	619	68	254	47	10	43	7	40	8	24	4	23	4	1742
Montenegro	Red mud	B-5/19	124	223	353	649	65	235	44	9	41	6	38	8	23	4	24	4	1726
Montenegro	Red mud	B-6/19	99	169	309	578	65	246	46	9	39	6	32	6	19	3	18	3	1549
Montenegro	Red mud	B-6/19	108	185	325	603	65	238	45	9	39	6	34	7	20	3	21	3	1603
Montenegro	Red mud	B-6/19	122	224	388	637	70	256	46	10	43	7	39	8	23	4	23	4	1782
Montenegro	Red mud	B-6/19	123	221	364	656	65	231	43	9	40	6	38	8	24	4	24	4	1737
Slovenia	Red mud	Kidričevo -	85	131	182	363	33	116	21	4	19	3	22	5	15	2	15	2	935

This activity has received funding from the European Institute of Innovation and Technology (EIT), a body of the European Union, under the Horizon 2020, the EU Framework Programme for Research and Innovation

All concentrations of REEs and Scandium were converted to REO and prices in USD/ton REO were sourced from several papers published by USGS (US) DERA (Germany) or Statista (Table 411) to calculate in-situ prices of REO and Scandium(III) oxide per ton of bauxite or red mud. The results are shown in Table 42 and Table 43.

Table 41. Conversion factors REE to REO and Sc to Sc_2O_3 plus price information sourced from several publications.

Z	REE	REE Name	REO	REE2REO	LREE/HREE	Price [US/t REO]	Product description	Source of Price
21	Sc	Scandium	Sc2O3	1.5338	X	4 800 000	Scandium oxide, 99.99% purity, 5-kilogram lot size	USGS (2014-2018)
39	Y	Yttrium	Y2O3	1.2699	X	6 440	Yttrium (oxide), min. 99,999 %, fob China	DERA (2014-2018)
57	La	Lanthanum	La2O3	1.1728	LREE	2 880	Lanthanum (oxide), min. 99 %, fob China	DERA (2014-2018)
58	Ce	Cerium	Ce2O3	1.1713	LREE	2 630	Cerium (oxide), min. 99 %, fob China	DERA (2014-2018)
59	Pr	Praseodymium	Pr2O3	1.1703	LREE	69 140	Praseodymium (oxide), min. 99 %, Europe	DERA (2014-2018)
60	Nd	Neodymium	Nd2O3	1.1664	LREE	66 400	Neodymium (oxide), min. 99 % fob China	DERA (2014-2018)
62	Sm	Samarium	Sm2O3	1.1596	LREE	2 920	Samarium (oxide), min. 99 % fob China	DERA (2014-2018)
63	Eu	Europium	Eu2O3	1.5825	LREE	246 900	Europium (oxide), min. 99 % fob China	DERA (2014-2018)
64	Gd	Gadolinium	Gd2O3	1.1423	LREE	27 000	Gadolinium oxide	Statista (2015)
65	Tb	Terbium	Tb2O3	1.1510	HREE	512 060	Terbium (oxide), min. 99,9 %, fob China	DERA (2014-2018)
66	Dy	Dysprosium	Dy2O3	1.1477	HREE	238 860	Dysprosium (oxide), min. 99 % fob China	DERA (2014-2018)
67	Ho	Holmium	Ho2O3	1.1455	HREE	55 000	Holmium (oxide)	Statista (2015)
68	Er	Erbium	Er2O3	1.1664	HREE	37 470	Erbium (oxide), min. 99 % , fob China	DERA (2014-2018)
69	Tm	Thulium	Tm2O3	1.1421	HREE	160 000	Thulium (oxide), min. 99 % , fob China	Alibaba.com (12.Feb2020)
70	Yb	Ytterbium	Yb2O3	1.1387	HREE	53 000	Ytterbium (oxide)	Statista (2013)
71	Lu	Lutetium	Lu2O3	2.2916	HREE	1 258 000	Lutetium (oxide)	Statista (2015)

The highest in-situ values for REOs and Sc_2O_3 are within red muds of Montenegro and Slovenia. These red muds have in-situ values of REOs of around 60 to 80 USD per ton of material and 600 to 900 USD in-situ values of Sc_2O_3 per ton of material, followed by several locations of bauxite in Croatia and Montenegro from around 600 USD per ton downwards for Sc_2O_3 and 90 USD per ton downwards for REOs (see Table and Table).

The reader should note that these in-situ values are an indication without consideration of technical and/or economic feasibility, viz. processing recoveries or any other modifying factor relevant for any reserve estimation. However, these in-situ values set an economic framework, which has to cover all costs of

1) extraction of a bulk REO-enriched concentrate (no standard technique available up to date),
2) separation into individual REO (standard technique available),
3) transport
4) all other costs related to a natural resource project, e.g. mining, governmental, legal, social and environmental impact and others.

As soon as a production scale technology for the extraction of a bulk REO-enriched concentrate is in place, it is recommended to collect appropriate data for a more detailed resource estimation on selected locations of red mud or bauxite based on representative estimates on concentrations of REOs and Sc_2O_3 and bulk tonnages.

This activity has received funding from the European Institute of Innovation and Technology (EIT), a body of the European Union, under the Horizon 2020, the EU Framework Programme for Research and Innovation

Table 42. In-situ values of REOs and Scandium oxide for several locations in Croatia and Hungary; Units are in USD per ton of bauxite or red mud; top 10 % are marked in red and top 10 % to 20 % are marked in yellow for each Sc_2O_3, TOTAL REE and TOTAL REE with Sc_2O_3

Country-Province	Material	Site	Sc2O3 USD/t	Y2O3 USD/t	La2O3 USD/t	Ce2O3 USD/t	Pr2O3 USD/t	Nd2O3 USD/t	Sm2O3 USD/t	Eu2O3 USD/t	Gd2O3 USD/t	Tb2O3 USD/t	Dy2O3 USD/t	Ho2O3 USD/t	Er2O3 USD/t	Tm2O3 USD/t	Yb2O3 USD/t	Lu2O3 USD/t	TOTAL REOs USD/t	TOTAL REOs with Sc2O3 USD
Croatia-Dalmatia and Lika	Bauxite	Ćosići 1	346.0	0.4	0.2	0.4	1.2	4.3	0.0	0.9	0.3	1.0	2.8	0.1	0.3	0.2	0.4	2.9	15.6	361.6
Croatia-Dalmatia and Lika	Bauxite	Ćosići 2	544.8	2.0	0.7	1.0	3.7	14.0	0.1	3.8	1.4	4.4	12.4	0.6	1.2	0.6	1.3	9.5	56.8	601.6
Croatia-Dalmatia and Lika	Bauxite	Glijev S	338.7	2.1	0.8	0.9	3.4	12.5	0.1	2.8	1.1	2.9	8.2	0.4	0.8	0.4	0.9	6.6	43.8	382.5
Croatia-Dalmatia and Lika	Bauxite	Glijev S	397.6	2.1	0.8	1.0	3.9	15.7	0.1	3.6	1.3	3.5	9.8	0.5	0.9	0.5	1.0	7.7	52.5	450.1
Croatia-Dalmatia and Lika	Bauxite	Glijev S	434.4	1.8	0.8	1.0	3.8	14.5	0.1	3.3	1.1	3.3	9.5	0.5	1.0	0.5	1.1	8.1	50.5	484.8
Croatia-Dalmatia and Lika	Bauxite	Gljev	419.6	3.7	1.0	1.2	4.3	17.5	0.2	4.7	1.8	5.4	15.8	0.8	1.7	1.0	1.9	14.2	75.2	494.8
Croatia-Dalmatia and Lika	Bauxite	Gljev	441.7	2.2	0.8	0.8	3.5	13.6	0.1	3.4	1.3	3.8	10.9	0.5	1.1	0.6	1.2	8.7	52.6	494.3
Croatia-Dalmatia and Lika	Bauxite	Imotski	471.2	0.7	0.4	1.2	2.0	7.7	0.1	1.8	0.6	1.8	4.7	0.2	0.4	0.3	0.6	4.2	26.6	497.8
Croatia-Dalmatia and Lika	Bauxite	Jukići-Đidar	463.8	1.4	0.7	1.0	3.0	11.8	0.1	2.5	0.7	2.3	6.8	0.3	0.7	0.4	1.0	7.4	40.1	503.9
Croatia-Dalmatia and Lika	Bauxite	Košute	257.7	0.5	0.4	0.6	1.8	6.5	0.1	1.3	0.4	1.3	3.5	0.2	0.3	0.2	0.5	3.3	20.7	278.3
Croatia-Dalmatia and Lika	Bauxite	MAM B-1	287.1	0.6	0.5	0.7	2.4	8.1	0.1	1.5	0.5	1.5	4.1	0.2	0.4	0.2	0.5	3.6	24.9	312.0
Croatia-Dalmatia and Lika	Bauxite	MAM B-1	294.5	0.5	0.3	0.7	1.4	4.9	0.0	1.1	0.4	1.1	3.0	0.1	0.3	0.2	0.4	3.1	17.5	312.0
Croatia-Dalmatia and Lika	Bauxite	MAM B-1	301.9	0.7	0.4	0.7	1.9	6.7	0.1	1.3	0.4	1.3	3.7	0.2	0.4	0.2	0.5	3.8	22.5	324.4
Croatia-Dalmatia and Lika	Bauxite	MAM B-1	309.2	0.6	0.4	0.6	1.8	6.3	0.1	1.3	0.5	1.4	3.9	0.2	0.4	0.2	0.5	3.7	21.9	331.1
Croatia-Dalmatia and Lika	Bauxite	MAM B-1	316.6	0.3	0.2	0.5	0.7	2.5	0.0	0.5	0.2	0.6	1.6	0.1	0.2	0.1	0.3	2.0	9.7	326.3
Croatia-Dalmatia and Lika	Bauxite	MAM B-1	323.9	0.5	0.3	0.5	1.7	6.1	0.1	1.7	0.5	1.7	4.7	0.2	0.4	0.3	0.6	3.9	23.3	347.2
Croatia-Dalmatia and Lika	Bauxite	MAM B-1	353.4	0.6	0.3	0.7	1.5	5.2	0.0	1.1	0.4	1.2	3.5	0.2	0.4	0.2	0.5	3.8	19.5	372.9
Croatia-Dalmatia and Lika	Bauxite	MAM B-1	360.7	0.5	0.3	0.6	1.2	4.3	0.0	1.0	0.3	1.0	2.8	0.1	0.3	0.2	0.4	3.2	16.3	377.0
Croatia-Dalmatia and Lika	Bauxite	MAM B-1	368.1	0.6	0.3	0.8	1.3	4.5	0.0	1.2	0.4	1.2	3.6	0.2	0.4	0.2	0.6	4.1	19.3	387.4
Croatia-Dalmatia and Lika	Bauxite	MAM B-1	375.5	0.3	0.2	0.6	0.8	3.0	0.0	0.8	0.2	0.7	2.1	0.1	0.2	0.2	0.4	2.7	12.3	387.8
Croatia-Dalmatia and Lika	Bauxite	MAM B-1	419.6	0.6	0.3	0.7	1.7	6.6	0.1	2.0	0.6	2.0	5.6	0.2	0.5	0.3	0.7	5.3	27.4	447.0
Croatia-Dalmatia and Lika	Bauxite	Mamutovac	390.2	0.5	0.3	0.6	1.6	5.7	0.1	1.3	0.4	1.2	3.4	0.2	0.3	0.2	0.5	3.4	19.7	409.9
Croatia-Dalmatia and Lika	Bauxite	Mamutovo	419.6	1.2	0.6	0.8	2.3	8.1	0.1	1.8	0.6	2.1	6.0	0.3	0.6	0.4	0.8	6.0	31.7	451.3
Croatia-Dalmatia and Lika	Bauxite	Mamutovo	522.7	0.8	0.4	0.9	2.0	8.2	0.1	2.3	0.8	2.4	6.2	0.3	0.5	0.3	0.7	5.7	31.6	554.3
Croatia-Dalmatia and Lika	Bauxite	Mamutovo	537.4	1.0	0.4	1.4	2.8	11.7	0.1	3.2	1.1	3.1	7.5	0.3	0.7	0.4	0.9	6.9	41.4	578.9
Croatia-Dalmatia and Lika	Bauxite	Mamutovo	595.3	1.1	0.4	1.8	2.7	11.0	0.1	2.8	1.1	3.2	8.2	0.4	0.7	0.4	1.0	7.1	42.1	638.5
Croatia-Dalmatia and Lika	Bauxite	Moseć	338.7	0.5	0.2	0.4	1.0	3.4	0.0	0.6	0.2	0.8	2.4	0.1	0.3	0.2	0.4	3.0	13.5	352.2
Croatia-Dalmatia and Lika	Bauxite	Moseć	382.8	1.1	0.5	0.9	2.5	8.8	0.1	1.9	0.7	2.0	5.4	0.3	0.5	0.3	0.6	4.4	29.7	412.6
Croatia-Dalmatia and Lika	Bauxite	Moseć	404.9	1.5	0.3	0.8	2.5	9.6	0.1	2.3	0.8	2.4	6.7	0.3	0.7	0.4	0.8	5.6	34.8	439.7
Croatia-Dalmatia and Lika	Bauxite	Moseć	441.7	0.8	0.4	0.9	2.1	7.6	0.1	1.9	0.6	2.0	5.5	0.3	0.5	0.3	0.6	4.6	28.3	470.1
Croatia-Dalmatia and Lika	Bauxite	Moseć Jama	375.5	0.7	0.2	0.4	1.2	4.5	0.0	1.3	0.4	1.4	4.1	0.2	0.4	0.3	0.6	4.2	19.9	395.4
Croatia-Dalmatia and Lika	Bauxite	Moseć Jama	390.2	0.8	0.3	0.4	1.8	6.5	0.1	1.6	0.5	1.6	4.5	0.2	0.4	0.3	0.6	4.2	23.7	413.9
Croatia-Dalmatia and Lika	Bauxite	Obrovac	390.2	1.1	0.5	1.0	3.0	11.4	0.1	2.7	0.8	2.5	6.9	0.3	0.6	0.4	0.8	5.8	37.9	428.1
Croatia-Dalmatia and Lika	Bauxite	Obrovac	463.8	0.8	0.4	0.8	2.2	7.9	0.1	1.8	0.6	1.9	5.3	0.2	0.5	0.3	0.7	5.2	28.8	492.6
Croatia-Dalmatia and Lika	Bauxite	Ričina	390.2	0.5	0.3	0.7	1.5	5.4	0.0	1.2	0.4	1.3	3.6	0.2	0.4	0.2	0.5	3.7	19.9	410.1
Croatia-Dalmatia and Lika	Bauxite	Ričina	471.2	1.6	0.7	1.1	3.6	13.9	0.1	3.4	1.3	3.6	9.6	0.4	0.8	0.4	0.9	6.6	48.3	519.4
Croatia-Dalmatia and Lika	Bauxite	Rudopolje	243.0	0.6	0.2	0.6	1.0	3.8	0.0	0.8	0.3	1.1	3.4	0.2	0.4	0.2	0.5	4.1	17.2	260.2
Croatia-Dalmatia and Lika	Bauxite	Rudopolje	272.4	0.6	0.1	0.7	0.7	2.8	0.0	0.7	0.3	1.1	3.2	0.2	0.4	0.2	0.5	3.7	15.2	287.6
Croatia-Dalmatia and Lika	Bauxite	Rudopolje	309.2	1.5	0.5	0.8	2.2	7.9	0.1	1.5	0.7	2.2	6.5	0.3	0.7	0.5	1.0	7.2	33.6	342.8
Croatia-Dalmatia and Lika	Bauxite	Stari Gaj, Ot	427.0	0.5	0.3	1.3	1.6	5.5	0.1	1.5	0.4	1.5	4.2	0.2	0.4	0.3	0.7	4.8	23.1	450.1
Croatia-Dalmatia and Lika	Bauxite	Stari Gaj, Ot	390.2	0.4	0.3	1.0	1.4	4.9	0.0	1.2	0.4	1.2	3.3	0.2	0.3	0.2	0.5	3.7	19.2	409.4
Croatia-Dalmatia and Lika	Bauxite	Stari Gaj, Ot	360.7	0.4	0.2	0.6	1.1	3.8	0.0	1.0	0.3	1.0	2.8	0.1	0.3	0.2	0.5	3.5	15.7	376.5
Croatia-Dalmatia and Lika	Bauxite	Strmendola	228.2	0.3	0.4	0.8	1.3	3.8	0.0	0.7	0.2	0.6	1.9	0.1	0.2	0.1	0.3	1.9	12.6	240.8
Croatia-Dalmatia and Lika	Bauxite	Strmendola	265.0	0.3	0.2	0.7	0.9	3.2	0.0	0.5	0.2	0.6	1.7	0.1	0.2	0.1	0.3	1.9	10.9	275.9
Croatia-Dalmatia and Lika	Bauxite	Strmendola	463.8	0.9	0.5	0.7	2.9	10.6	0.1	2.2	0.7	2.1	5.5	0.2	0.5	0.3	0.6	4.3	32.4	496.2
Croatia-Dalmatia and Lika	Bauxite	Tošići-Dujić	404.9	2.9	0.8	1.1	3.7	15.7	0.2	4.6	1.7	4.7	12.7	0.6	1.2	0.7	1.4	9.7	61.8	466.7
Croatia-Dalmatia and Lika	Bauxite	Tošići-Dujić	449.1	3.3	0.6	0.9	3.0	11.5	0.1	3.8	1.5	4.6	13.5	0.7	1.4	0.8	1.6	11.5	58.9	508.0
Croatia-Dalmatia and Lika	Bauxite	Tošići-Dujić	493.3	6.0	0.6	1.0	2.9	12.3	0.1	4.1	1.6	4.6	12.9	0.7	1.5	0.8	1.6	12.1	62.7	556.0
Croatia-Dalmatia and Lika	Bauxite	Tošići-Dujić	508.0	1.5	0.7	1.1	3.2	11.2	0.1	2.6	0.9	2.8	8.1	0.4	0.8	0.5	1.1	7.6	42.3	550.3
Croatia-Dalmatia and Lika	Bauxite	Tošići-Dujić	552.2	11.0	1.6	1.1	9.1	40.6	0.4	11.5	5.6	14.7	40.9	2.3	4.2	2.0	3.3	23.4		723.6
Croatia-Dalmatia and Lika	Bauxite	Turban Kosa	493.3	0.5	0.2	0.4	1.3	4.8	0.0	1.2	0.4	1.2	3.6	0.2	0.4	0.2	0.5	3.7	18.6	511.8
Croatia-Dalmatia and Lika	Bauxite	Turban Kosa	559.5	1.0	0.4	1.0	1.9	6.9	0.1	2.0	0.7	2.4	7.2	0.3	0.7	0.4	0.9	6.5	32.5	592.0
Croatia-Dalmatia and Lika	Bauxite	Vrace	265.0	0.5	0.3	0.5	1.4	4.8	0.0	1.0	0.4	1.2	3.4	0.2	0.4	0.2	0.5	3.8	18.7	283.7
Croatia-Dalmatia and Lika	Bauxite	Vrace	294.5	0.6	0.5	1.2	3.0	10.9	0.1	1.5	0.5	1.4	3.7	0.2	0.4	0.2	0.5	3.5	28.2	322.7
Croatia-Istria	Bauxite	Dragozetići-	0.0	0.4	0.3	2.0	1.0	3.1	0.0	0.6	0.3	0.8	2.3	0.1	0.3	0.2	0.4	3.1	14.9	14.9
Croatia-Istria	Bauxite	Dragozetići-	0.0	0.6	0.4	0.7	1.6	5.1	0.0	1.1	0.4	1.3	4.1	0.2	0.4	0.3	0.6	4.4	21.1	21.1
Croatia-Istria	Bauxite	Karojba-1	0.0	0.5	0.4	0.4	1.4	4.5	0.0	0.8	0.3	0.9	2.7	0.1	0.3	0.2	0.5	3.3	16.3	16.3
Croatia-Istria	Bauxite	Karojba-2	0.0	0.5	0.4	0.4	1.4	4.5	0.0	0.8	0.3	1.0	3.0	0.1	0.3	0.2	0.5	3.5	17.0	17.0
Croatia-Istria	Bauxite	Kaštelir-1	0.0	0.4	0.6	0.7	1.4	3.5	0.0	0.6	0.2	0.7	2.4	0.1	0.3	0.2	0.4	3.1	14.7	14.7
Croatia-Istria	Bauxite	Kaštelir-2	0.0	0.4	0.3	0.4	1.3	4.0	0.0	0.7	0.3	0.8	2.5	0.1	0.3	0.2	0.4	2.9	14.8	14.8
Croatia-Istria	Bauxite	Kaštelir-3	0.0	0.5	0.2	0.4	1.1	3.9	0.0	0.9	0.3	1.1	3.3	0.2	0.3	0.2	0.5	3.3	16.3	16.3
Croatia-Istria	Bauxite	Kaštelir-4	0.0	0.4	0.3	0.3	1.1	3.4	0.0	0.6	0.2	0.7	2.1	0.1	0.2	0.2	0.3	2.6	12.5	12.5
Croatia-Istria	Bauxite	Minjera2-1	0.0	0.5	0.4	0.7	1.5	3.8	0.0	0.4	0.2	0.7	2.6	0.2	0.4	0.2	0.5	3.8	16.0	16.0
Croatia-Istria	Bauxite	Rovinj1-1	0.0	0.7	0.4	1.8	1.8	5.8	0.0	1.2	0.4	1.4	4.2	0.2	0.4	0.3	0.5	3.9	23.0	23.0
Croatia-Istria	Bauxite	Rovinj1-2	0.0	0.8	0.6	0.9	3.3	11.8	0.1	1.9	0.7	1.7	4.3	0.2	0.4	0.2	0.6	4.1	31.5	31.5
Croatia-Istria	Bauxite	Rovinj1-3	0.0	0.9	0.9	1.5	5.0	18.1	0.1	3.0	1.0	2.4	5.6	0.2	0.4	0.3	0.5	4.0	44.1	44.1
Croatia-Istria	Bauxite	Rovinj1-4	0.0	0.7	0.5	1.0	3.0	10.5	0.1	2.0	0.7	1.9	4.8	0.2	0.4	0.3	0.6	4.0	30.5	30.5
Croatia-Istria	Bauxite	Rovinj1-5	0.0	0.6	0.5	0.9	2.9	9.8	0.1	1.7	0.5	1.6	4.2	0.2	0.4	0.2	0.5	3.7	27.9	27.9
Croatia-Istria	Bauxite	Rovinj1-6	0.0	0.4	0.3	0.7	1.9	6.8	0.1	1.1	0.3	0.9	2.4	0.1	0.2	0.1	0.3	2.4	18.1	18.1
Croatia-Istria	Bauxite	Šterna-1	0.0	0.4	0.3	0.9	1.5	5.0	0.0	1.1	0.4	1.1	2.9	0.1	0.3	0.2	0.3	2.5	16.9	16.9
Croatia-Istria	Bauxite	Učka-1	0.0	0.6	0.3	0.5	1.4	4.7	0.0	1.1	0.4	1.1	3.4	0.2	0.3	0.2	0.4	3.1	17.7	17.7
Croatia-Istria	Bauxite	Učka-2	0.0	0.6	0.3	0.8	1.4	4.2	0.0	0.8	0.3	1.0	3.2	0.2	0.4	0.3	0.6	4.1	18.0	18.0
Hungary	Bauxite	Csabrendek	0.0	0.9	0.5	0.6	3.7	13.7	0.1	2.8	0.8	2.4	6.4	0.3	0.6	0.4	0.8	6.1	40.2	40.2
Hungary	Bauxite	Dudar	0.0	0.9	0.5	0.9	2.7	9.7	0.1	1.9	0.6	1.8	5.0	0.2	0.5	0.3	0.6	4.4	30.2	30.2
Hungary	Bauxite	Iharkút	0.0	1.9	0.6	0.9	3.2	12.1	0.1	2.5	0.9	2.6	7.3	0.4	0.8	0.5	1.0	7.9	42.7	42.7
Hungary	Bauxite	Nagyharsán	0.0	1.5	0.7	0.9	3.1	11.6	0.1	2.3	0.8	2.3	6.7	0.3	0.8	0.5	1.0	7.7	40.3	40.3
Hungary	Bauxite	Óbarok	0.0	0.4	0.5	0.8	2.4	8.5	0.1	1.6	0.5	1.2	2.8	0.1	0.2	0.1	0.3	2.2	21.8	21.8
Hungary	Red mud	Cell No. IX.	0.0	1.2	0.7	1.3	3.9	13.9	0.1	2.5	0.9	2.4	6.8	0.3	0.6	0.4	0.9	6.6	42.7	42.7
Hungary	Red mud	Cell No. VII.	0.0	0.9	0.7	1.3	3.4	11.7	0.1	2.1	0.7	2.0	5.7	0.3	0.5	0.3	0.8	6.1	36.7	36.7
Hungary	Red mud	Cell No. VIII	0.0	1.2	0.7	1.3	3.8	13.7	0.1	2.6	0.9	2.5	7.0	0.3	0.7	0.5	0.9	6.9	42.9	42.9

This activity has received funding from the European Institute of Innovation and Technology (EIT), a body of the European Union, under the Horizon 2020, the EU Framework Programme for Research and Innovation

Table 43. In-situ values of REOs and Scandium oxide for several locations in Montenegro and Slovenia; Units are in USD per ton of bauxite or red mud; top 10 % are marked in red and top 10 % to 20 % are marked in yellow for each Sc_2O_3, TOTAL REE and TOTAL REE with Sc_2O_3

Country-Province	Material	Site	Sc2O3 USD/t	Y2O3 USD/t	La2O3 USD/t	Ce2O3 USD/t	Pr2O3 USD/t	Nd2O3 USD/t	Sm2O3 USD/t	Eu2O3 USD/t	Gd2O3 USD/t	Tb2O3 USD/t	Dy2O3 USD/t	Ho2O3 USD/t	Er2O3 USD/t	Tm2O3 USD/t	Yb2O3 USD/t	Lu2O3 USD/t	TOTAL REOs USD/t	TOTAL REOs with Sc2O3 USD
Montenegro	Bauxite	BAJOV DO;	198.8	0.3	0.1	0.2	0.4	1.4	0.0	0.3	0.1	0.4	1.5	0.1	0.2	0.1	0.2	1.8	7.1	205.9
Montenegro	Bauxite	BAJOV DO;	265.0	0.3	0.2	0.4	0.7	2.0	0.0	0.4	0.2	0.6	1.9	0.1	0.2	0.2	0.3	2.4	9.9	275.0
Montenegro	Bauxite	BAJOV DO;	279.8	0.4	0.2	0.2	0.9	3.2	0.0	0.7	0.2	0.8	2.6	0.1	0.3	0.2	0.4	3.3	13.7	293.5
Montenegro	Bauxite	BAJOV DO;	287.1	0.3	0.2	0.3	0.8	2.4	0.0	0.5	0.2	0.7	2.3	0.1	0.3	0.2	0.4	3.1	11.8	298.9
Montenegro	Bauxite	BAJOV DO;	323.9	0.4	0.2	0.8	0.8	2.6	0.0	0.6	0.2	0.7	2.3	0.1	0.3	0.2	0.4	3.0	12.7	336.7
Montenegro	Bauxite	BAJOV DO;	338.7	0.4	0.2	0.9	1.1	3.6	0.0	0.8	0.3	0.9	2.7	0.1	0.3	0.2	0.4	3.1	15.0	353.6
Montenegro	Bauxite	BAJOV DO;	375.5	0.5	0.4	0.9	1.7	5.4	0.0	1.1	0.4	1.3	3.5	0.2	0.4	0.2	0.6	4.3	20.8	396.2
Montenegro	Bauxite	BAJOV DO;	412.3	0.5	0.5	1.2	2.3	7.7	0.1	1.6	0.5	1.7	4.4	0.2	0.4	0.3	0.6	4.8	26.9	439.2
Montenegro	Bauxite	BIJELE POLJ	220.9	0.2	0.1	0.2	0.3	1.3	0.0	0.3	0.1	0.4	1.0	0.1	0.1	0.1	0.2	1.3	5.5	226.3
Montenegro	Bauxite	BIJELE POLJ	287.1	1.1	0.8	0.7	5.3	19.6	0.1	3.2	1.0	2.5	6.3	0.3	0.5	0.3	0.7	4.7	47.1	334.2
Montenegro	Bauxite	BIJELE POLJ	316.6	0.4	0.1	0.2	0.4	1.5	0.0	0.4	0.2	0.6	2.2	0.1	0.3	0.2	0.4	2.9	9.8	326.4
Montenegro	Bauxite	BIJELE POLJ	323.9	0.4	0.2	0.5	0.8	2.7	0.0	0.6	0.2	0.7	2.3	0.1	0.3	0.2	0.4	2.8	12.2	336.2
Montenegro	Bauxite	BIJELE POLJ	338.7	0.5	0.3	0.5	0.8	2.5	0.0	0.6	0.2	0.8	2.5	0.1	0.3	0.2	0.4	3.0	12.8	351.5
Montenegro	Bauxite	BIJELE POLJ	353.4	0.5	0.3	0.7	1.7	5.8	0.1	1.2	0.4	1.3	3.4	0.2	0.4	0.2	0.5	3.7	20.2	373.6
Montenegro	Bauxite	BIJELE POLJ	360.7	0.4	0.2	0.8	0.8	2.9	0.0	0.7	0.2	0.8	2.4	0.1	0.3	0.2	0.4	2.9	13.0	373.8
Montenegro	Bauxite	BIJELE POLJ	375.5	0.3	0.1	0.2	0.4	1.4	0.0	0.3	0.1	0.6	1.9	0.1	0.2	0.1	0.3	2.5	8.6	384.0
Montenegro	Bauxite	BIJELE POLJ	434.4	0.3	0.1	0.2	0.3	1.1	0.0	0.3	0.1	0.5	1.8	0.1	0.2	0.1	0.3	2.5	8.0	442.4
Montenegro	Bauxite	BIOČKI STA	485.9	1.9	0.9	1.3	4.9	20.3	0.2	4.6	1.5	4.1	10.2	0.5	0.9	0.5	1.1	8.2	61.2	547.1
Montenegro	Bauxite	BOKA KOTO	206.1	0.4	0.3	0.5	1.3	4.3	0.0	0.8	0.3	0.8	2.3	0.1	0.2	0.1	0.3	2.4	14.2	220.4
Montenegro	Bauxite	BOROVA BR	478.5	1.1	1.1	1.3	4.0	14.1	0.1	3.0	1.1	3.1	7.7	0.3	0.7	0.4	0.8	6.1	45.0	523.6
Montenegro	Bauxite	BRŠNO; DEF	368.1	0.7	0.4	1.1	1.5	4.8	0.0	1.0	0.4	1.2	3.8	0.2	0.4	0.3	0.5	4.2	20.4	388.6
Montenegro	Bauxite	CRVENJACI;	390.2	0.8	0.5	1.1	2.1	7.1	0.1	1.4	0.5	1.5	4.4	0.2	0.4	0.3	0.6	4.4	25.3	415.5
Montenegro	Bauxite	CRVENO PR	390.2	1.4	1.1	1.1	3.4	12.1	0.1	2.2	0.8	2.5	7.1	0.4	0.7	0.5	0.9	6.9	41.2	431.4
Montenegro	Bauxite	ĐELOV DO;	301.9	0.5	0.3	0.6	1.1	3.6	0.0	0.7	0.3	1.0	3.1	0.2	0.3	0.2	0.5	3.4	15.7	317.6
Montenegro	Bauxite	ĐURAKOV D	419.6	1.0	0.5	1.1	2.7	9.7	0.1	2.0	0.7	2.0	5.5	0.3	0.6	0.4	0.8	5.9	33.2	452.8
Montenegro	Bauxite	GORNJEPOL	206.1	0.5	0.1	0.2	0.6	2.3	0.0	0.5	0.2	0.7	2.4	0.1	0.3	0.2	0.4	2.8	11.3	217.5
Montenegro	Bauxite	GORNJEPOL	213.5	0.4	0.2	0.8	1.1	3.9	0.0	0.7	0.3	0.9	2.4	0.1	0.2	0.2	0.3	2.6	14.2	227.7
Montenegro	Bauxite	GORNJEPOL	220.9	0.7	0.2	0.5	1.1	3.7	0.0	0.8	0.4	1.2	3.4	0.2	0.3	0.2	0.4	3.2	16.3	237.2
Montenegro	Bauxite	GORNJEPOL	228.2	1.6	0.9	2.7	5.6	20.9	0.2	3.4	1.4	3.7	9.2	0.4	0.8	0.5	0.9	6.6	58.7	286.9
Montenegro	Bauxite	GORNJEPOL	250.3	0.5	0.1	0.3	0.8	3.1	0.0	0.7	0.3	1.0	3.0	0.2	0.3	0.2	0.5	3.9	14.9	265.2
Montenegro	Bauxite	GORNJEPOL	265.0	1.0	0.4	0.7	2.0	7.3	0.1	1.4	0.6	1.9	5.2	0.2	0.5	0.3	0.7	4.8	27.2	292.2
Montenegro	Bauxite	GREBENICI,	390.2	0.8	0.5	0.7	2.0	6.1	0.0	1.0	0.4	1.3	4.0	0.2	0.4	0.3	0.6	4.6	22.9	413.1
Montenegro	Bauxite	JELINA PEĆI	309.2	0.3	0.1	0.3	0.5	1.6	0.0	0.4	0.2	0.6	1.8	0.1	0.2	0.1	0.3	2.3	9.0	318.2
Montenegro	Bauxite	KRUŠČICA;	287.1	0.2	0.1	0.2	0.4	1.3	0.0	0.3	0.1	0.4	1.4	0.1	0.2	0.1	0.2	1.9	7.1	294.2
Montenegro	Bauxite	LAZINE; Mir	287.1	0.3	0.3	0.5	0.9	2.4	0.0	0.4	0.1	0.6	1.8	0.1	0.2	0.1	0.3	2.4	10.4	297.5
Montenegro	Bauxite	LIVEROVIĆI;	412.3	1.0	0.9	1.1	3.9	12.6	0.1	2.1	0.7	2.1	5.8	0.3	0.6	0.4	0.8	5.8	38.1	450.4
Montenegro	Bauxite	MEĐEĐE; DE	257.7	0.3	0.2	0.4	0.9	3.3	0.0	0.7	0.2	0.7	1.8	0.1	0.2	0.1	0.3	2.0	11.1	268.8
Montenegro	Bauxite	MILOVIĆI; C	235.6	0.7	0.3	0.4	1.5	5.6	0.0	1.1	0.4	1.2	3.3	0.2	0.3	0.2	0.4	3.0	18.7	254.3
Montenegro	Bauxite	PAKLARICA;	309.2	0.4	0.2	0.4	1.3	4.4	0.0	0.9	0.3	0.9	2.5	0.1	0.3	0.2	0.4	2.7	15.0	324.2
Montenegro	Bauxite	PIVA, Rudin	353.4	0.6	0.2	1.0	0.8	2.7	0.0	0.6	0.3	1.0	3.2	0.2	0.4	0.3	0.6	4.8	16.7	370.1
Montenegro	Bauxite	SAVINA GRA	235.6	0.5	0.3	0.5	1.3	4.7	0.0	0.9	0.3	1.0	2.7	0.1	0.3	0.2	0.3	2.5	15.7	251.3
Montenegro	Bauxite	ŠTITOVO II;	162.0	1.7	0.4	0.3	2.2	10.1	0.1	3.0	1.2	3.4	8.7	0.4	0.8	0.4	0.9	6.3	39.9	201.9
Montenegro	Bauxite	ŠTITOVO II;	390.2	0.7	0.4	1.1	1.9	6.8	0.1	1.5	0.5	1.6	4.4	0.2	0.4	0.3	0.6	4.8	25.2	415.4
Montenegro	Bauxite	ŠTITOVO II;	397.6	0.7	0.4	1.0	2.0	7.2	0.1	1.5	0.5	1.4	4.1	0.2	0.4	0.3	0.6	4.7	25.0	422.6
Montenegro	Bauxite	ŠTITOVO II;	427.0	0.8	0.4	1.0	1.9	6.9	0.1	1.5	0.5	1.5	4.2	0.2	0.5	0.3	0.6	4.9	25.3	452.3
Montenegro	Bauxite	ŠTITOVO II;	471.2	0.9	0.5	1.2	2.4	9.1	0.1	2.1	0.7	2.1	5.5	0.3	0.5	0.3	0.7	5.5	31.9	503.1
Montenegro	Bauxite	ŠTITOVO II;	500.6	1.6	1.3	1.1	5.8	20.3	0.2	4.4	1.4	4.1	11.1	0.5	1.0	0.6	1.3	9.3	63.8	564.5
Montenegro	Bauxite	ŠTITOVO II;	515.4	1.0	0.5	1.1	2.7	10.1	0.1	2.5	0.9	2.6	7.0	0.3	0.6	0.4	0.9	6.8	37.7	553.0
Montenegro	Bauxite	STUDENAC;	287.1	0.4	0.2	0.4	0.8	2.5	0.0	0.5	0.2	0.7	2.2	0.1	0.3	0.2	0.4	2.7	11.4	298.5
Montenegro	Bauxite	TREBOVINJS	449.1	0.4	0.2	0.4	0.8	2.9	0.0	0.7	0.3	0.8	2.4	0.1	0.2	0.2	0.3	2.5	12.1	461.2
Montenegro	Bauxite	ULCINJ ARE	220.9	0.4	0.4	0.7	1.6	5.2	0.0	0.9	0.3	0.9	2.5	0.1	0.2	0.2	0.4	2.5	16.3	237.2
Montenegro	Bauxite	VELIKA GOR	206.1	0.4	0.5	0.9	2.1	6.4	0.0	1.0	0.3	1.0	2.6	0.1	0.3	0.2	0.4	2.6	18.8	225.0
Montenegro	Bauxite	VELIKA GOR	213.5	0.4	0.4	0.7	1.6	4.6	0.0	0.8	0.3	0.8	2.3	0.1	0.2	0.2	0.3	2.7	15.3	228.8
Montenegro	Bauxite	VELIKA GOR	220.9	0.4	0.4	0.6	1.6	4.7	0.0	0.9	0.3	0.9	2.7	0.1	0.3	0.2	0.4	2.7	16.2	237.1
Montenegro	Bauxite	VELIKA GOR	235.6	0.3	0.4	0.7	1.7	4.8	0.0	0.8	0.2	0.8	2.3	0.1	0.2	0.2	0.3	2.6	15.6	251.2
Montenegro	Bauxite	VELIKA GOR	287.1	0.3	0.4	0.9	1.6	4.7	0.0	0.8	0.3	0.9	2.5	0.1	0.3	0.2	0.4	2.8	16.2	303.3
Montenegro	Bauxite	VELJA DUBC	338.7	1.0	0.6	0.7	2.6	9.2	0.1	1.8	0.6	1.9	5.4	0.3	0.5	0.3	0.7	5.3	31.0	369.7
Montenegro	Bauxite	ZAGRAD; DE	478.5	1.0	0.8	1.3	3.5	12.0	0.1	2.3	0.8	2.3	6.2	0.3	0.6	0.4	0.9	6.4	38.7	517.2
Montenegro	Red mud	B-1/19	257.7	0.5	0.3	0.6	1.4	5.1	0.0	1.0	0.3	1.0	2.8	0.1	0.3	0.2	0.4	2.9	17.0	274.7
Montenegro	Red mud	B-1/19	596.3	1.0	0.7	1.3	3.2	11.5	0.1	2.3	0.8	2.4	6.4	0.3	0.6	0.4	0.9	6.4	38.3	634.6
Montenegro	Red mud	B-2/19	684.7	1.3	0.8	1.5	3.8	13.5	0.1	2.6	0.9	2.7	7.5	0.4	0.8	0.5	1.0	7.7	45.0	729.7
Montenegro	Red mud	B-2/19	773.0	1.4	1.2	1.8	5.2	18.7	0.1	3.6	1.2	3.5	9.4	0.4	0.9	0.6	1.2	8.8	58.0	831.0
Montenegro	Red mud	B-2/19	787.8	1.5	1.0	1.7	4.5	16.0	0.1	3.1	1.1	3.2	8.6	0.4	0.9	0.5	1.2	9.1	53.1	840.8
Montenegro	Red mud	B-3/19	677.3	1.4	0.9	1.5	4.3	15.1	0.1	2.9	1.0	3.0	8.0	0.4	0.8	0.5	1.1	8.0	49.0	726.3
Montenegro	Red mud	B-3/19	736.2	1.4	0.9	1.7	4.2	14.9	0.1	2.9	1.0	3.0	8.1	0.4	0.8	0.5	1.1	8.4	49.2	785.5
Montenegro	Red mud	B-3/19	780.4	1.4	0.9	1.7	4.5	16.1	0.1	3.2	1.1	3.2	8.8	0.4	0.9	0.5	1.2	8.7	52.9	833.3
Montenegro	Red mud	B-4/19	743.6	1.4	0.9	1.7	4.4	15.9	0.1	3.2	1.1	3.2	8.8	0.4	0.8	0.5	1.2	8.4	52.0	795.6
Montenegro	Red mud	B-4/19	773.0	1.4	0.9	1.7	4.5	15.5	0.1	3.1	1.0	3.1	8.6	0.4	0.9	0.5	1.2	8.5	51.4	824.4
Montenegro	Red mud	B-4/19	839.3	1.5	1.1	1.9	4.9	16.8	0.1	3.4	1.1	3.4	9.5	0.4	1.0	0.6	1.3	9.4	56.3	895.6
Montenegro	Red mud	B-5/19	699.4	1.3	0.9	1.6	4.4	15.9	0.1	3.2	1.1	3.0	8.0	0.4	0.7	0.4	1.0	7.2	49.3	748.7
Montenegro	Red mud	B-5/19	831.9	1.7	1.4	1.8	6.0	21.9	0.2	4.2	1.5	4.1	11.0	0.5	1.0	0.6	1.3	9.7	67.0	898.9
Montenegro	Red mud	B-5/19	883.5	1.8	1.2	1.9	5.5	19.7	0.2	3.8	1.3	4.0	11.0	0.5	1.1	0.7	1.4	10.4	64.5	948.0
Montenegro	Red mud	B-5/19	912.9	1.8	1.2	2.0	5.3	18.2	0.1	3.7	1.3	3.8	10.5	0.5	1.0	0.7	1.5	10.3	61.8	974.7
Montenegro	Red mud	B-6/19	728.9	1.4	1.0	1.8	5.3	19.0	0.2	3.6	1.2	3.4	8.8	0.4	0.8	0.5	1.1	8.1	56.6	785.5
Montenegro	Red mud	B-6/19	795.1	1.5	1.1	1.9	5.2	18.4	0.2	3.6	1.2	3.6	9.4	0.5	0.9	0.6	1.2	8.9	58.1	853.2
Montenegro	Red mud	B-6/19	898.2	1.8	1.3	2.0	5.6	19.8	0.2	3.8	1.3	3.9	10.8	0.5	1.0	0.6	1.4	10.3	64.4	962.6
Montenegro	Red mud	B-6/19	905.6	1.8	1.2	2.0	5.2	17.9	0.1	3.5	1.2	3.8	10.5	0.5	1.0	0.6	1.4	10.6	61.5	967.1
Slovenia	Red mud	Kidričevo -	625.8	1.1	0.6	1.1	2.7	9.0	0.1	1.7	0.6	2.0	6.0	0.3	0.7	0.4	0.9	6.9	34.1	659.9

This activity has received funding from the European Institute of Innovation and Technology (EIT), a body of the European Union, under the Horizon 2020, the EU Framework Programme for Research and Innovation

References

Benedek, K., Pécskay, Z., Szabó, C., Jósvai, J., Németh, T. (2004): Paleogene igneous rocks inthe Zala Basin (Western Hungary): link to the paleogene magmatic activity along thePeriadriatic Lineament. Geologica Carpathica Bratislava 55 (1), 43–50.

Besić, Z., Vuković, V., Cicović, B.(1965): Boksiti Crne Gore l, Rudnici boksita-Nikšić, Nikšić, p. 165

Császár, G. (2002): Urgon Formations in Hungary. *Geologica Hungarica, Sereis Geologica* Tom. 25, Budapest, p 209

Csontos, L. & Vörös, A. (2004): Mesozoic plate tectonic reconstruction of the Carpathian region. Palaeogeography, Palaeoclimatology, Palaeoecology 210, 1–56.

Deady, É., Mouchos, E.,Goodenough, K., Williamson, B., Wall, F. (2014): ERES2014: 1st European Rare Earth Resources Conference, Milos 04/7/09/2014 , 1-12

Dragović, D.R. (1988): Bijeli boksiti Crne Gore; Izdanje Univerzitet "Veljko Vlahović" u Titogradu, Nikšić (88).

Dunkl I. (1990): A középhegységi eocén-fedős bauxitok törmleékes cirkonkristályainak fission-track kor: a korai eocén vulkanizmus bizonyítéka. *Ált. Földt. Szemle (General Geological Review*), **25**, 163-177 (Fission-track age of zircon crystals from Eocene bauxites of the Transdnubian Central Range) (in Hungarian)

Dunkl, I. (1992): Origin of the Eocene-covered karst bauxites of the Transdanubian Central Range (Hungary): evidence from early Eocene volcanism. *Eur. J. Miner*., **4**. 581-595

Gabrić, A., Lukšić, B. (1975): Geološka istraživanja boksitonosnog područja Imotski. Fond stručne dokum. 275/75, Institut za geološka istraživanja, Zagreb.

Gabrić, A. (1978): Geološka istraživanja boksitonosnih terena područja Sinj – Imotski. Fond stručne dokum. 34/78, Geološki zavod – Zagreb

Gabrić, A., Lukšić, B. (1986): Geološka istraživanja i rudne rezerve boksitonosne eocenske sinklinale u reviru Turban Kosa – Ćosići – Rebići kod imotskog. Fond stručne dokum. 19/86, Geološki zavod – Zagreb

Gádori, V., Szepeshegyi, I. (Eds) (1987): Bauxitbányászat a Bakonyban (Bauxite mining in the Bakony Hills), Tapolca, p 265, (in Hungarian)

Gawlick, H.-J. & Missoni, S. (2019): Middle-Late Jurassic sedimentary mélange formation related to ophiolite obduction in the Alpine-Carpathian-Dinaridic Mountain Range. – Gondwana Research 74:144-172.

This activity has received funding from the European Institute of Innovation and Technology (EIT), a body of the European Union, under the Horizon 2020, the EU Framework Programme for Research and Innovation

Gawlick, H.-J., Sudar, M.N., Missoni, S., Suzuki, H., Lein, R. & Jovanovic, D., (2017): Triassic-Jurassic geodynamic evolution of the Dinaridic Ophiolite Belt (Inner Dinarides, SW Serbia). Journal of Alpine Geology 55, 1–167.

Grubic, A. (1999): Problematics of Yugoslav bauxites. Bulletin of Geoinstitute 36: 7-24.

Gu, H., Wang, N., Hargreaves, J. S. J. (2018): Sequential extraction of valuable trace elements from Bayer process-derived waste red mud samples. Journal of Sustainable Metallurgy, Vol. 4, pp. 147-154.

Haas, J., Kovács, S., Gawlick, H.-J., Gradinaru, E., Karamata, S., Sudar, M., Péró, Cs, Mello, J., Polák, M., Ogorelec, B., Buser, S., 2011. Jurassic evolution of the tectonostratigraphic units of the Circum-Pannonian Region. Jahrbuch der Geologischen Bundesanstalt 151, 281–354.

Jankovic, S., Jelenkovic, R. & Vujic, S. (2003): Mineral resources and potential prognosis of metallic and non-metallic mineral raw materials in Serbia and Montenegro at the end of the XXth century. – 1-875, Engineering Academy of Serbia and Montenegro.

Jović, V., Radusinović, S., Pajović, M. (2009): Rare earth elements in the karstic bauxites of Zagrad (Niksicka Zupa,Montenegro), Goldschmidt Conference Abstracts 2009, p. A607.

Kelemen, P., Dunkl, I., Csillag, G., Mindszenty, A., von Eynatten, H., Józsa, S. (2017): Tracing multiple resedimentation on an isolated karstified plateau: The bauxite-bearing red clay of the Southern Bakony Mts., *Hungary. Sed.Geol*., **358**, 84-96

Koren, K., Lapajne, S. (2017): Final review of the Program for the operational monitoring of groundwater for the closed landfill of non-hazardous waste Rdeče blato-Talum d.d., December 2013, Program of measures in case of exceeding warning-level changes in the groundwater parameters, landfill of non-hazardous waste Red Mud, December 2013, and Reports on monitoring the condition of underground waters at the landfill of non-hazardous Red Mud-Talum waste for 2016, March 2017. Geological Survey of Slovenia, Ljubljana:, 2017. 21 p.

Kovacs, S., Sudar, Gradinaru, E., M., Gawlick, H.-J., Karamata, S., Haas, J., Pero, C., Gaetani, M., Mello, J., Polak, M., Aljinovic, D., Ogorelic, B., Kolar-Jurkovsek, T., Jurkovsek, B. & Buser, S. (2011): Triassic Evolution of the Tectonostratigraphic Units of the Circum-Pannonian Region. - Jahrbuch der Geologischen Bundesanstalt, 151: 199-280.

Kruk, B., Dedić, Ž., Kovačević Galović, E., Kruk, Lj. (2014): Osnove gospodarenja mineralnim sirovinama na području općine Promina u Šibensko-kninskoj županiji, Fond stručne dokumentacije, Hrvatski geološki institut, Zagreb, str. 87.

Lukšić, B. (1994): Litostratigrafski odnosi u krovinskim naslagama paleogenskih boksita područja Imotskog. Magistarski rad. Sveučilište u Zagrebu, PMF I RGNF fakultet, Zagreb.

This activity has received funding from the European Institute of Innovation and Technology (EIT), a body of the European Union, under the Horizon 2020, the EU Framework Programme for Research and Innovation

Lukšić, B., Pencinger, V., Jurić, A., Juric, J. (2004): Elaborat o rezervama boksita u eksploatacijskom polju „Mamutovac“, Fond stručne dokumentacije, Hrvatski geološki institut, br. 32/04, Zagreb.

Lukšić, B.,Miko, S., Pencinger, V., Dedić, Ž. (2006): Rudarsko-geološka studija Šibensko-kninske županije, Fond stručne dokumentacije, Hrvatski geološki institut, Zagreb.

Markovic, S. (2002): Hrvatske Mineralne Sirovine. -1-543, Institut za geoloska istrazivanja, Zavod zu geologiju, Zagreb,

Mindszenty, A., Gál-Sólymos, K., Csordás-Tóth, A., Imre, I., Felvári, Gy., Ruttner, A., Böröczky T. (1991): Extraclasts from Cretaceous/Tertiary bauxites of the Transdanubian Central Range and the Northern Calcareous Alps. Preliminary results and tentative geological interpretation. *Jubilaeumsschrift 20 Jahre Geol Zusammenarbeit Österreich-Ungarn, Teil I.* 309-345, Vienna

Missoni, S. & Gawlick, H.-J. (2011): Evidence for Jurassic subduction from the Northern Calcareous Alps (Berchtesgaden; Austroalpine, Germany). International Journal of Earth Sciences 100, 1605–1631.

Nagy, S. (1989): A nagyharsányi bauxit reambulációs vizsgálata (The Nagyharsány Bauxite revisited), MSc Theses, ELTE Budapest, Dept. of Mineralogy, manuscript, pp.154, (in Hungarian)

Noszky, J. jr (1957): Kiértékelő jelentés az 1952-ben a Villányi-hegységben végzett bauxitföldtani reambuláló vizsgálatokról (Report on bauxite geological reambuation in the Villány Mts in 1952 manuscript, in Hungarian), Hungarian Geological Institute, 197p

Pajović, M. (2009): Genesis and genetic types of karst bauxites, *Iranian Journal of Earth Sciences,* **1**, 44-56

Pajovic, M., Mirkovic, M., Svrkota, R., Ilic, D. & Radusinovic, S. (2017): Geologija boksitonosnog rejona Vojnik-Maganik (Crna Gora)/Geology of the Vojnik-Maganik baxite-bearing region (Montenegro). Spararet issues of the Geological Bulletin XXI: 1-431, Geological Survey of Montenegro.

Pencinger, V. (1987): Izvještaj o radovima na istraživanju boksita šireg područja Imotskog u godini 1986. Fond stručne dokum. 28/87, Geološki zavod – Zagreb

Pueyo, E. L., Mauritsch, H. J, Gawlick, H.-J, Scholger, R. & Frisch, W. (2007): New evidence for block and thrust sheet rotations in the central northern Calcareous Alps deduced from two pervasive remagnetization events. - Tectonics 26, TC5011.

Radusinović ,S., Jelenković, R., Pačevski, A., Simić, V., Božović, D., Holclajtner-Antunović, I., Životić, D. (2017): Content and mode of occurrences of rare earth elements in the Zagrad karstic bauxite deposit (Nikšić area, Montenegro). Ore Geology Reviews, 80, 406-428.

This activity has received funding from the European Institute of Innovation and Technology (EIT), a body of the European Union, under the Horizon 2020, the EU Framework Programme for Research and Innovation

Rivera, R.M. (2019): Innovative technologies for rare earth element recovery from bauxite residue. KU Leuven, PhD. thesis, p. 191.

Rivera, R.M., Ounoughene, G., Borra, C.R., Binnemans, K., Van Gerven, T. (2017): Neutralisation of bauxite residue by carbon dioxide prior to acidic leaching. Minerals Engineering 112, 92–102.

Sakač, K., Šinkovec, B., Jungwirth, E., Lukšić, B. (1984): Opća obilježja geološke građe i ležišta boksita područja Imotskog. Geol. Vjesnik 37, 153-174, Zagreb.

Schmid, S.M., Bernoulli, D., Fügenschuh, B., Matenco, L., Schefer, S., Schuster, R., Tischler, M. & Ustaszewski, K. (2008): The Alpine-Carpathian-Dinaride-orogenic system: correlation and evolution of tectonic units. - Swiss Journal of Geosciences, 101: 139-183, Birkhaeuser Verlag AG, Basel.

Taylor, S.R., and McLennan, S.M. (1985): The Continental Crust: Its Composition and Evolution: Oxford (Blackwell Scientific).

Tessier A., Campbel P.G.C., Bisson M. (1979): Sequential extraction procedure for the speciation of particulate trace metals. Anal. Chem. 51(7), pp. 844–851.

Timotijevic, S. (1995): Metalogenetsko prognoziranje Lezista Boksita Zapadne Srbije. – Posebna izdanja Geoinstitua 34: 1-170, Belgrade.

Timotijevic, S. (2001): Kredni Boksiti Srbije. - Posebna izdanja Geoinstitua 27: 1-94, Belgrade.

Vujec, S. (1996): Rudarstvo u Hrvatskoj. *Rudarsko-geološko-naftni zbornik*, **8**, 11-17 (in Croatian)

Sources:

Red mud project: http://redmud.org/

Shangai Metal Market: https://www.metal.com/

This activity has received funding from the European Institute of Innovation and Technology (EIT), a body of the European Union, under the Horizon 2020, the EU Framework Programme for Research and Innovation

ANNEX – Normalized REE distribution patterns in selected bauxite deposits

In order to illustrate relative abundances of REE in bauxite deposits explored within WP2, normalized REE distribution patterns for selected bauxite deposits are presented in Figures A-1 to A-12.

Croatia

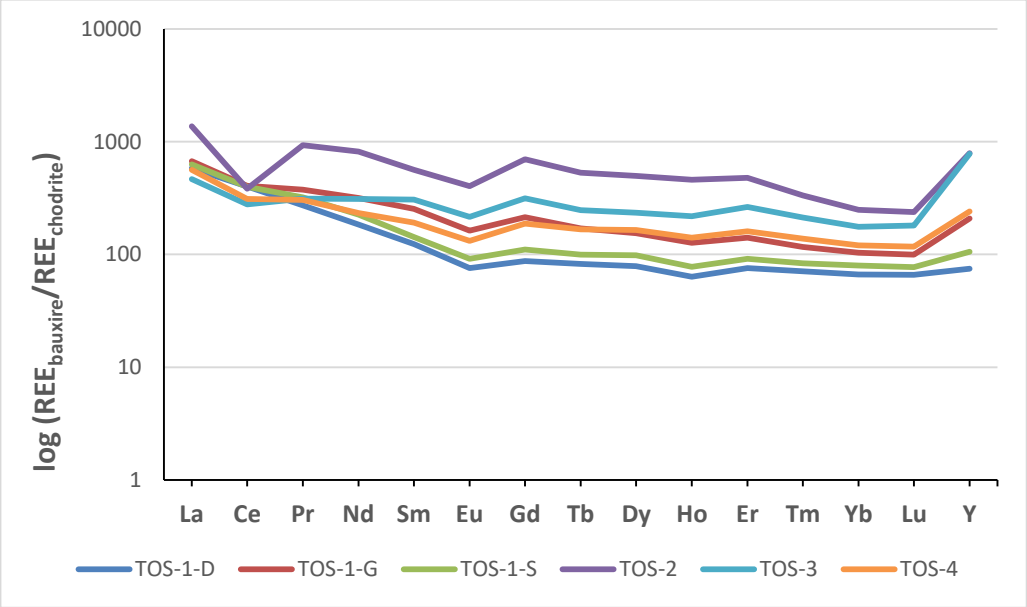

Figure A-1 Chondrite-normalized REE distribution in bauxite of Tošići-Dujići deposit

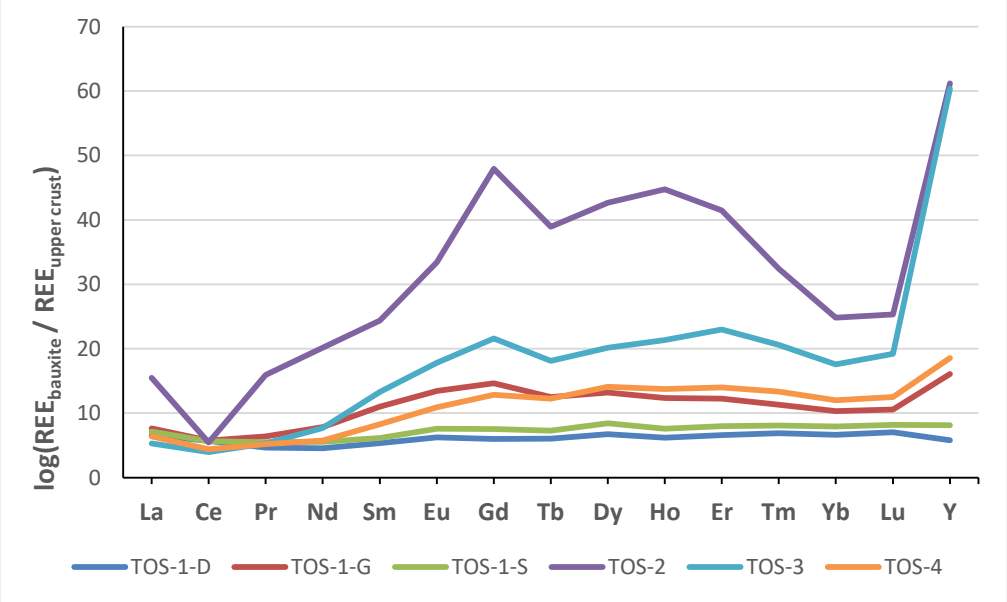

Figure A-2 Upper crust-normalized REE distribution in bauxite of Tošići-Dujići deposit

This activity has received funding from the European Institute of Innovation and Technology (EIT), a body of the European Union, under the Horizon 2020, the EU Framework Programme for Research and Innovation

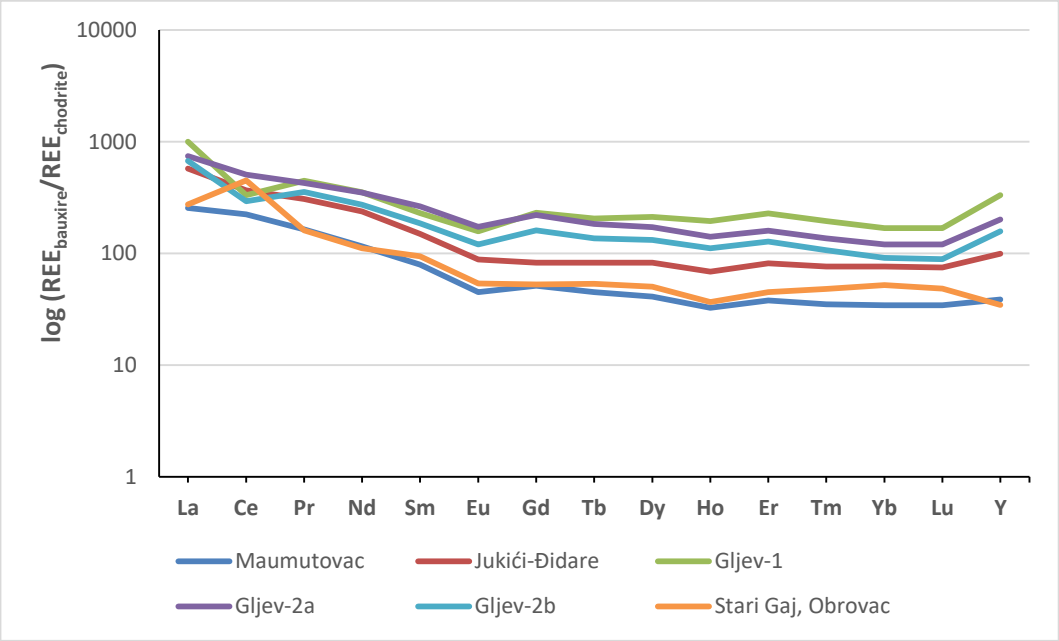

Figure A-3 Chondrite-normalized REE distribution in bauxite of several deposits in Croatia

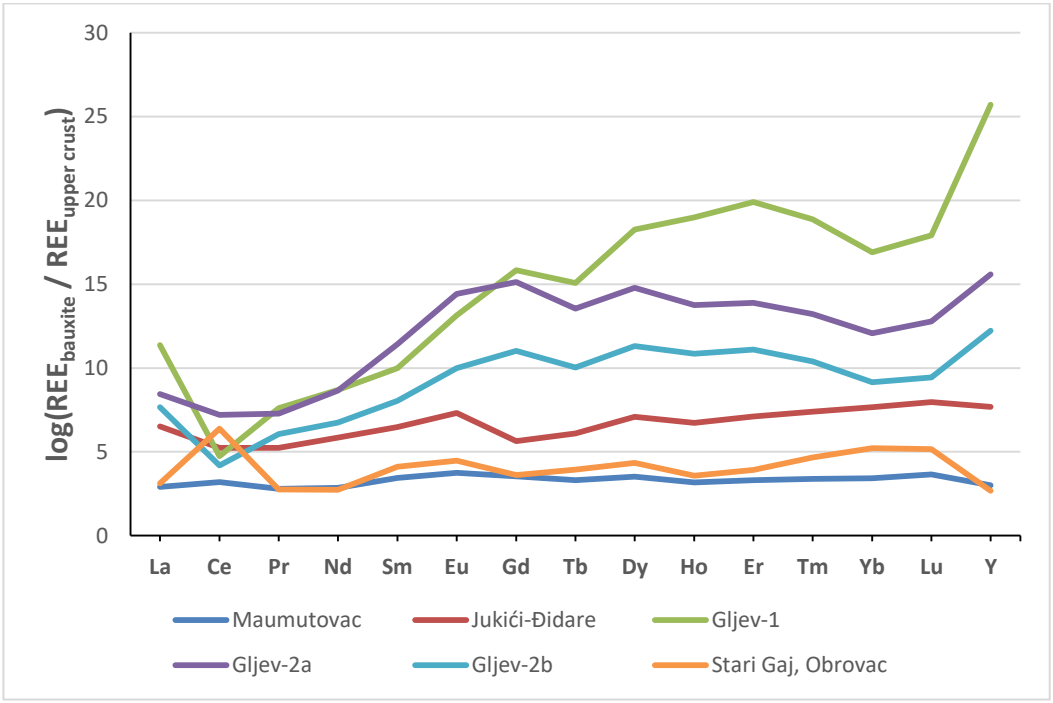

Figure A-4 Upper crust-normalized REE distribution in bauxite of several deposits in Croatia

This activity has received funding from the European Institute of Innovation and Technology (EIT), a body of the European Union, under the Horizon 2020, the EU Framework Programme for Research and Innovation

Hungary

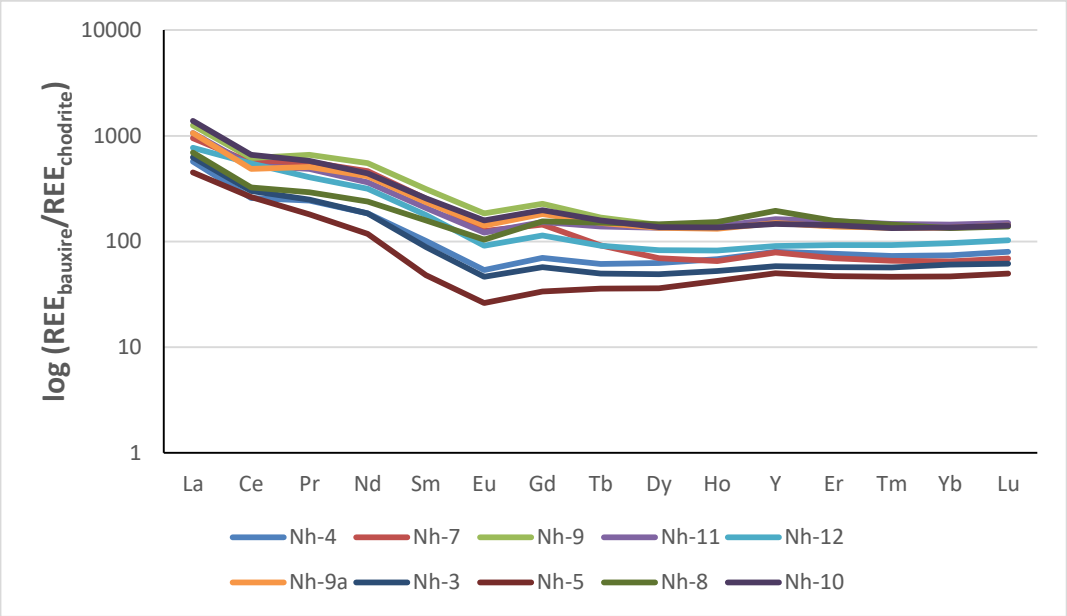

Figure A-5 Chondrite-normalized REE distribution in bauxite of Nagyharsány deposit

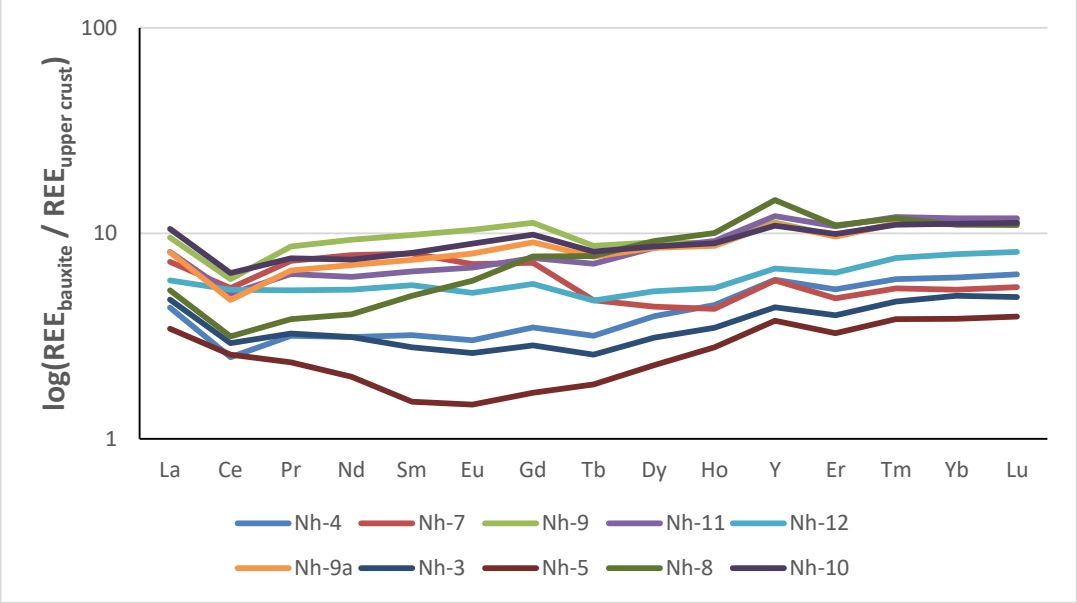

Figure A-6 Upper crust-normalized REE distribution in bauxite of Nagyharsány deposit

This activity has received funding from the European Institute of Innovation and Technology (EIT), a body of the European Union, under the Horizon 2020, the EU Framework Programme for Research and Innovation

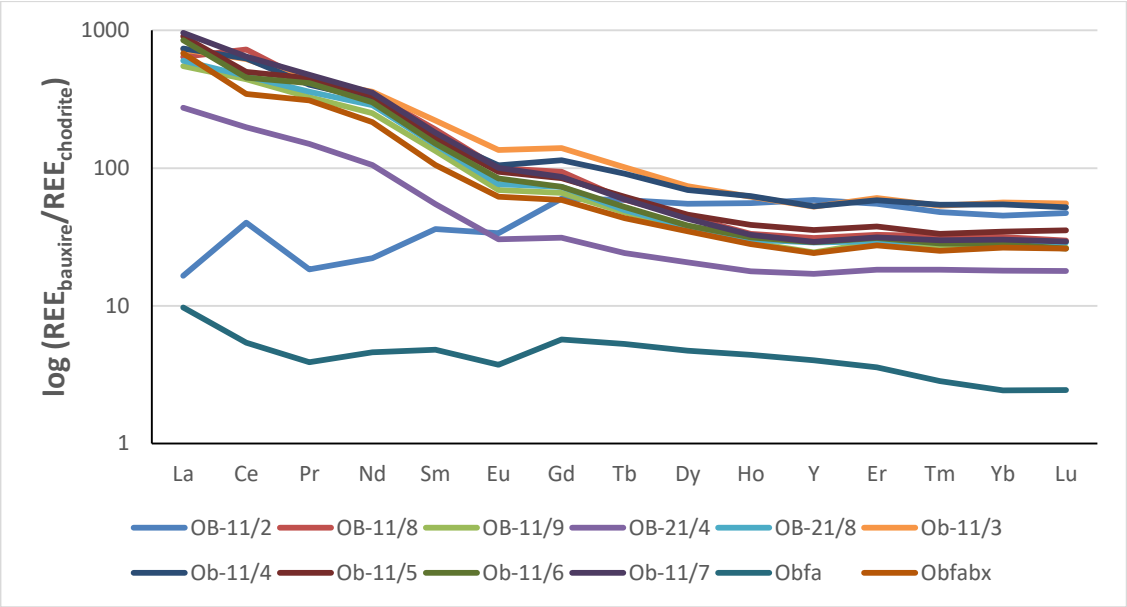

Figure A-7 Chondrite-normalized REE distribution in bauxite of Óbarok deposit

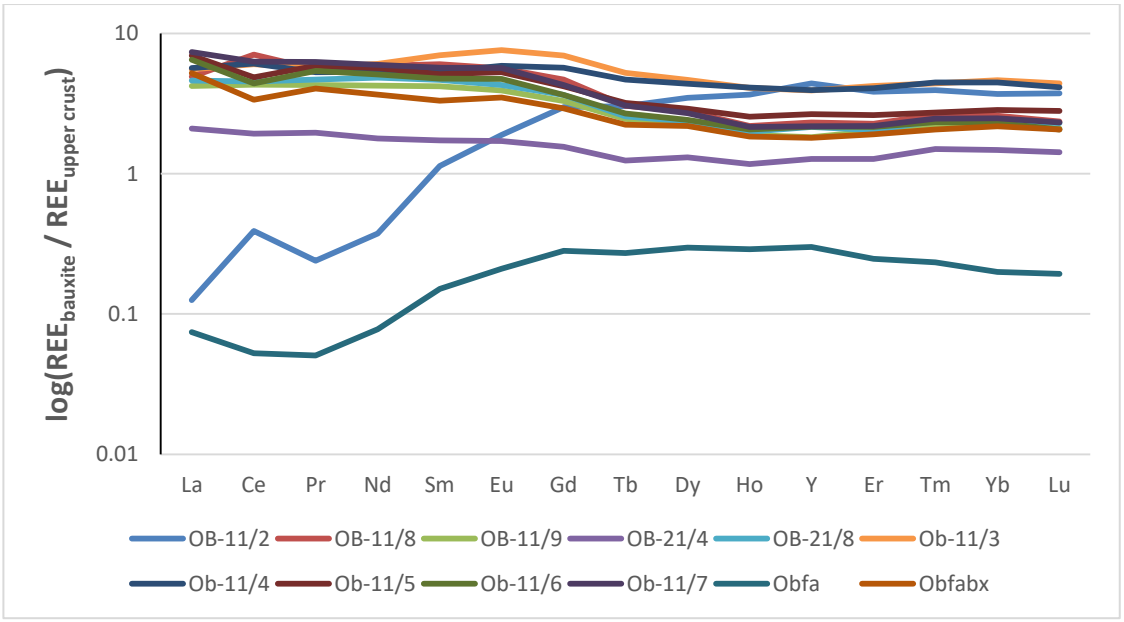

Figure A-8 Upper crust-normalized REE distribution in bauxite of Óbarok deposit

This activity has received funding from the European Institute of Innovation and Technology (EIT), a body of the European Union, under the Horizon 2020, the EU Framework Programme for Research and Innovation

Montenegro

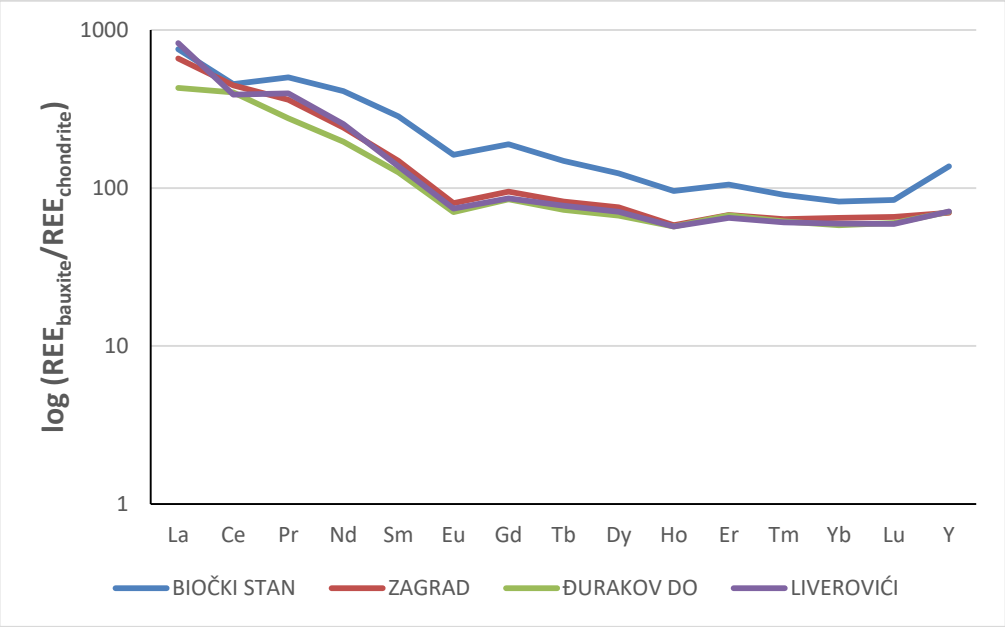

Figure A-9 Chondrite-normalized REE distribution in bauxite of several deposits in Montenegro

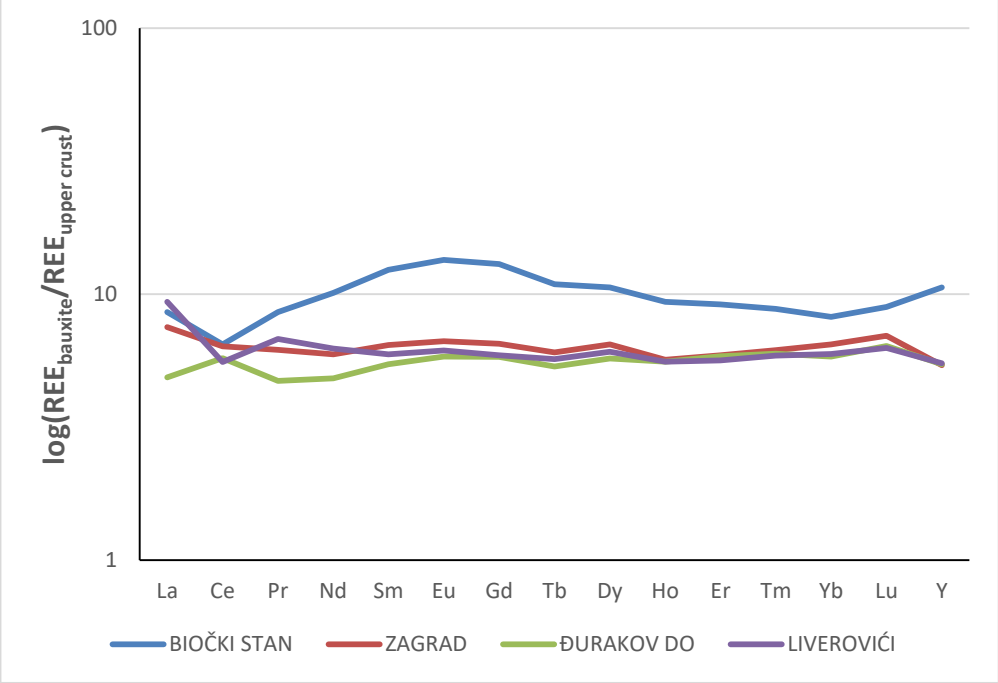

Figure A-10 Upper crust-normalized REE distribution in bauxite of several deposits in Montenegro

This activity has received funding from the European Institute of Innovation and Technology (EIT), a body of the European Union, under the Horizon 2020, the EU Framework Programme for Research and Innovation

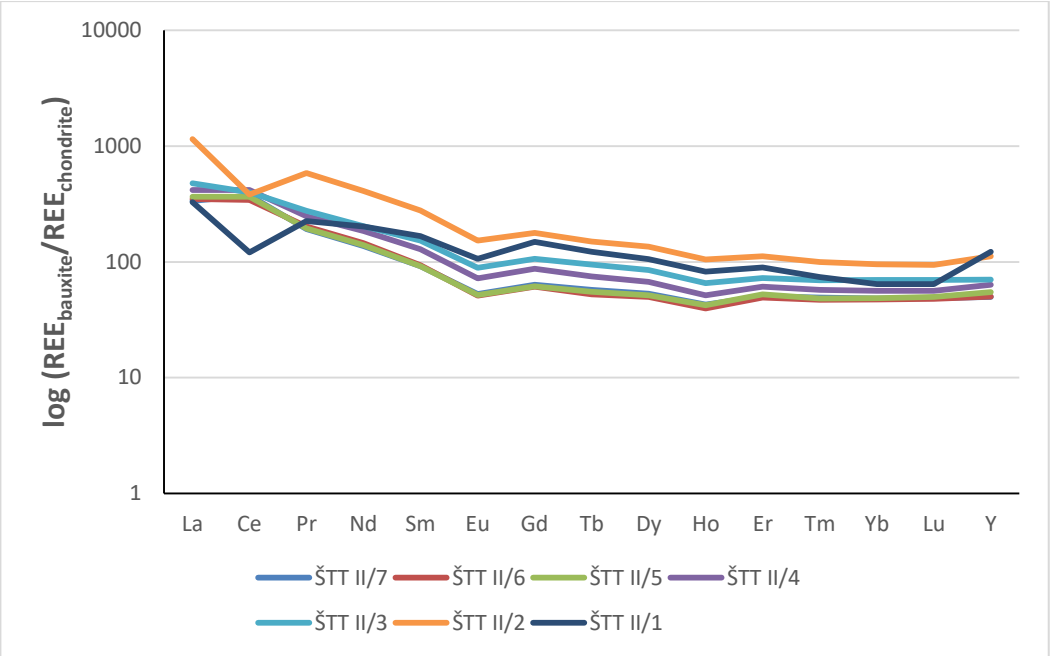

Figure A-11 Chondrite-normalized REE distribution in bauxite of Šitovo deposit

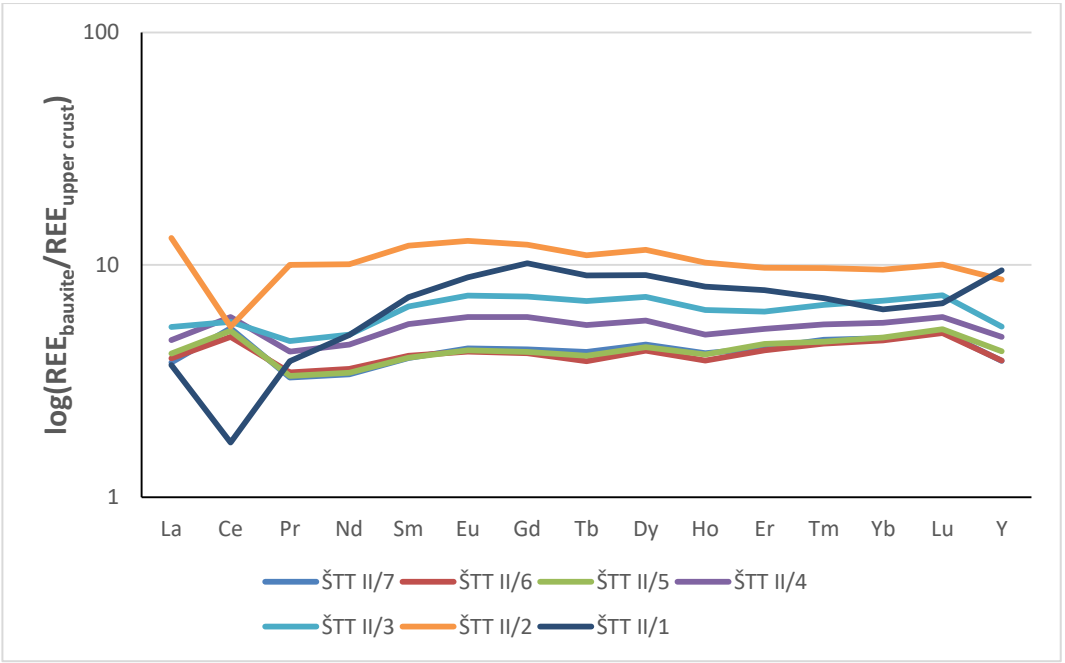

Figure A-12 Upper crust-normalized REE distribution in bauxite of Šitovo deposit

This activity has received funding from the European Institute of Innovation and Technology (EIT), a body of the European Union, under the Horizon 2020, the EU Framework Programme for Research and Innovation

The REEBAUX activities in 2019 were supported by:

This activity has received funding from the European Institute of Innovation and Technology (EIT), a body of the European Union, under the Horizon 2020, the EU Framework Programme for Research and Innovation

and the partner institutions.

This activity has received funding from the European Institute of Innovation and Technology (EIT), a body of the European Union, under the Horizon 2020, the EU Framework Programme for Research and Innovation